8.72 cm

ION IMPLANTED SOLAR CELLS

by

THEODORE M. VANDERWEL, B.ENG.

PART A: MCMASTER (ON-CAMPUS) PROJECT*

A Report Submitted to the School of Graduate Studies
in Partial Fulfilment of the Requirements
for the Degree
Master of Engineering

Department of Engineering Physics
McMaster University
Hamilton, Ontario, Canada
April 1978

*One of two project reports: The other part is designated PART B: OFF-CAMPUS PROJECT.

MASTER OF ENGINEERING (1978)
Department of Engineering Physics

MCMASTER UNIVERSITY
Hamilton, Ontario

TITLE: Ion Implanted Solar Cells

AUTHOR: Theodore M. Vanderwel, B.Eng. (McMaster)

SUPERVISOR: Dr. J. Shewchun

NUMBER OF PAGES: iv, 96

ABSTRACT

Ion implantation is investigated as a technique to fabricate solar cells on monocrystalline silicon. The electrical properties of the implanted layer, as determined using the Hall Effect, and solar cell performance have been studied for varying implant species (As and P), implanted dopant concentration (10^{18} - 10^{21} cm^{-3}), implanted substrate temperature (55° to 300°K) and annealing temperature (700° to 900°C). Some progress has been made toward the optimization of the various parameters.

ACKNOWLEDGEMENTS

I wish to thank my Supervisor, Dr. J. Shewchun for his advice and support during the course of my research. I would also like to express my gratitude to J.B. Neilson for his ideas and assistance in all phases of the work, and to Dr. R.S. Walker and Dr. D.A. Thompson for advice and assistance in the implantation techniques. Finally, I would like to thank the technicians and graduate students in the Engineering Physics Department for many stimulating and often rewarding discussions.

TABLE OF CONTENTS

EXPERIMENTAL: SOLAR CELLS

EXPERIMENTAL: HALL SAMPLES

RESULTS

APPENDIX I

APPENDIX II

INTRODUCTION

In this day of energy crises and fuel embargoes, it is becoming increasingly important to find an alternate energy source for the future. Photovoltaic cells, semiconductor devices which convert sunlight directly to electrical power, either alone or in conjunction with thermal conversion units, may be such a viable energy alternative. There are also several other applications for photovoltaics, such as isolate or orbital power supplies requiring long lives under a variety of environmental conditions. It is unlikely that a single type of solar cell would fill the widely varying requirements of these diverse applications. It is therefore necessary to investigate the advantages and disadvantages of different designs and fabrication techniques.

There are several different types of solar cells being presently studied. Shallow single crystal p-n junctions seem to be the mainstay of the photovoltaics field with the best efficiencies (i.e. best power area ratio) and longest life. Competing structures include the thin film heterojunction which promises better power: cost and power: weight ratios and the newer MOS devices. The purpose of this project is to investigate the use of ion implantation as the doping mechanism in single crystal cells. Conventional cells rely on diffusion from either a gas source or a spin-on emulsion to turn over the type of the surface layer; thereby forming the p-n junction, but variations in doping profile, junction depth, and dopant gradient near the junction are all limited by the diffusion process. Greater control over junction formation is possible using implantation and hence better solar cell performance may be possible provided no less obvious disadvantages appear.

Much work has been done in the use of implantation doping in the fabrication of devices and integrated circuits. However, little has been done to investigate its potential in the production of solar cells(1,2). Several advantages of the use of ion implantation are apparent. There is greater control of the dopant distribution than with conventional diffusion techniques. In particular, very shallow junctions are possible, allowing the formation of the "blue-shifted" cell(3), which shows an enhanced response to the short wavelength end of the spectrum. If this is not at the cost of some red response, this should result in increased efficiency, in particular for AMO (orbital) applications although it is hoped that terrestrial applications should also benefit. Also, the lateral geometry control available with the implantation technique facilitates the fabrication of grating cells(4) which also show an enhanced blue response due to the increased effective diffusion length as a result of bringing the higher carrier lifetime of bulk material to the surface, and should also show correspondingly increased efficiency.

The aim of this project, then, is to isolate the characteristics of implantation doping that are of particular concern in the manufacture of solar cells. To achieve this, several simple planar geometry solar cells, similar in design to the conventional diffused cells, were prepared by implanting p-type silicon wafers with n-type dopants (Arsenic or Phosphorus) at energies from 20keV to 120keV, with the substrate temperature held fixed at from 40°K to 300°K during the implant. The samples were vacuum annealed to remove the bombardment damage, aluminum ohmic contacts were evaporated on and the resulting solar cell characteristics were determined using a solar simulator and automated I-V plotter (See Figure 1 and 2).

To help identify the implantation parameters having the most effect on cell behaviour, several key implantations, as chosen according to cell performance, were duplicated in a geometry suitable for Hall measurements (see Figure II-1) and these were electrically characterized.

EXPERIMENTAL: SOLAR CELLS

A Sample Preparation

The substrates used for this work were commercial p-type (B doped) silicon wafers, (111) orientation, with resistivities in the range 0.1 to 10 ohm cm. It was possible that there were variations in quality, but judging from the results these were not significant. Before use the samples were scribed and cleaved into 1 cm by 1.5 cm sections, which were then subjected to a standard cleaning procedure as follows:

15 minutes in boiling $H_2SO_4 + H_2O_2$ (2:1)
Cool 5 minutes
Rinse thoroughly with de-ionized water
2 minutes in HF + H_2O (1:10)
Rinse
15 minutes in boiling H_2O + HCl + H_2O_2 (4:1:1)
Rinse and blow dry with N_2 gas.

Throughout this procedure the samples were kept submerged in a quartz beaker, to avoid oxidation or contamination by contact with the air. The HCl etch stabilizes the surface after the HF etch and reduces the adsorption of atmospheric contaminants.

Energies and doses for the implants were calculated to give a uniformly doped surface layer using the data from Gibbons et al(5). The lowest energy ion beam that was easily stabilized was found to be 20 keV. As can be seen from Figure 4 this leaves a very low dopant concentration near the surface, making good ohmic contact to the device difficult. Two possible solutions were found. After the implant a thin surface layer could be removed by growing an oxide 300Å thick and stripping it in 10% HF, or a "through-the-oxide" implant could be used to obtain an appreciable impurity concentration at the silicon surface. By comparing the stopping powers of silicon and silicon dioxide, it was found that an oxide thickness of 130Å would be adequate. This thin oxide could be removed after the annealing procedure. Both methods were tried and were found equivalent, but as the oxidation rate of implanted silicon varies depending on the implant, it was decided that the through-the-oxide implant was preferable. The next step in preparation was therefore to grow an oxide 130Å thick on the sample. This was done, immediately after cleaning, in a quartz tube three element furnace at 800°C in a steam atmosphere. The oxidation time was 19 minutes 10 seconds, which gives an oxide 130Å thick according to the graph given in Sze(6), page 81. Sample oxides were measured by ellipsometry and had thicknesses of 140 ± 10Å.

After oxide growth the samples were moved to the implantation facility, while being handled as little as possible. As sample preparation and implantation were done in different buildings, there is some concern that the time interval and exposure between final oxidation and evacuation in the implantation target chamber may lead to some surface contamination of the sample. It is hoped that the

130Å oxide is sufficient protection for the silicon surface, particularly since this layer is removed in the final processing and contacting, but the possibility of recoil implantation of any adsorbed contaminants cannot be dismissed. It is recommended, therefore, that an evacuable desicator be used for sample shuttling in any future work.

B Implantation

The implantations were done with the 150keV ion accelerator(7) in the Tandem Accelerator Lab at McMaster. The ion beam, from a Danfysik 911A Universal Ion source, is accelerated, focussed through a 2 mm aperture, then electrostatically swept across a second 2 mm aperture to ensure a uniform implant, and the two apertures were sufficiently off axis to avoid the implantation of neutrals, which would not be swept and hence cause a hot spot. The current on target was 10 to 200 nanoamps swept over an oval of 1 cm^2 area (see Figure 3). Dosimetry was by means of a current digitizer and scalar connected to integrate the target current. In a preliminary study, the calculated dosimetry was checked using the in situ backscattering facility and good agreement was found.

To calculate implanted impurity depth profiles, the distributions were approximated by gaussians, with moments as prepared by Gibbons et al(5) using LSS theory. Each sample was aligned in a "random" direction to avoid channeling, and implanted with several different energies, at doses calculated to give uniform concentrations from the silicon surface to the peak of the deepest implanted layer. The junction depth was taken as the intersection of the approximated implant distribution with the background dopant level. An example plot is given in Figure 4. Table 1 lists calculated average concentrations and junction depths for various implant conditions.

C Final Processing

The samples require annealing and deposition of aluminum contacts before the solar cells are complete. Annealing was done in a quartz tube three element vacuum furnace at a pressure of 10^{-6} torr, at temperatures ranging from 700°C to 900°C. Ten minute isochronal anneals were chosen as sufficient to reach the first annealing plateau commonly observed in silicon annealing(8).

After the anneal, the 130Å oxide window was etched off in 10% HF and aluminum contact pads were evaporated on the top and bottom in a vacuum evaporator, through a brass mask in the desired design (see Figure 3). Finally, the contacts were sintered for 10 minutes at 400°C under vacuum in the annealing furnace. Contacts made to an unimplanted sample were tested and showed an ohmic characteristic. Tests made on the Hall samples (next section) confirmed that all contacts made to both implanted and substrate sides of the cell were ohmic.

D Testing

The cell efficiencies were determined by measuring the illuminated I-V characteristics. Contact was made to the aluminum contact pads by an indium block below and a copper wire probe held in a micromanipulator on top. Illumination was provided by an Air Mass 2 solar simulator consisting of four 300 watt tungsten-iodine lamps with dichroic filters. The output spectrum is shown in Figure 1. Input power to the cell at AM2 is 75mW/cm^2. The I-V characteristic was measured on a system based on a Hewlett-Packard HP 9820 computer and including a digital voltmeter, programmable power supply, and xy plotter. Figure 2 shows a block diagram of the system and a typical output plot is given in Figure 5. Significant values are the open circuit voltage (V_{oc}), the short-circuit current (I_{sc}), and the maximum output power (0_{mp}). The fill factor C_{ff}, defined as $0_{mp}/V_{oc}I_{sc}$ is a useful quantity, and the efficiency, 0_{mp} divided by total incident power, is the parameter being maximized in this study. The cells were illuminated only in the area of the contact grid (see Figure 3) to avoid edge effects and to define the input power.

Dark I-V characteristics were also measured, to give an indication of the quality of the p-n junctions formed.

EXPERIMENTAL: HALL SAMPLES

A Sample Preparation

The same substrate material was used for the Hall samples as for the solar cells, and the same standard cleaning procedure. Sample size was changed to 7mm × 10mm. In order to measure the Hall coefficient and resistivity a bar shaped implanted region was required (Figure 6). The implanted region was defined by protecting the area not to be implanted with a thick oxide during implantation. Immediately after cleaning the samples were placed in the oxidation furnace at 900°C in a steam atmosphere for 105 minutes, growing an oxide 4000Å thick according to Sze(6) page 81. A film of Shipley AZ 1350 photoresist was then spun onto the samples at 4000 RPM and pre-baked 5 minutes at 100°C. The photoresist was then exposed through an image of the implant pattern, developed, and baked for 1 hour at 100°C. The sample was etched for 4 minutes in 50% HF solution to etch the implant window, the remaining photoresist removed with acetone, and the sample rinsed in de-ionized water. Finally a thin oxide was grown, as for the solar cells, in 800°C steam for 19 minutes 10 seconds.

B Implantation

The Hall samples were implanted on the same equipment and in the same manner as the solar cells.

C Final Processing

The annealing and contact deposition procedures were identical with those used for the solar cells, except that a different brass mask was used for the contact evaporation (see Figure 6). Note that the oxide etch prior to contact deposition removed only the thin oxide over the Hall bar, leaving the thick oxide over the unimplanted region as an insulator over the substrate. This considerably reduced the alignment requirements for the contacts.

A back contact to the substrate was also added at this point. As the assumption that the implanted bar-shaped region is isolated from the substrate(9) is necessary to the evaluation of the raw Hall data, the I-V characteristics of the bar-to-substrate interface were checked to ensure that it was a good diode. Also, as a check on the applicability of the Hall tests to the previously done solar cell measurements, the photovoltaic characteristics of these samples were also determined, and found to be comparable to the earlier work.

Following the 400°C sintering step, gold wires were bonded to the contact pads with an ultrasonic wirebonder to facilitate Hall testing.

D Testing

The resistivities and Hall coefficients of the samples were measured at room temperature on a computerized system described in detail by Shewchun et al(10). The system, controlled by a computer sequencer, switched the sample current and the magnetic field through positive and negative values while measuring the Hall voltage. It also measured the conductivity voltage in each direction, the current, the magnetic field, and the sample temperature. Readings can be made automatically at fixed intervals of up to 20 minutes. The data is typed or punched on paper tape as it is measured, and later analysed on a CDC 6400 computer to give calculated values of the Hall coefficient, Hall mobility, carrier concentration, and resistivity. The calculations and program are described in more detail in Appendix I and the apparatus is discussed in Appendix II.

RESULTS

Several implantation parameters were varied, and the dependence of the cell performance was studied. Results are given here primarily with cell efficiency as the dependent variable, but I_{SC}, V_{OC}, and C_{FF} are included to help clarify the physical mechanism responsible for the observed behaviour. The standard cells in the following studies, determined in a preliminary examination to have "reasonable" photovoltaic characteristics, are 10 ohm-cm, arsenic implanted at room termperature to maximum energy of 80 keV, have an average implanted concentration of $10^{20} cm^{-3}$, and were annealed at 800°C. In each case, all the above parameters were constant except the observed variable.

A Implant Temperature

Earlier published results(11) have suggested that better electrical activity is obtained in silicon by total amorphization of the surface layer during implantation followed by epitaxial regrowth of the damaged region in the anneal stage. It was therefore expected that by holding the substrate at low temperatures during the implant, allowing little or no annealing, a greater amount of damage would accummulate and a more completely amorphous layer would result, improving the subsequent epitaxial regrowth during the anneal. This effect was not observed, however, as shown in

Figure 7, where it can be seen that the best efficiencies were obtained with the room temperature implant.

The dominant effect in this case was the variation of I_{SC} from 20 ma/cm^2 for the room temperature sample. Relatively constant V_{OC} and C_{FF} indicate that the barrier formation and sheet resistivity of the surface layer were not greatly affected by the lower implant temperature, but that the carrier generation rate or lifetime has degraded. This could be due to increased surface contamination from condensation on the sample at these low temperatures (e.g. mercury from the mercury vapour pump) possibly resulting in contaminants in the implanted region due to a recoil mechanism.

B Anneal Temperature

The temperature at which the damaged layer of the sample is regrown in the anneal step should be critical to cell performance. As reported in the literature(8,12) both the electrically active fraction of the implanted ions and the carrier mobility are strong functions of anneal temperature. Several standard cells were evaluated after anneals at temperatures ranging from 700°C to 900°C. As shown in Figure 8, from 700°C to 800°C cell performance improves with increasing anneal temperature, but over 800°C, V_{OC} drops off accompanied by a less rapid drop in C_{FF}, resulting in a dramatic decrease in efficiency.

A degradation of carrier lifetimes and diffusion length was at first expected to occur at higher anneal temperatures, but this would result in a decrease in I_{SC}, which was not observed. The drop in V_{OC} suggests a decrease in junction barrier height, perhaps attributable to an enhanced diffusion resulting in a less abrupt junction, or a decrease in dopant concentration.

Hall measurements on duplicate samples determined that the latter was the functional mechanism. As shown in Figure 9, the carrier concentration versus anneal temperature behaves similar to the solar cell efficiency curve, while the mobility peaks at 750°C and degrades very slightly for higher anneal temperatures (Figure 10). Also, the resistivity of the implanted material increases for the higher temperatures, accounting for the lower C_{FF}.

The reason for the lower dopant concentrations with the hot anneals is not immediately obvious. It has been suggested that compensation occurs. That is, the electrically active fraction of arsenic atoms continues to increase, consistent with the work of Baldo et al(8), but that at higher temperatures, some inactive p-type dopants go substitutional, dropping the net n-dopant concentration. Another possibility is that diffusion does become significant, and the implanted impurities diffuse deeper into the substrate resulting in a thicker but less concentrated surface n-layer.

The photovoltaic response of the Hall samples was tested under the solar simulator and was found to behave similar to the solar cell samples (Figure 11).

C Implanted and Substrate Dopant Concentration

The effect of both the implanted and the background impurity concentrations on cell efficiency was examined using arsenic implanted cells to a maximum energy of 80 keV at room temperature and annealed at 800°C. The results are shown in Figure 12. It was expected that for greater dopant concentrations on both sides of the junction, the increased barrier height would result in a greater V_{oc}. It is clearly seen in Figure 12, however, that the efficiency drops off dramatically when the substrate resistivity is reduced to 0.1 ohm cm. This is probably due to a reduction in carrier lifetimes as was indicated by a decrease in I_{sc}.

In a shallow junction cell, the majority of the minority carriers are generated in the bulk material, and so the bulk lifetimes and the surface layer resistivity should be the dominant factors in cell behaviour. The best results would therefore be expected for a cell with a high substrate resistivity, giving long lifetimes, and a high implanted surface concentration to give a low sheet resistance. This is found to be true for diffused cells(13) and, as shown in Figure 12, also for implanted cells. There may be some depth dependence hidden in these results (see Table 1), but the magnitude of this effect over the range of depths here (600Å to 1000Å) should be negligible. Hall tests on the duplicates of these samples showed, as should be expected, a lower carrier concentration and higher mobility in samples which have not been as heavily implanted (Figures 13, 14).

D Junction Depth

Junction depth is a very critical parameter in the design of solar cells. The first and most obvious criterion is to maximize the number of carriers generated within a diffusion length of the junction. If α is the absorption coefficient then:

$$\phi(x) = \phi_0 \exp(-\alpha x)$$

is the photon flux at a depth x. For simplicity, assume one absorbed photon generates one carrier. The problem is then to maximize

$$\begin{aligned}\phi_{abs} &= \phi(d_j + L_p) - \phi(d_j - L_n) \\ &= \phi_0 \exp(d_j)[\exp(L_p) - \exp(-L_n)]\end{aligned}$$

where d_j is junction depth and L_p and L_n are minority carrier diffusion lengths in the p-type substrate and the implanted n-layer, respectively.

For the implanted layer however, L_n is very short, leading to impossibly shallow junctions at which point the series collection resistance due to the thin n-layer causes I^2R losses, observed as a decreased C_{FF} and I_{SC}. Also, with very shallow junctions, effects such as surface recombination andinhomogeneities in junction depth and concentration become significant.

Implantation to energies of 120 keV restricts us to shallow junctions (1500Å with As) compared to conventional diffused cells with junction depths of 5000 to 10,000Å typically, and the latter arguments above seem to be the more significant. This behaviour is observed in Figure 15, where monotonic increase in efficiency with depth is observed. The improved performance of the deeper junctions was due primarily to an increase in C_{FF} indicating that the sheet resistance of the surface layer was the dominant effect. This was also discussed in the previous section.

The behaviour of the arsenic implanted cells lead to the use of phosphorus to obtain a deeper junction. Arsenic had originally been chosen because of its covalent radius match to silicon, which would allow a greater dopant concentration without too much crystal strain or reduced diffusion lengths. Phosphorus, however, with its smaller radius, seems to give a better cell, even at the same calculated junction depth, and even higher efficiencies are possible with the deeper junctions (Figure 15). It is understandable that the carrier lifetime of the implanted layer should not have a great effect on efficiency, but the improved efficiency at the same depth is difficult to explain.

Hall measurements of the depth study samples (Figures 16, 17) show constant concentration at all depths for arsenic implants, indicating good reproducability in the implant conditions. The phosphorus samples, however, show a concentration variation for doses calculated to give constant concentration, indicating that either the gaussian dopant profiles are not a good enough approximation for phosphorus(14,15) or the electrically active fraction of the implanted phosphorus is depth dependent. The Hall mobilities of all samples were fairly constant at about 40 $cm^2/v.s.$

E Spectral Response

The simple equation for the previous section can be slightly improved by indicating explicitly that α is a function of wavelength, λ, of the incident photons. That is,

$$\phi(x) = \int_{\lambda} d\lambda[\phi_0(\lambda)\ \exp(\alpha(\lambda)x)]$$

This implies that the spectral response of the cell will be dependent on junction depth. Since for most materials, α is larger for the smaller wavelength (blue) end of the visible spectrum(16), most of these higher energy photons will be absorbed very near the silicon surface. Therefore, the closer the junction is to the surface, the better the collection efficiency for carriers generated by the blue light will be. That is, shallow junction cells should be "blue-shifted". This result was indeed observed as shown in Figure 18.

For purposes of demonstration, the spectral responses of the four arsenic implanted cells of the depth study were determined and are presented in Figure 18 normalized to coincide at $\lambda = 7{,}000\mathring{A}$. It should be noted that although the shallower junctions showed a higher relative blue response, the overall performances were as shown in Figure 15. That is, the deeper junctions had higher collection efficiencies.

One possible way to achieve both the enhanced blue response and still maintain the advantages of the deeper junction is the grating structure solar cell (Figure 19) as discussed by Loferski(4). By implanting deep stripes and leaving the surface between stripes undamaged, the carriers generated near the surface by the blue light can still be collected efficiently as the collecting junction is always within a diffusion length of the generating site. In this way the longer bulk diffusion lengths are used to best advantage. Preliminary work in this area has shown that the resolution attainable using conventional photoresist techniques to make thick oxide implantation masks is sufficient for grating cells in silicon, but may be difficult for other materials with shorter diffusion lengths such as GaAs.

SUMMARY

The use of ion implantation as a solar cell fabrication technique has been investigated. Most of the parameters which could be adjusted were studied, and some progress was made toward the optimization of cell efficiency. It was found that:

1. Low temperature implants do not improve the electrical characteristics of the cell.
2. Optimum annealing was found at 800°C. Below 800°C, incomplete activiation occurs, and above 800°C compensation begins to take place.
3. The best doping combination was found to be a high implanted concentration (10^{20} cm^{-3}) for low sheet resistivity, and a low substrate impurity concentration (10^{15} cm^{-3}) for long carrier lifetimes.
4. As junction depth is increased to 3000Å, cell efficiency increases, but the enhanced blue response of the shallow junction cells is lost.

Optimizing the above criteria as outlined allows the fabrication of reproducable cells of 7% efficiency, without the use of an anti-reflection coating or an improved bottom contact, which is comparable to current commercial standards.

TABLE I

Species	C_B (cm^{-3})	E (keV)	ϕ (μc-cm^{-2})	E	ϕ	E	ϕ	E	ϕ	C_{AVE} (cm^{-3})	D_j (Å)
As	10^{15}	20	0.15	40	0.25	80	0.42			10^{18}	870
As	10^{15}	20	1.5	40	2.5	80	4.2			10^{19}	930
As	10^{15}	20	15	40	25	80	42			10^{20}	1000
As	2×10^{16}	20	0.15	40	0.25	80	0.42			10^{18}	775
As	2×10^{16}	20	1.5	40	2.5	80	4.2			10^{19}	850
As	2×10^{16}	20	15	40	25	80	42			10^{20}	910
As	5×10^{17}	20	0.15	40	0.25	80	0.42			10^{18}	600
As	5×10^{17}	20	1.5	40	2.5	80	4.2			10^{19}	740
As	5×10^{17}	20	15	40	25	80	42			10^{20}	825
As	10^{15}	20	15							10^{20}	340
As	10^{15}	20	15	40	25					10^{20}	570
As	10^{15}	20	15	40	25	80	42			10^{20}	1000
As	10^{15}	20	15	40	25	80	42	120	55	10^{20}	1400
P	10^{15}	20	40							10^{20}	700
P	10^{15}	20	25	40	62					10^{20}	1300
P	10^{15}	20	25	40	28	60	88			10^{20}	1800
P	10^{15}	20	25	40	48	80	115			10^{20}	2400
P	10^{15}	20	25	40	35	60	62	100	135	10^{20}	3000

Table 1: List of Implants

C_B is substrate carrier concentration.

C_{AVE} is average implanted concentration.

D_j is junction depth.

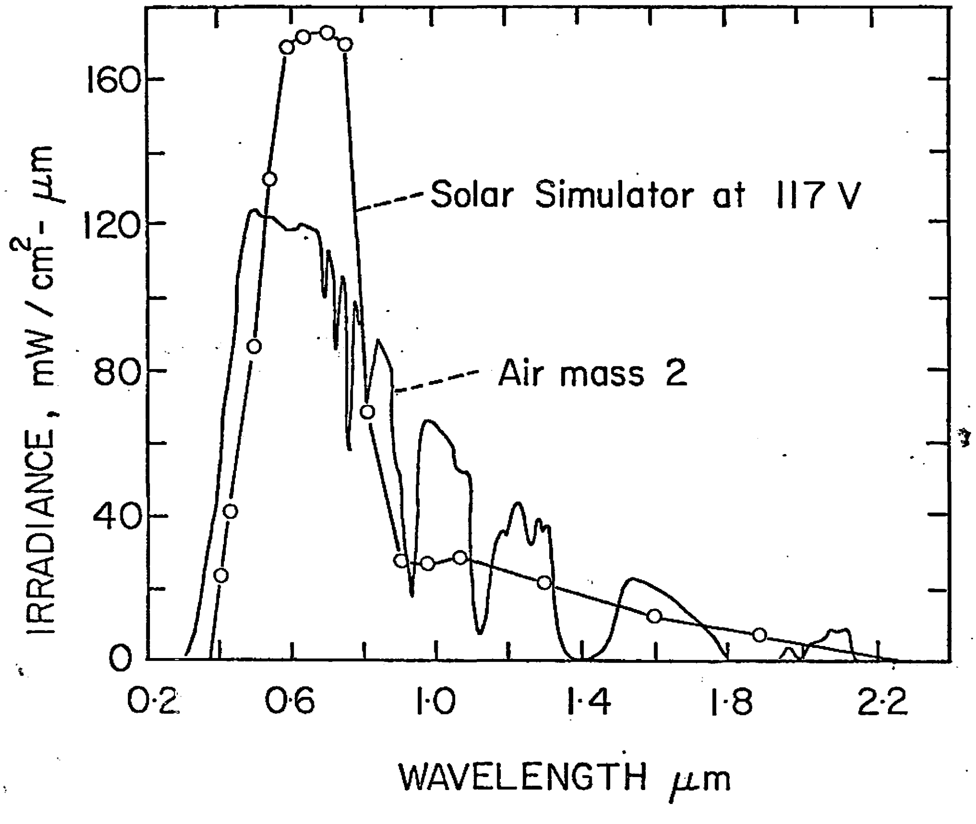

Figure 1: Solar Simulator Spectrum

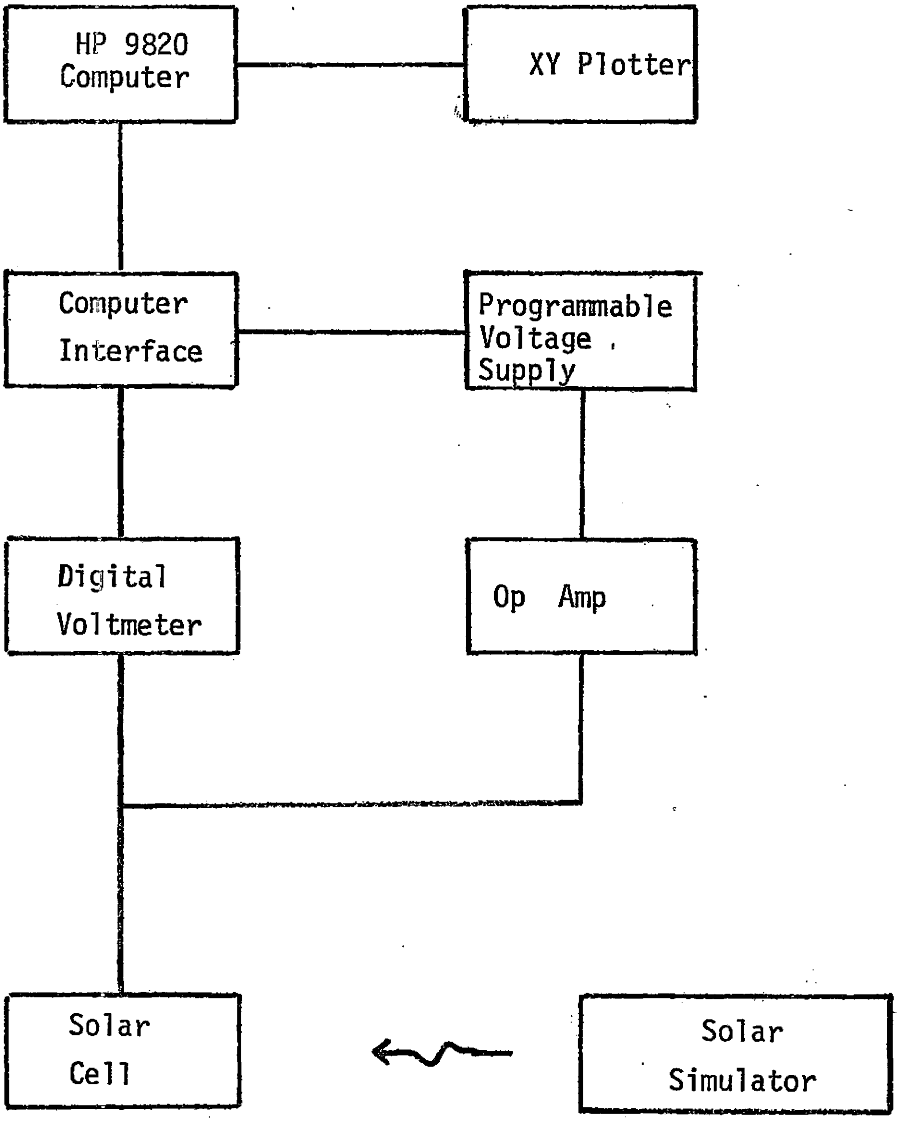

FIGURE 2: Solar Cell Testing System

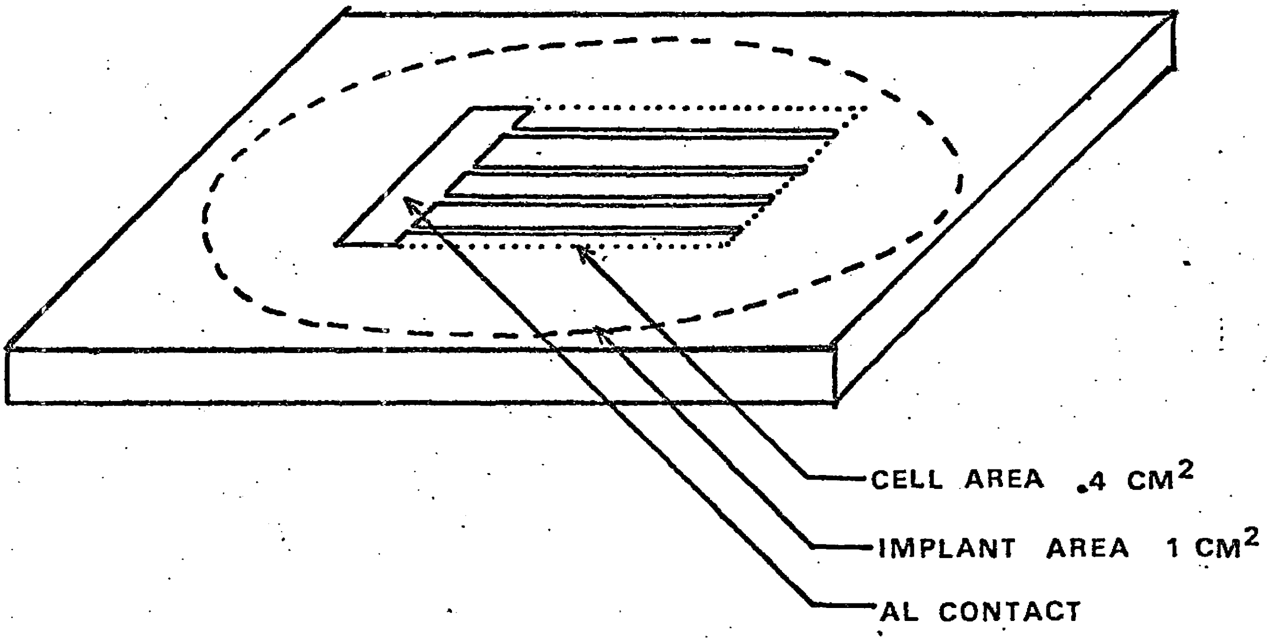

Figure 3: Solar Cell configuration.

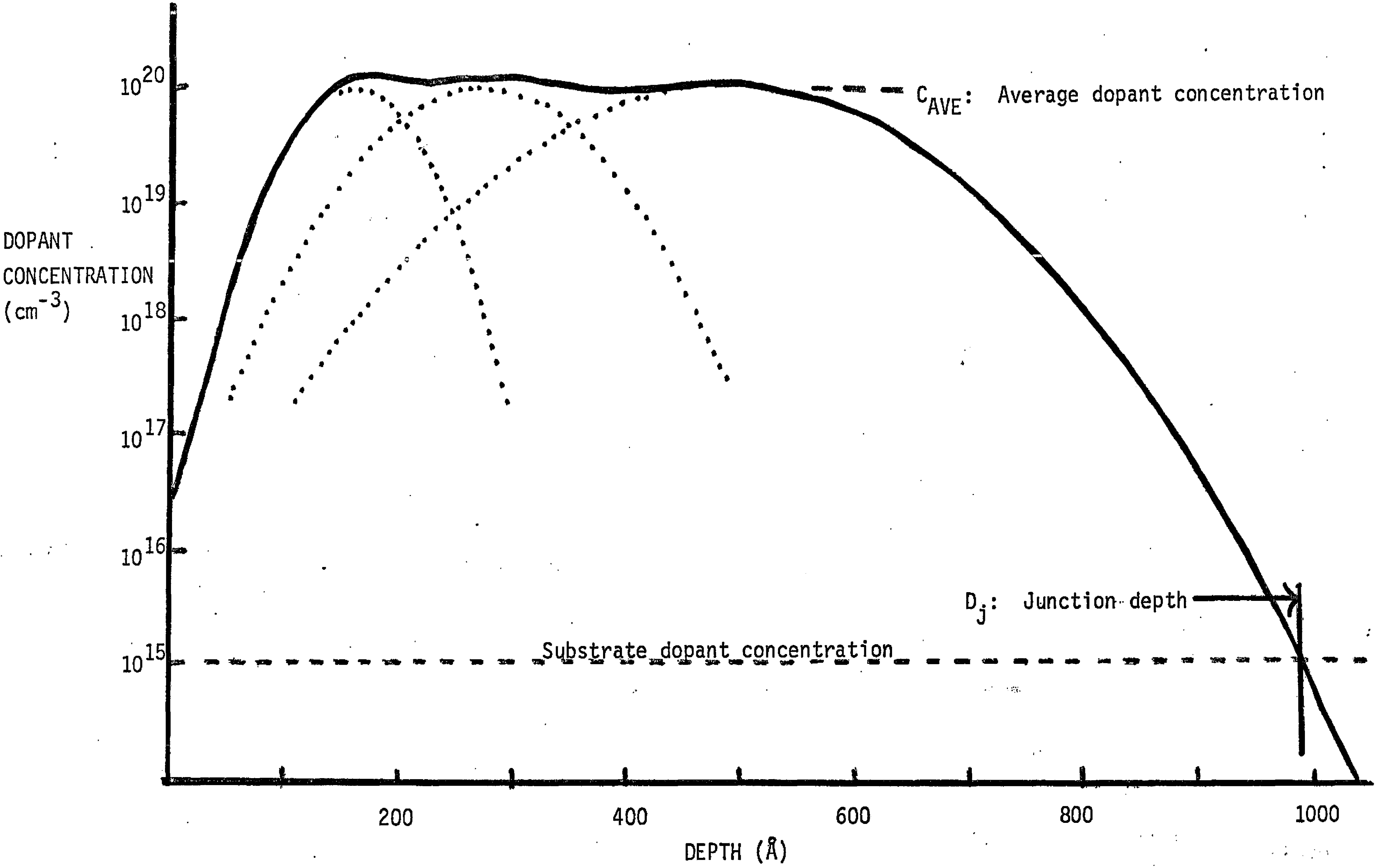

FIGURE 4: Calculated Dopant Concentration: Sample Plot

For arsenic implants of 15 $\mu C/cm^2$ at 20 keV, 25 at 40 keV, and 42 at 80 keV.

Curve parameters from Gibbons et al$^{(7)}$

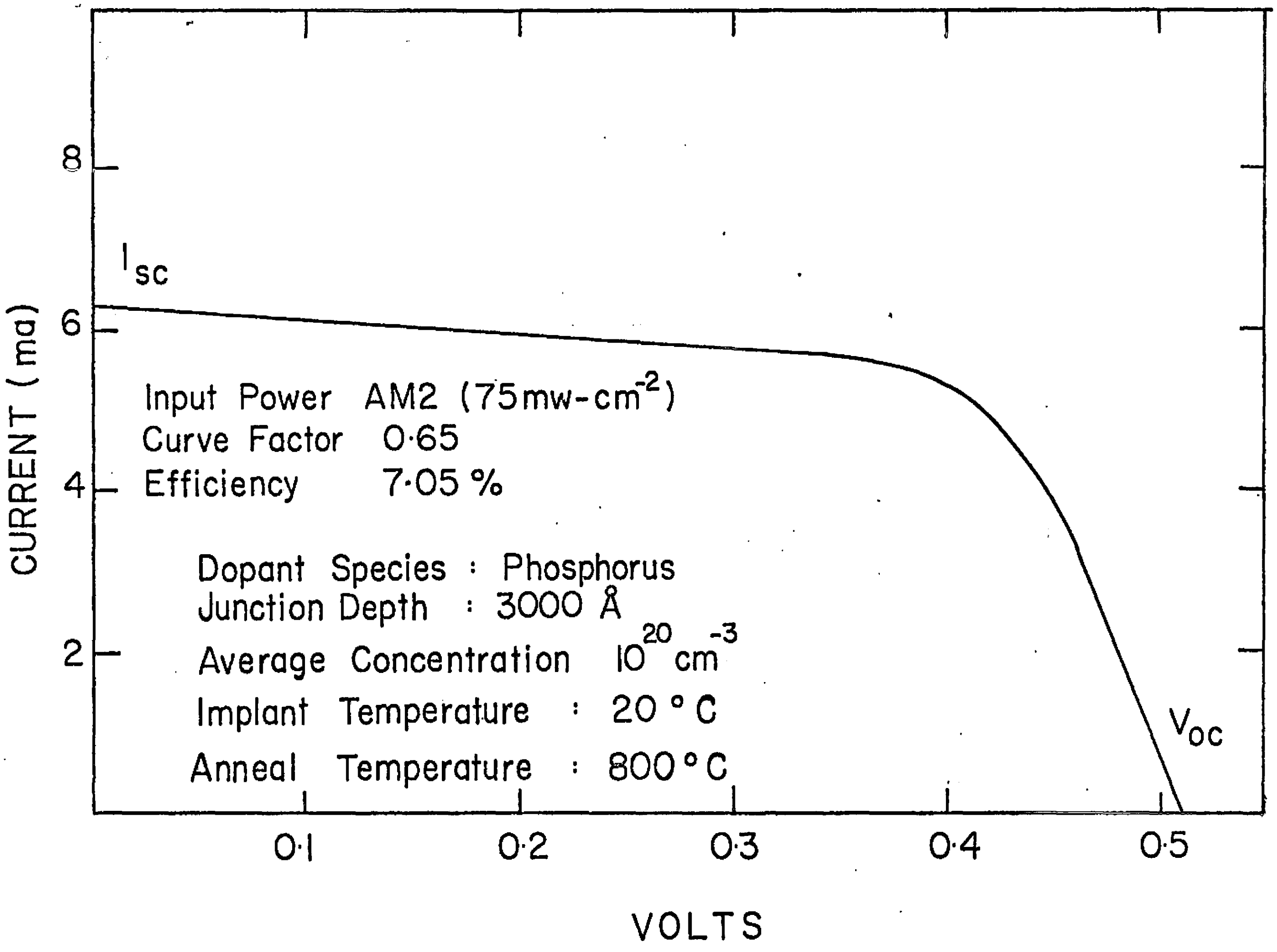

FIGURE 5: SOLAR CELL TEST I-V PLOT

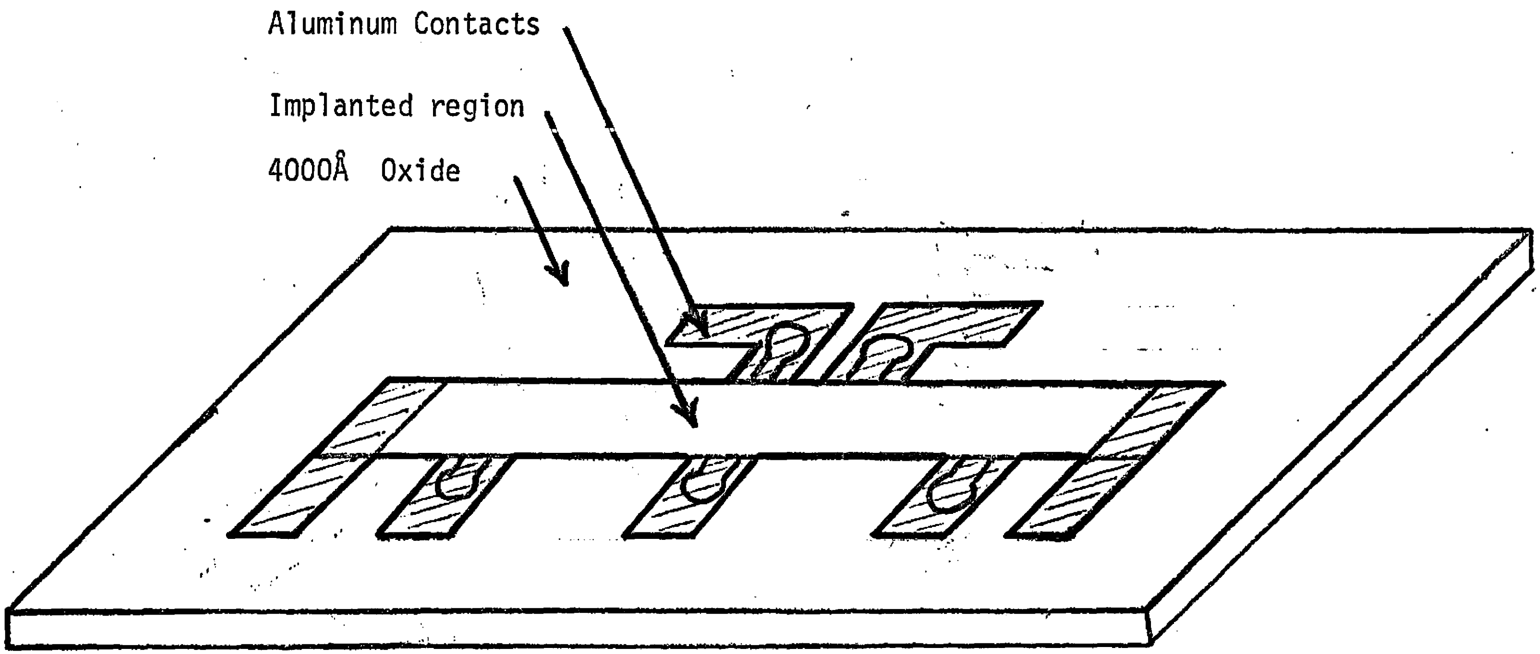

FIGURE 6: Hall Sample Configuration

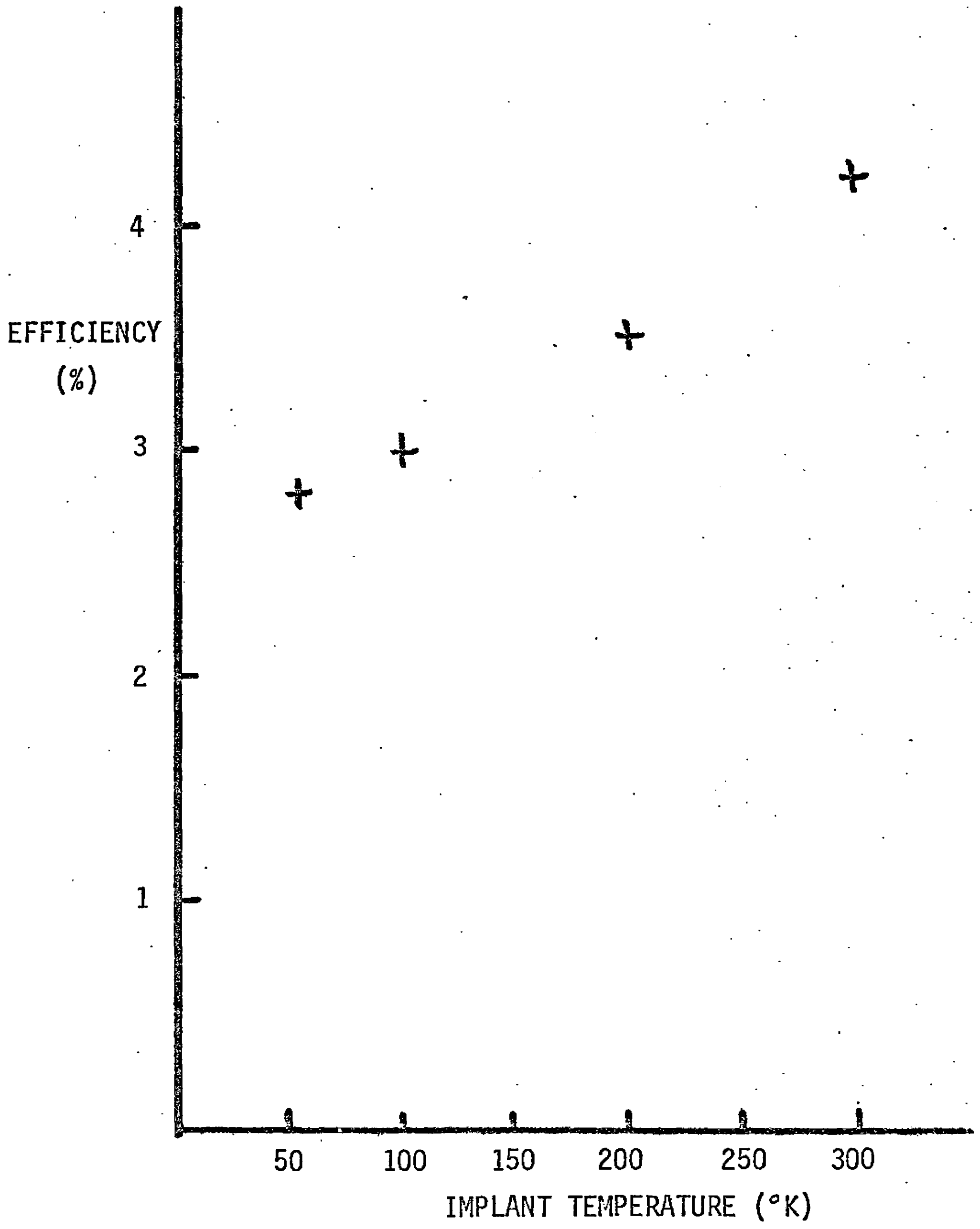

FIGURE 7: Efficiency vs Implant Temperature
80 keV arsenic in 10 ohm-cm silicon. Concentration 10^{20} cm^{-3}
Anneal temperature 800°C.

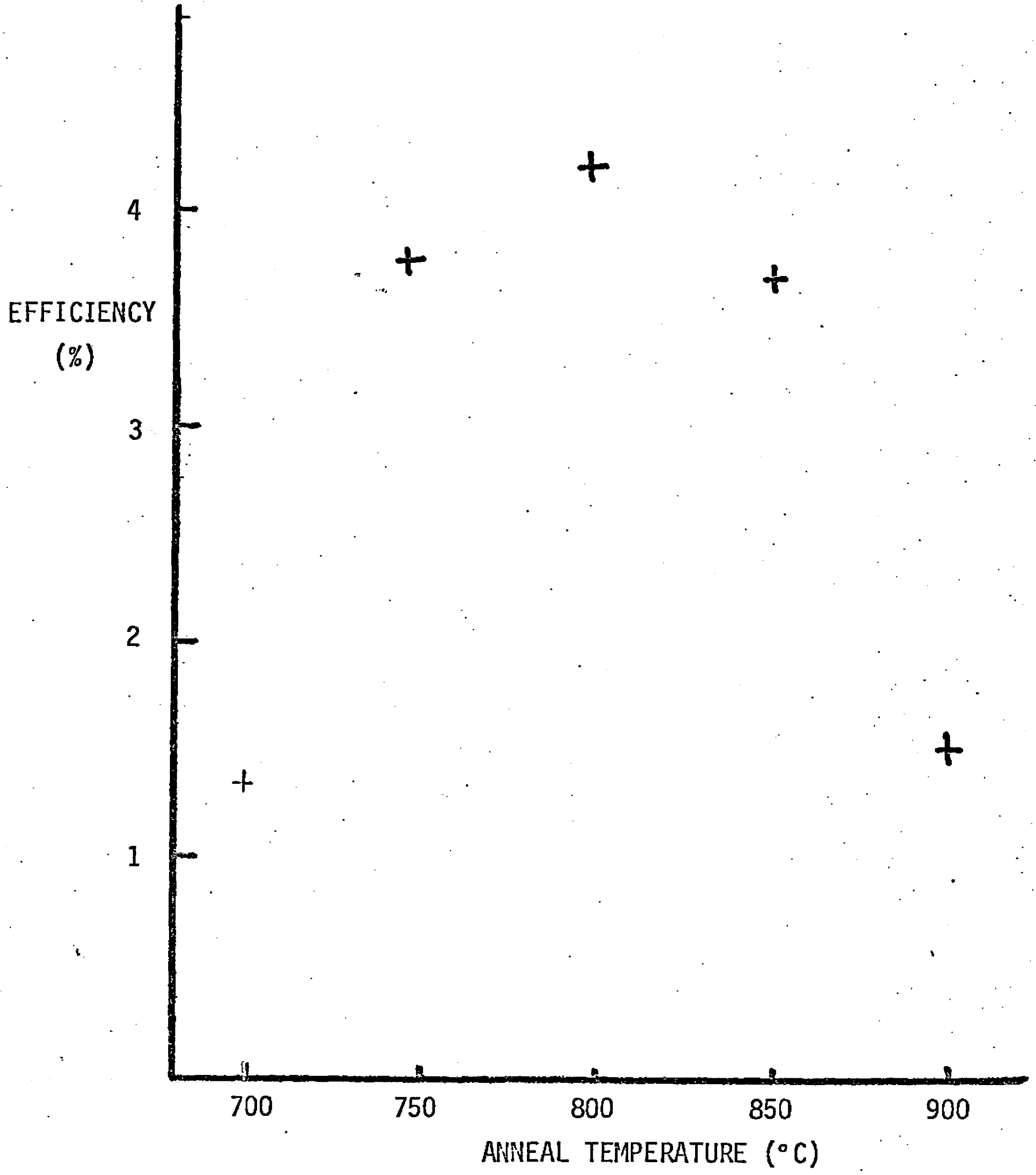

FIGURE 8: Efficiency vs Anneal Temperature
Cells as in 7. Implant temperature 20°C.

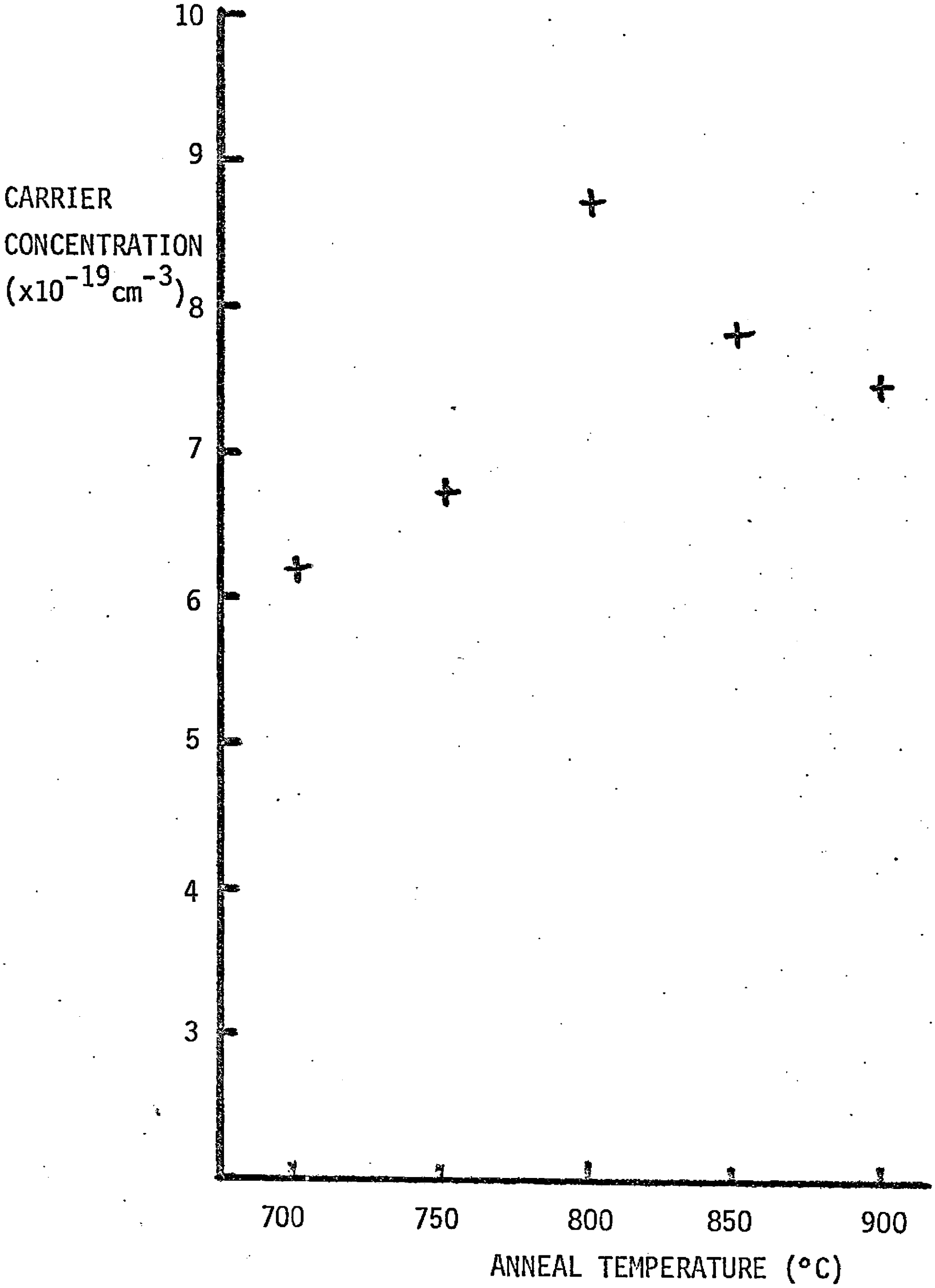

FIGURE 9: Carrier Concentration vs Anneal Temperature
80 keV arsenic in 10 ohm-cm silicon. Implant Temperature 20°C.

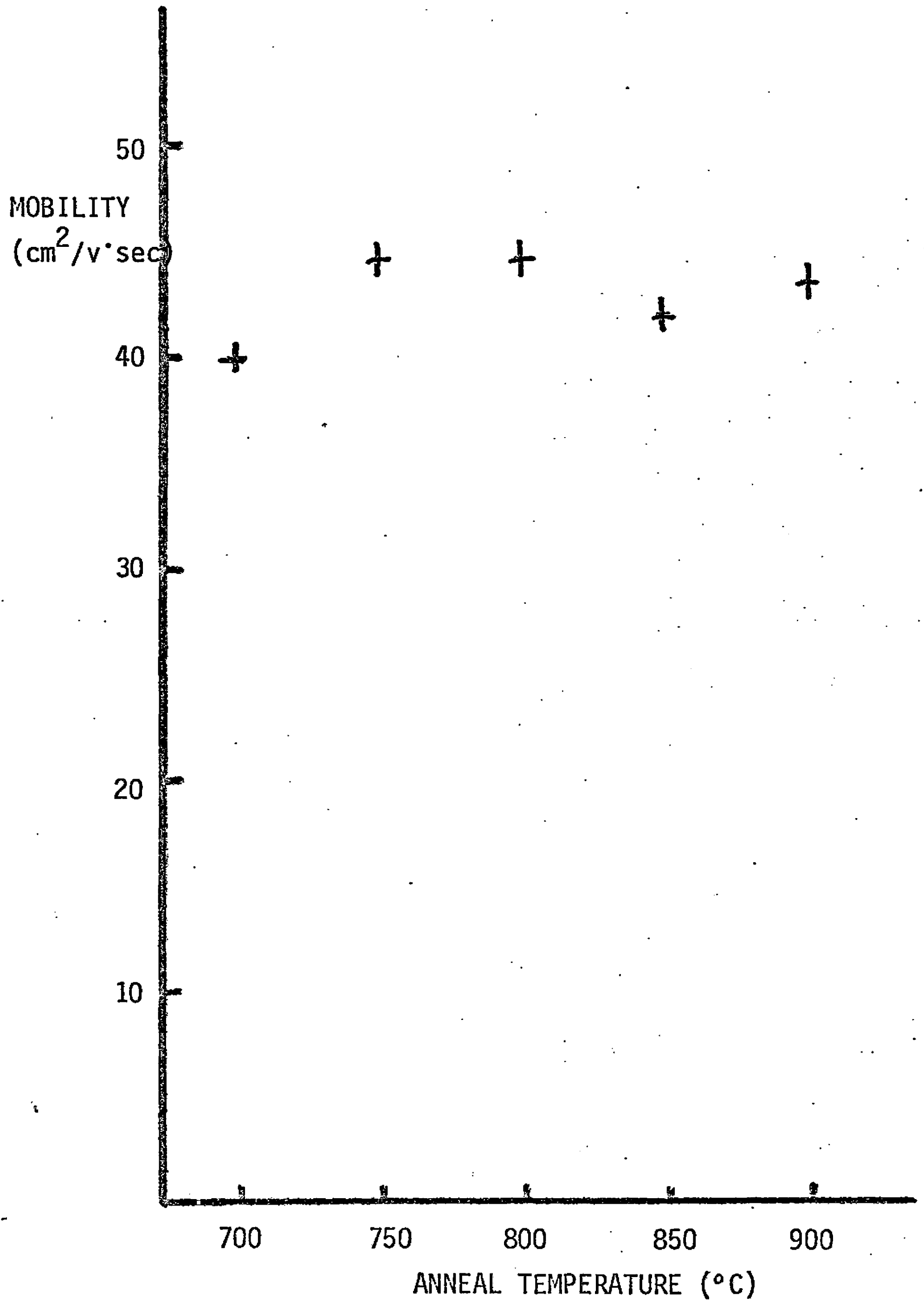

FIGURE 10: Mobility vs Anneal Temperature

Samples as in figure 9.

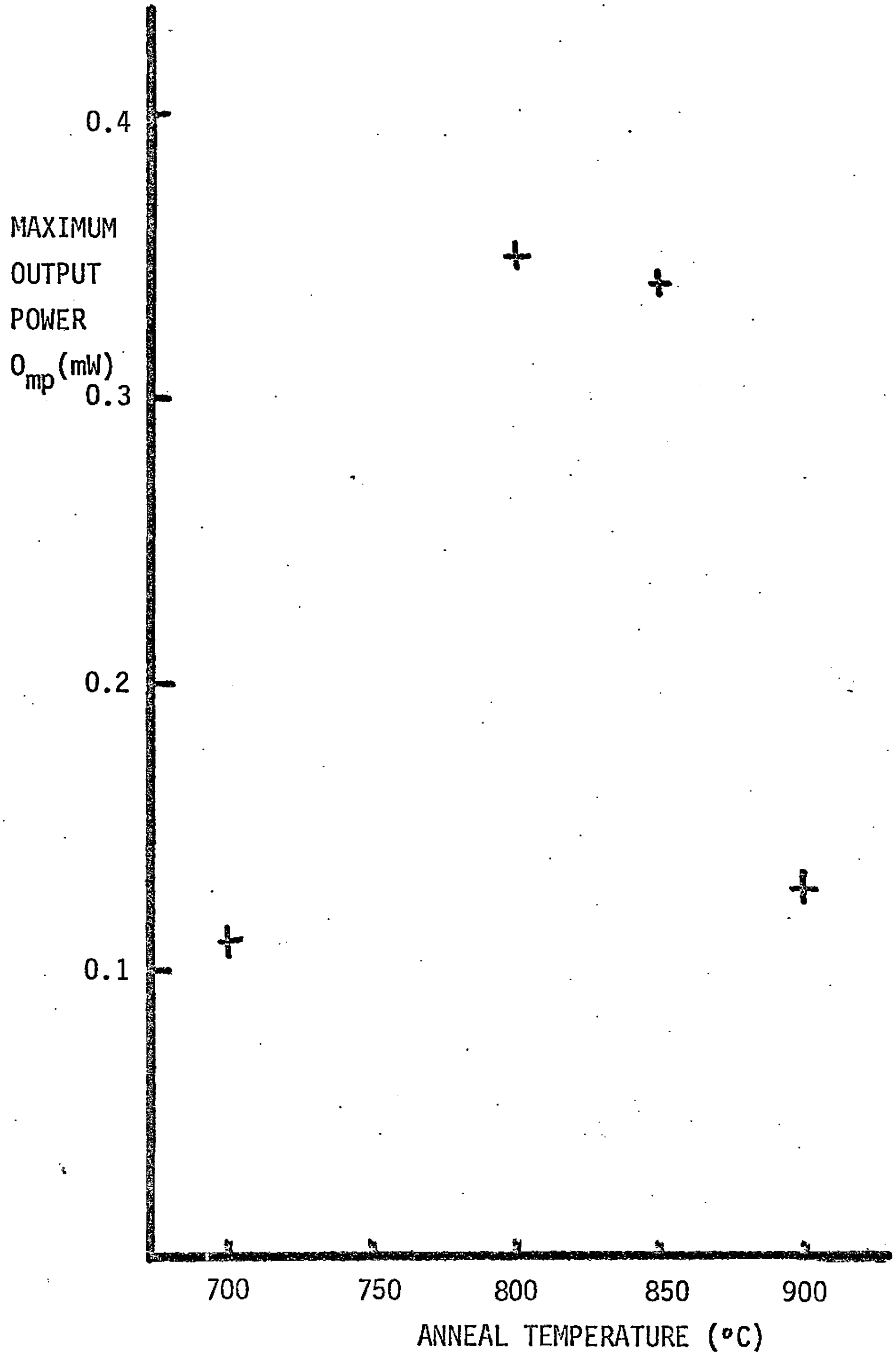

FIGURE 11: Hall Sample O_{mp} vs Anneal Temperature
Samples as in figure 9.

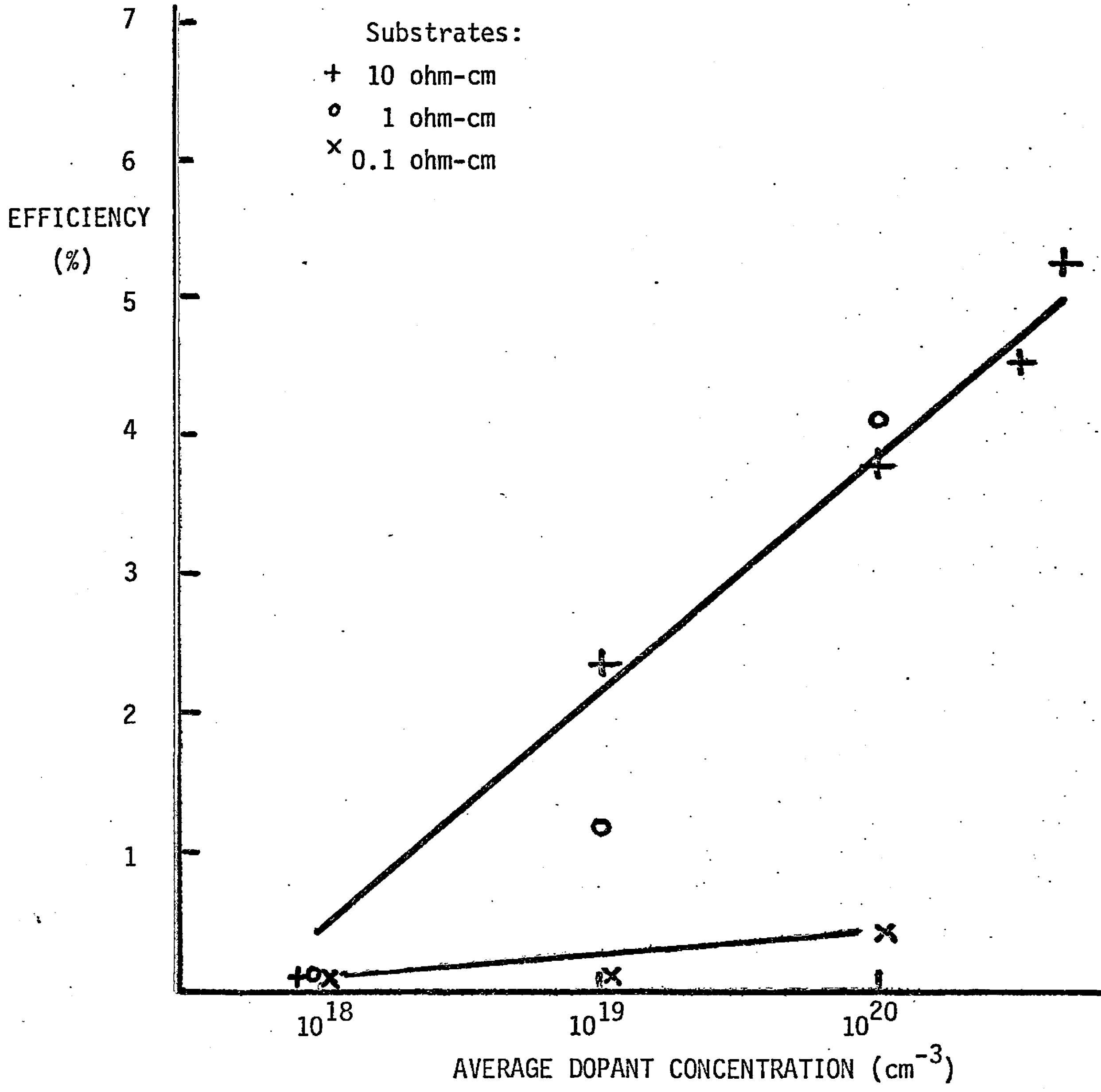

FIGURE 12: Efficiency vs Dopant Concentration
80 keV arsenic in silicon. Implant temperature 20°C.
Anneal temperature 800°C.

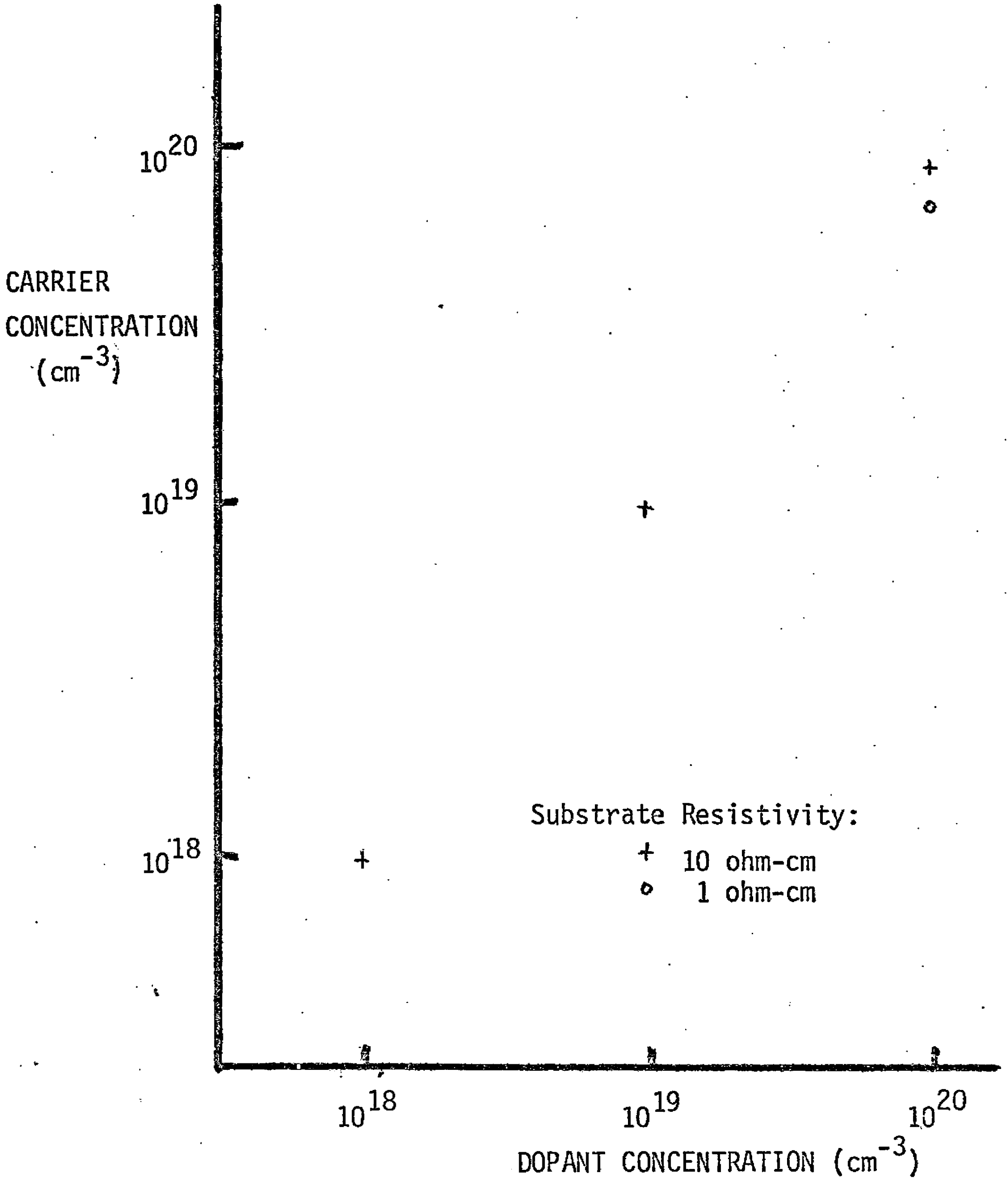

FIGURE 13: Carrier Concentration vs Dopant Concentration
Samples as in figure 12.

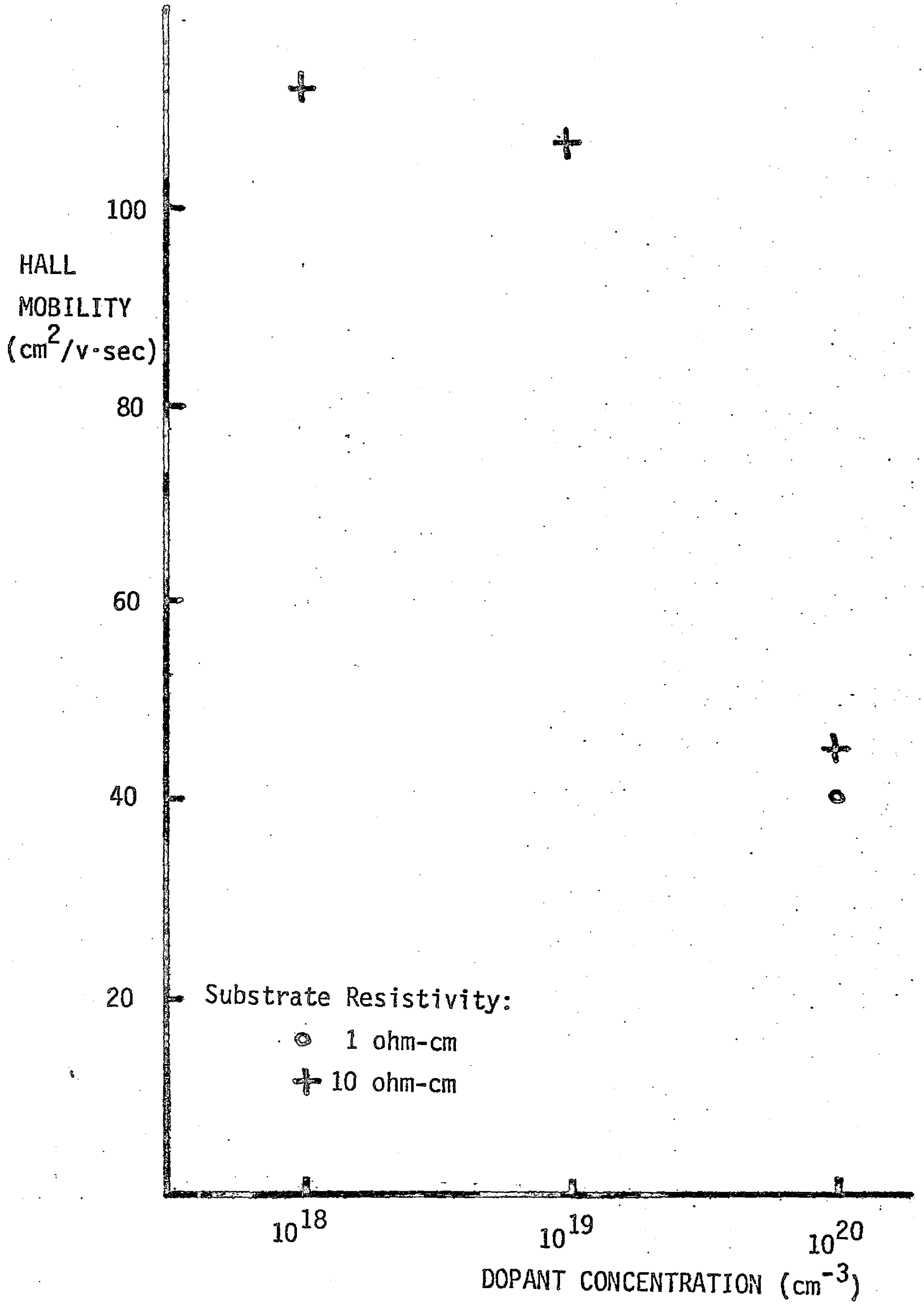

FIGURE 14: Hall Mobility vs Dopant Concentration 80 keV arsenic into silicon. Implant temperature 20°C. Anneal temperature 800°C.

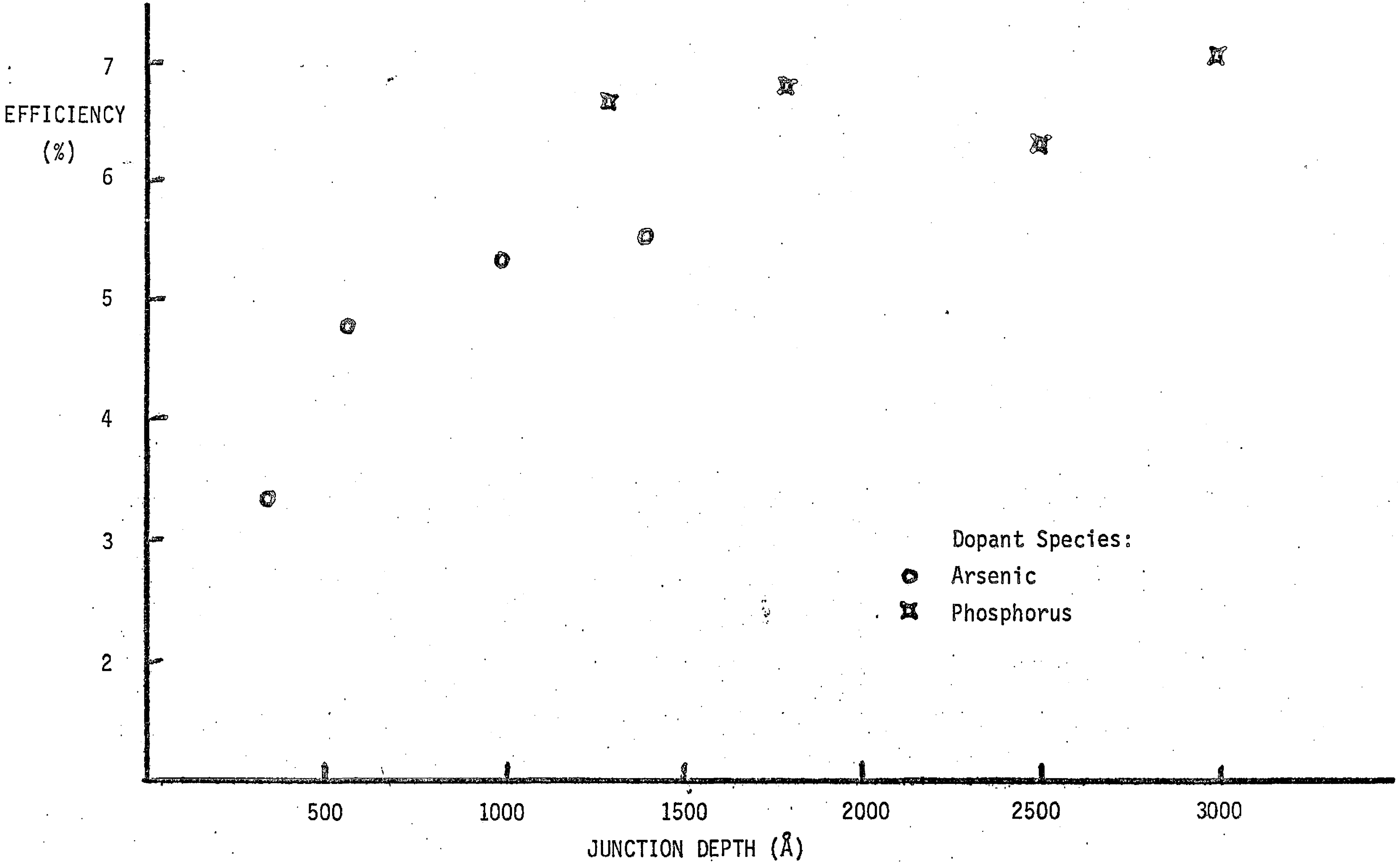

FIGURE 15: Efficiency vs Junction Depth

Dopant concentration 10^{20} cm^{-3}. Implant temperature 20°C. Anneal temperature 800°C. Substrate 10 ohm-cm silicon. Depths from Gibbons et al

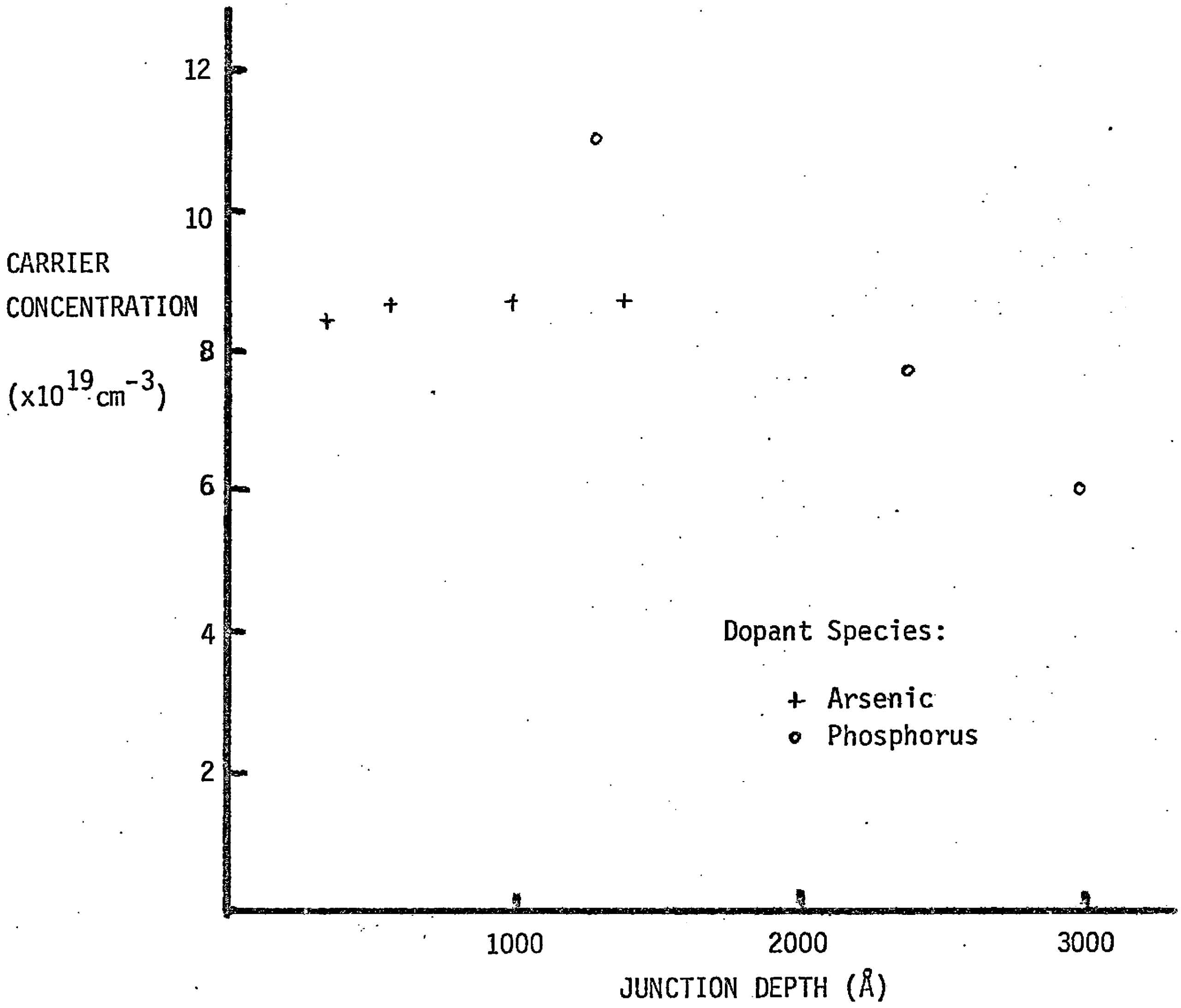

FIGURE 16 : Carrier Concentration vs Junction Depth
Substrate 10 ohm-cm silicon. Implant Temperature 20°C.
Anneal temperature 800°C. Depths from Gibbons et al

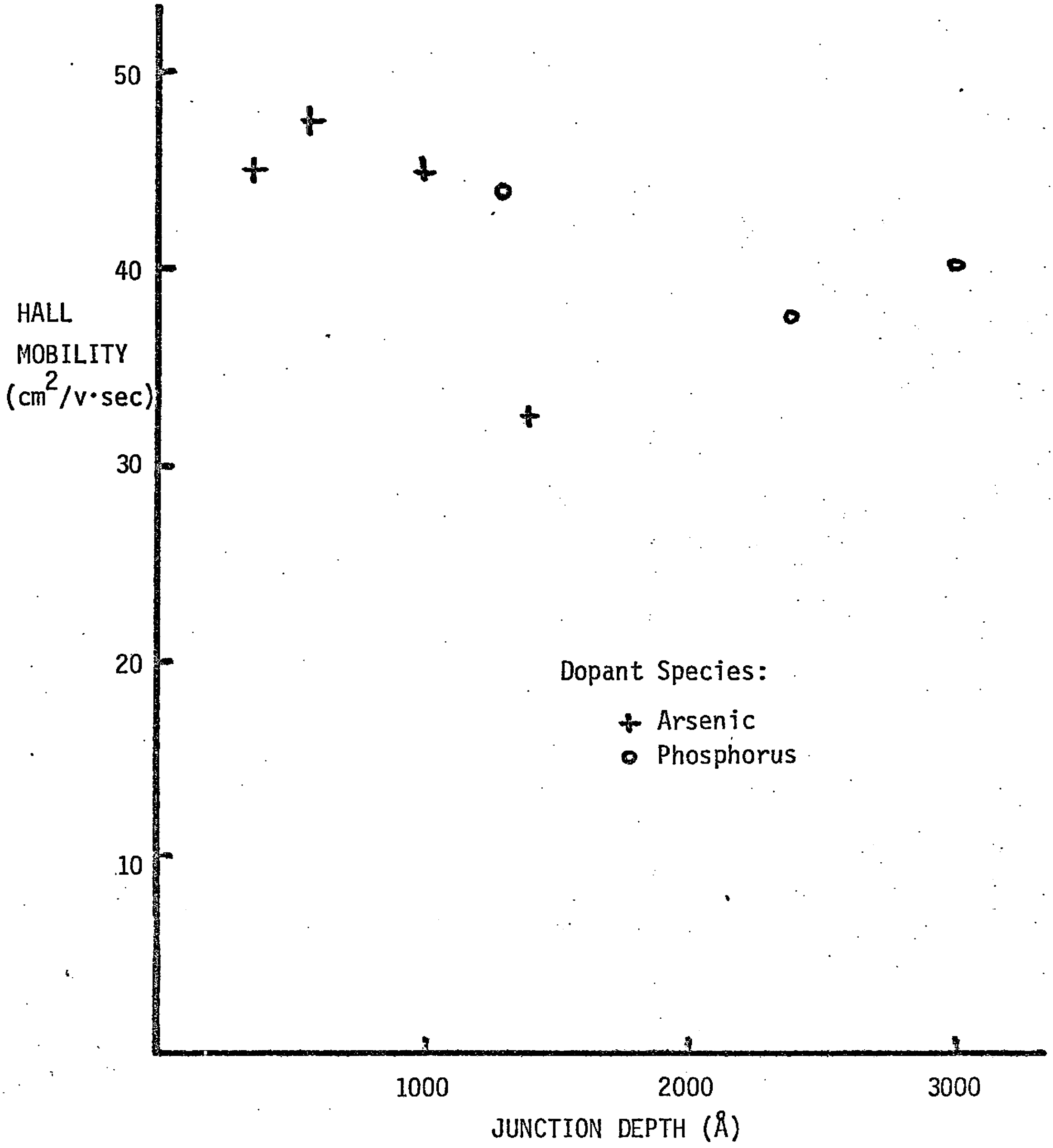

FIGURE 17: Hall Mobility vs Junction Depth

Samples as in figure 16.

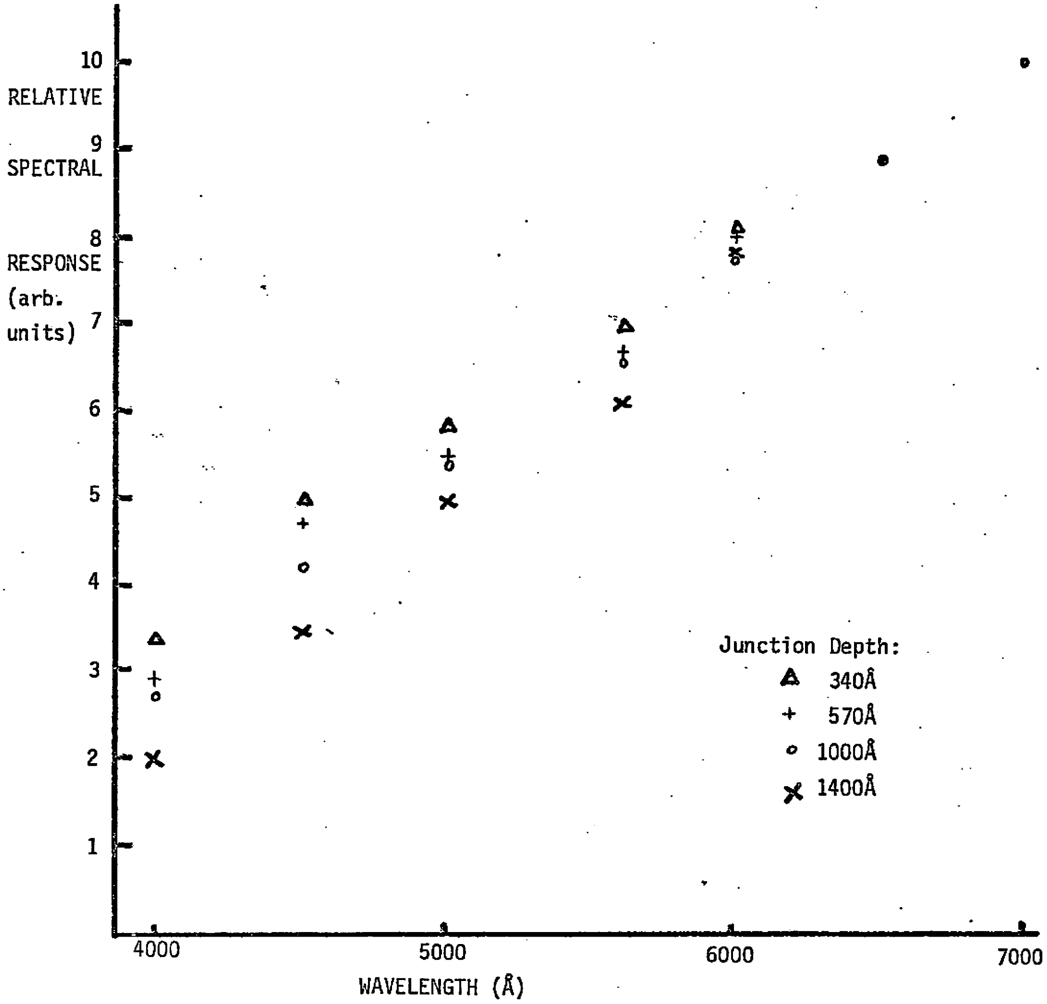

FIGURE 18: Spectral Response at Various Junction Depths
Concentration 10^{20} cm^{-3}; Arsenic in 10 ohm-cm silicon;
Implant temperature 20°C; Anneal temperature 800°C.
Depths from Gibbons et al(7).

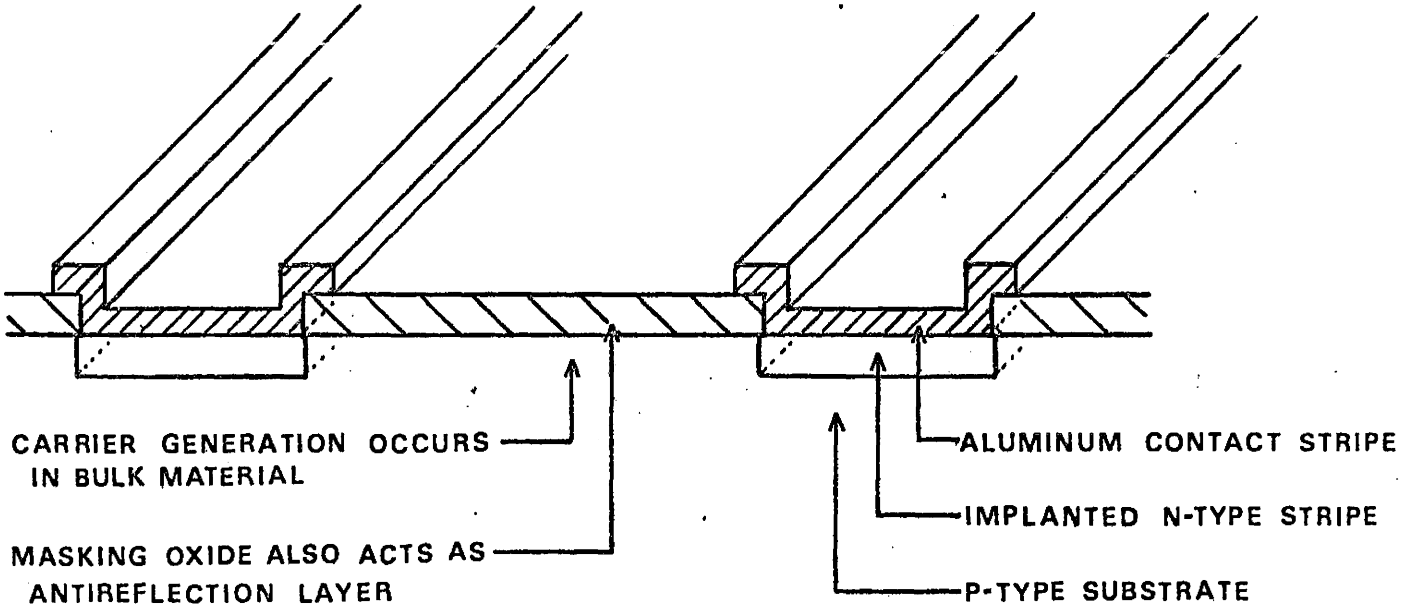

Figure 19: Proposed Grating Cell

APPENDIX I

Hall Effect Calculations and Program

It is assumed that the user has aquainted himself with the Hall Effect before attempting to use the automated system. If not, a brief report can be found in Sze(6), and a more complete discussion can be found in McKelvey(17) or Smith(18). As the program is written using only the simplified theory, that is all that is included here.

The basic setup is shown in Figure I-1 where an electric field is applied along the x-axis and a magnetic field along the z-axis. If the majority carriers are positive (i.e. p-type material), carrier motion due to the electric field will be in the -x direction. The Lorentz force ($q\vec{v}_x \times \vec{B}_z$) will exert a net downward force where the holes will collect until the charge separation on the y-axis sets up a field, $\vec{E}_y$, such that the electrostatic force exactly counters the Lorentz force. This is the Hall field given by:

$$E_y = (V_y/W) = R_H \, J_x \, B_z \qquad \text{I.1}$$

where R_H is the Hall coefficient given by:

$$R_H = r \, \frac{1}{q} \frac{p - b^2 n}{(p+bn)^2} \quad ; \; b \equiv \mu_n/\mu_p$$
$$; \; r \equiv \langle\tau^2\rangle/\langle\tau\rangle^2 \qquad \text{I.2}$$

where τ is the mean free time between carrier collisions. For simplicity, let $r = 1$.

From I.2, if n>>p,

$$R_H = r\left(\frac{-1}{qn}\right) \qquad \text{I.3}$$

and is p>>n,

$$R_H = r\left(\frac{+1}{qn}\right) \qquad \text{I.4}$$

When conductivity information is also available, as with the automated system, we also have, for n>>p:

$$\mu = \frac{\sigma}{qn} = |R_H\,\sigma| \qquad \text{I.5}$$

and for p>>n:

$$\mu_p = \frac{\sigma}{qp} = |R_H\,\sigma| \qquad \text{I.6}$$

The last four equations are the basis of the program. Restating these in terms of measurable quantities we have:

$$R_H = \frac{V_H t}{IB} \times 10^8 \qquad \text{I.7}$$

; V_H in volts
t in cm
I in Amps
B in Gauss
R_H in cm^3/Cb

$$n(\text{or } p) = \left|\frac{r}{qR_H}\right| \qquad \text{I.8}$$

; n(or p) in cm^{-3}

$$\sigma = \frac{I\ell}{V_c wt} \qquad \text{I.9}$$

; ℓ,w,t in cm
V_c in volts
σ in mho/cm

$$\mu_H = |R_H\,\sigma| \qquad \text{I.10}$$

; μ_H in cm^2/v.s

The following section contains a flowchart and parameter list for the program and is included here for completeness. For information regarding the use of the program see Appendix II.

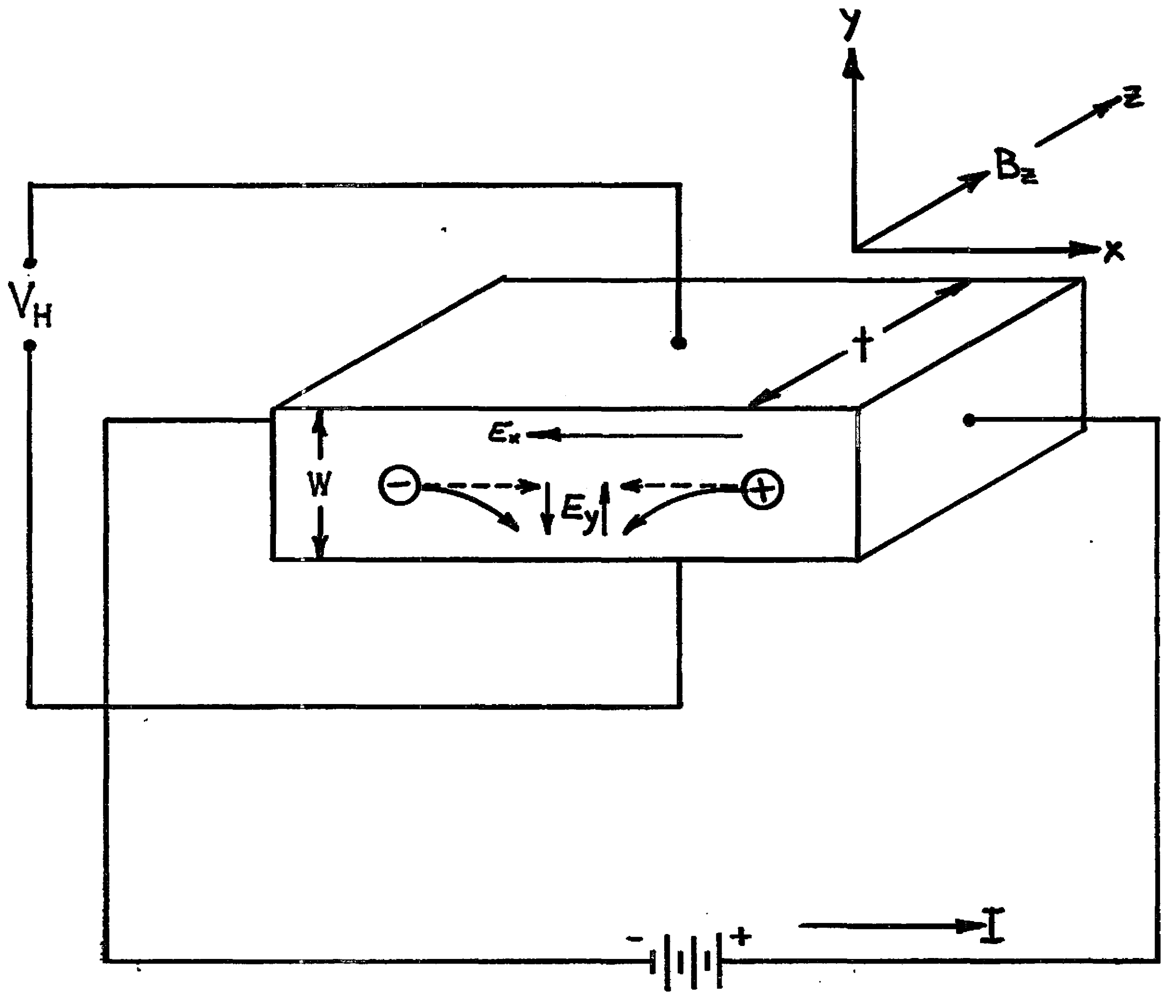

Figure I-1: Basic setup to measure the Hall Effect

Program Flow Chart*

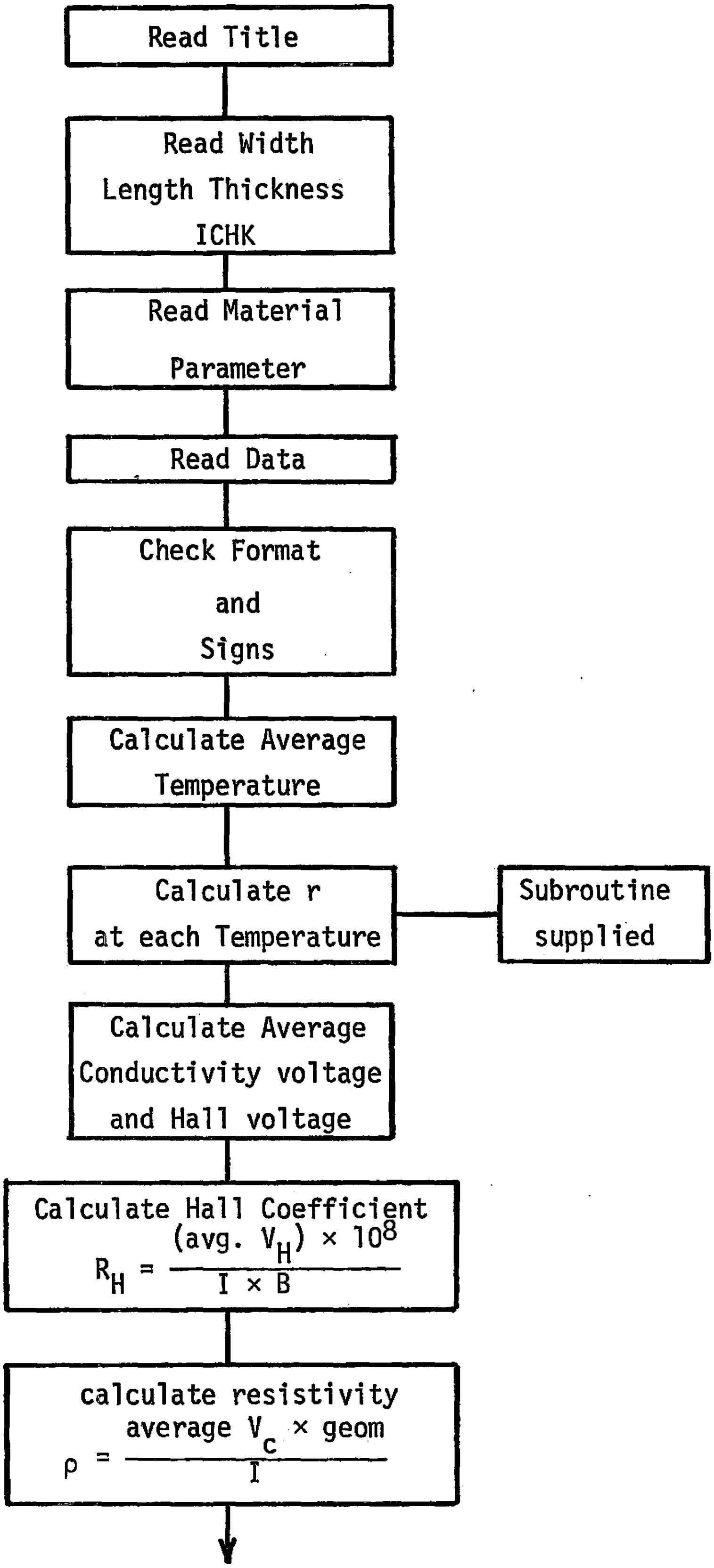

---

*Reference (19).

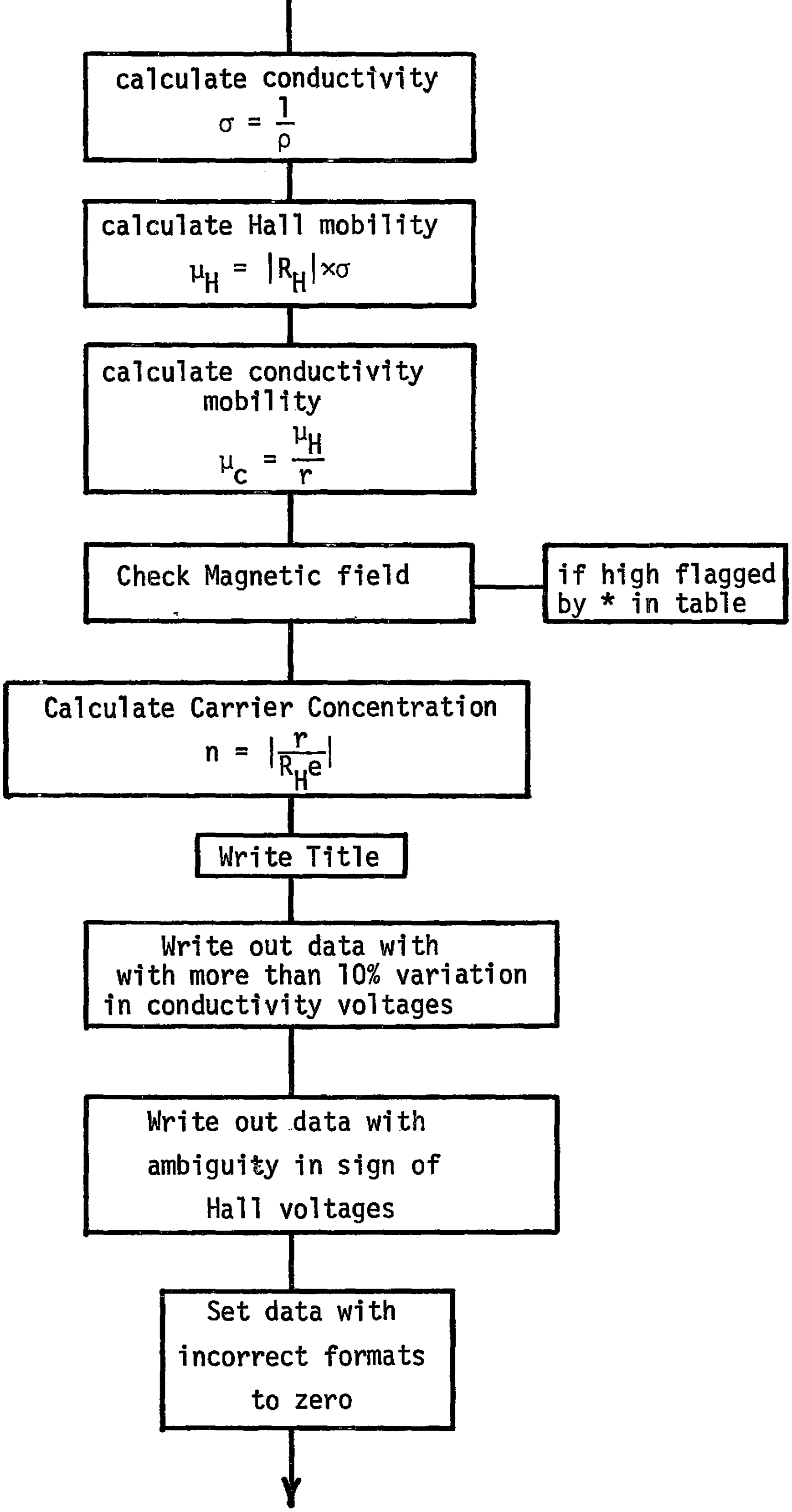
calculate conductivity
$\sigma = \frac{1}{\rho}$
calculate Hall mobility
$\mu_H = |R_H| \times \sigma$
calculate conductivity mobility
$\mu_c = \frac{\mu_H}{r}$
Check Magnetic field
if high flagged by * in table
Calculate Carrier Concentration
$n = |\frac{r}{R_H e}|$
Write Title
Write out data with with more than 10% variation in conductivity voltages
Write out data with ambiguity in sign of Hall voltages
Set data with incorrect formats to zero

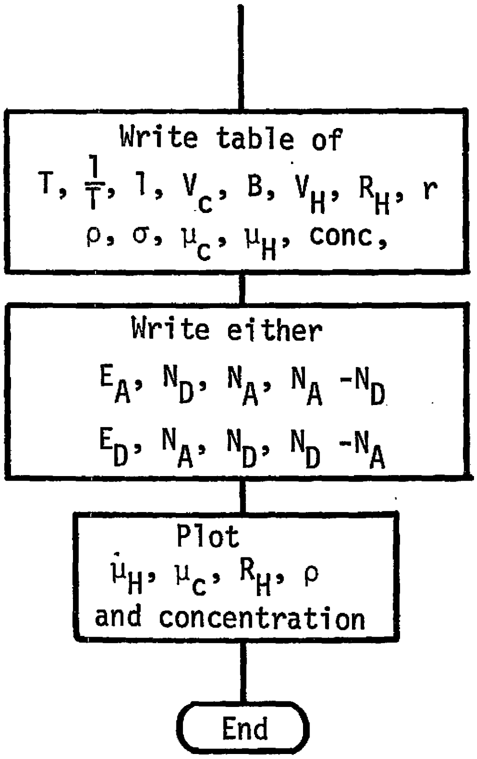
Write table of
T, $\frac{1}{T}$, I, V_c, B, V_H, R_H, r
ρ, σ, μ_c, μ_H, conc,
Write either
E_A, N_D, N_A, $N_A - N_D$
E_D, N_A, N_D, $N_D - N_A$
Plot
μ_H, μ_c, R_H, ρ
and concentration
End

PROGRAMME PARAMETER DEFINITIONS

AAA	array used in LESQ programme
AJIM	used in degeneracy check
ALHI	data point near RECLEE
ALLO	data point near RECLEE
ALNLEE	natural log of absolute value of compensation
ALNN	natural log of absolute value of carrier concentration
ALNX	ln $\|N_D-N_A\|$
AMOBCN	conductivity mobility of electrons in mixed conduction
AMOBCP	conductivity mobility of holes in mixed conduction
AN	electron concentration in mixed conduction
AP	hole concentration in mixed conduction
APETER	ln of normalized concentration
APNT	same as ALNN
AP1	parameters defined in Lee's paper
AP3	
AT	average temperature
AVC	average conductivity voltage
AVH	average hall voltage
B	magnetic field
BBB(1)	parameter of LESQ fit for ionization energy
BBB(2)	
COMPEN	compensated impurity density
CONC	concentration

CONCN	same as AN
CONCP	same as AP
COND	conductivity
DELTA	range in 1/T where ionization energy is determined
EFMASN	$\frac{m_e^*}{m_o}$ density of states effective mass
EFMASP	$\frac{m_h^*}{m_o}$ density of states effective mass
EGO	Ego
ENERGY	ionization energy in electron volts
ERLE	used in check on magnetic field
FLIM	ratio of two conductivity voltages
GAMMA	constant in intrinsic concentration
GEOM	(width x length)÷(thickness)
I	current
IEXP	current expressed as exponential
IVEX	same as VEX in integer form
LENGTH	conductivity length
MASS	either $\frac{m_e^*}{m_o}$ or $\frac{m_h^*}{m_o}$
MOBC	conductivity mobility
MOBH	Hall mobility
MOBRAT	$\mu H/\mu c$
MB	mobility
NP	number of data points used in LESQ for ionization energy

OVS	number of data points used in LESQ for determining Ego
R	scattering parameter (r)
RECHI	data point near RECLEE
RECIP	1/T
RECLEE	(1/TLEE)
RECLO	data point near RECLEE
RECMAX RECMIN	temperature range over which E_A or E_D is determined
RH	Hall coefficient
RHO	resistivity
RHOMAX	resistivity which corresponds to R_{max}
RMAX	maximum resistance that the Hall system can handle
RRECIP	same as RECIP
SLOPE	slope of ALNN with respect to RECIP
SS	see section on mixed conduction
T	temperature before averaging
THICK	thickness of sample
TLEE	temperatrue where LESQ straight line has a value ALNX
TMAX	1/RECMAX
TMIN	temperature that corresponds to RMAX
TRANS	array used for LESQ for Ego
TUK(1) TUK(2)	parameters of LESQ fit for Ego

VC	conductivity voltage
VEX	voltage read proportional to sample current
VGE	germanium thermometer voltage
VH	Hall voltage
WIDTH	width of sample

Information Necessary for Calculations

Card #1	Title [Format (13A6)]
Card #2	Width Length Thickness ICHK* [Format (3F 10.3, 50A1)]
Card #3	EFMASP, EFMASN, MOBRAT, RMAX, DELTA [Format (5E 10.3)]
Card #4	Name and Account [for plot heading]

DATA is entered in nonstandard format from the tape.

* ICHK if plots are desired write PLOT

if punched cards are desired write PUNCH

A subroutine exists to calculate the scattering parameter (r) at all temperatures. At present this subroutine assigns the value 1 to r at all temperatures. If a more complex dependence is required, a new subroutine must be written by the user.

ELECTRICAL PROPERTIES OF VARIOUS SEMICONDUCTORS

Semi-conductor	Energy gap, ev		Mobility,[a] cm^2/volt sec (T=300°K)		Mobility variation $\mu \alpha T^{-n}$		Band structure[b]	Effective mass m/m_o		Dielectric constant $\varepsilon/\varepsilon_o$	Refractive index
	300°K	0°K	Electrons	Holes	Electrons	Holes		Electrons	Holes		
Ge[c]	0.67	0.75	3,950 (3,900)[d]	3,400 (1,900)[d]	1.66	2.33	A	m_l=1.6 m_t=0.082	0.3, 0.4[e]	16	4.0
Si[c]	1.106	1.153	1,900 (1,350)[d]	425 (480)[d]	2.5	2.7	B	m_l=0.97 m_t=0.19	0.5, 0.16[e]	12	3.42
InSb	0.16	0.26	78,000	750	1.6	2.1	C	0.013	0.6	17	3.96
InAs	0.33	0.46	33,000	460	1.2	2.3	C	0.02	0.41	14.5	3.42
InP	1.29	1.34	4,600	150	2.0	2.4	C	0.07	0.4	14	3.26
GaSb	0.67	0.80	4,000	1,400	2.0	0.9	C	0.047	0.5	15	3.74
GaAs	1.39	1.58	8,500	400	1.0	2.1	C	0.072	0.5	12.5	3.30
GaP	2.24	2.40	110	75	1.5	1.5	B	.....	...	10	2.91
AlSb	1.63	1.75	200	420	...	1.8	Not C	.....	0.4	11	3.18
BP	2	....	.....	.....	...	...	Not C				

[a] The values of mobility are those obtained in the purest and most perfect material available to date. In most circumstances the actual mobilities are less than the value listed.

[b] A: germanium-like; conduction band minimum in <111> direction; valence band maximum at <000>.
B: silicon-like: conduction band minimum in <100> direction; valence band maximum at <000>.
C: GaAs-like: conduction band minimum at <000>; valence band maximum at <000>.
There are significant variations among the various semiconductors in details of the band structure beyond our A, B, C classification.

[c] E. M. Conwell, Properties of Silicon and Germanium, Proc. IRE, vol. 46, no. 6, June, 1958, has a fairly comprehensive discussion of the properties of silicon and germanium.

Calculated and experimental mobilities for III-V compounds at room temperature

Compound	Carrier	m^*/m_o	e_c^*/e	$\omega_1 \times 10^{13}$ (sec^{-1})	θ1 (°K)	Polar mobility (cm^2/V sec)	Observed mobility (cm^2/V sec)
InSb	Electron	0.013	0.13	3.5	260	200,000	78,000
	Hole	0.6				600	750
InAs	Electron	0.02	0.22	4.4	340	40,000	33,000
	Hole	0.41				500	460
InP	Electron	0.07	0.24	6.3	480	6,800	4,600
	Hole	0.4				500	150
GaSb	Electron	0.047	0.11	4.4	340	43,000	4,000
	Hole	0.5				1,200	1,400
GaAs	Electron	0.072	0.17	5.35	410	11,000	8,500
	Hole	0.5				600	400
AlSb	Hole	0.4	0.19	6.3	480	800	420

Scattering Mechanisms

Mechanism	$\mu \propto (m^*)^x T^y$		$\tau \propto E^z$	$R_H = -r/ne$
	x	y	z	r
Acoustic	-5/2	-3/2	-1/2	3π/8
Polar $T < \theta_1$	-3/2	Exponential	Independent	1.00 to 1.14
Ionized impurity	-1/2	3/2	~3/2	315π/512
Neutral impurity	1	Independent	Independent	1
Electron-hole	-1/2	3/2	~3/2	315π/512

C. Hilsum and A. C. Rose-Innes, "Semiconducting III-V Compounds" Pergamon Press, New York

APPENDIX II

The Automated Hall Effect Apparatus

The electrical characterizations done in this report were carried out using the automated Hall system in SSC 137. It has been fully reported on by Shewchun et al(10) regarding the nature of the system, but as yet, no "operator's manual" exists to aid beginners in the use of the machine. The purpose of this appendix is to provide enough information to act as a guide for anyone wishing to learn how to use the system.

First of all it should be noted that there exists a large green 3-ring binder containing detailed information on the construction of the controller and the dewar assembly which should be used as a reference in case of difficulty. Included there is a program listing, a brief photographic inventory, logic diagrams for the controller sequencer, and manufacturers leaflets and manuals for the various components including the vacuum system and the low temperature dewar. Also, data output is through the HP Coupler to a teletype which will probably have to be located and returned if the system has been down for any length of time. For assistance in this matter see the departmental technician (Mr. G. Leinweber) in BSB/B101.

The system is presently set up to accept samples in a slightly modified version of the standard six point Hall test bar configuration (Figure II-1). The double Hall voltage contacts on one side allow the user to remove the unwanted conductivity voltage contribution (due to misalignment of the contacts or film inhomogeneities) that tend to swamp the low Hall voltage of high carrier concentration samples. There are several sample preparation methods. An ultrasonic cutting head is available for cutting Hall bars from commercially available wafers, but the modified version is not yet available. In implanted samples, the junction formed by implanting into a substrate of opposite type is enough to isolate the bar. The author has also had experience with thin films and has found that evaporating through a suitable brass mask onto an insulating substrate is also quite acceptable. Sample size is variable, but the mounting area on the sample holder allows a maximum overall size of about 1 cm × 2 cm.

Using heat sink compound, and an insulator if necessary, the sample is mounted on the copper block at the end of a 1 meter rod that is inserted into the top of the dewar. Electrical connection to the metallized contacts on the sample is through the six pins and one extra wire found on the mounting block as in Figure II-2. The author has found that gold wire silver painted at both ends to pin and sample contact pad is quite sufficient provided the silver paint is allowed to dry thoroughly before evacuating the sample chamber.

When the sample is mounted, replace the copper and teflon shield over the sample and insert the assembly into the dewar making sure the O-ring at the top end of the assembly is securely in position in the dewar mouth. Reconnect the thermocouple jack to the small box at the right side of the equipment rack and submerge the reference thermocouple in liquid nitrogen. The sample chamber is evacuated by closing the bleed valve located on the rear wall behind the magnet power supply and switching on the rotary pump (#2 in Figure II-3). When the cable is reattached to the connector at the top of the mounting assembly, measurements can begin. The following is a step by step account of how to run the system. Thanks to Ara Kazandzian for his aid in compiling this.

Using The System To Measure Hall Effect At Room Temperature

1. Turn the water supply on for the magnet.
2. Start the magnet by pressing on "Norm" switch. Red "on" light along with "Norm" amber light will come on.
3. Adjust the current using "current adjust" knobs to desired current e.g. 10 amp. and turn on switch for the GAUSSMETER on the panel.
4. Turn DVM to MAN/EXT mode.
5. Set the interval to a desired time e.g. 4 minutes.
6. Turn the main power on "on the panel".
7. Turn the teletype to (external) left hand side "push on" teletype is ready, Note: let the tape punch on "Here is" for about 5 feet.
8. Switch to "auto" mode.
9. Push "start" button, by doing this. 26 sequential steps will be executed by the control unit.
10. Now the control unit takes over and it will automatically measure the VC_1, VH_1, TC_1, TG, I.
11. If the four Hall voltages appear to have a high condutivity component as in Figure I-4a, return to manual mode and cycle through to step 13. Set DVM to INT mode and zero the measured Hall voltage by use of the two potentiometers at the top of the mount assembly. Return DVM to MAN/EXT mode, and the controller

to semi-auto. The four Hall voltage should appear as in Figure I-4b. Goto step 8 and repeat.

12. At the end of the run switch teletype to "internal mode" push "here is" button and punch tape for 5 feet.
13. After the run is over the magnet will shut itself off.
14. Turn off water cooling supply.

Using The System to Measure Hall Effect at LN_2 Temperatures

Initial condition, sample is inside the sample chamber

1. Turn pump #2 on (located on the floor) make sure valve #6 (vent valve) is open and valve #5 closed. Fill cold trap for pump #2 with LN_2.
2. Turn mechanical pump #1 (located on the shelf) then open valve #3 and #12 to evacuate the vacuum chamber (make sure the air release valve for pump #1 is closed).
3. Turn on power switch located on thermocouple gauge panel.
4. Open vavle #1 to evacuate sampler chamber and also He vent, read TC_3 gauge on panel, pressure indicator will approach 1 micron.
5. Put LN_2 in the LN_2 fill of the Cryostat, wait for at least one hour to stabilize the temperature before starting the run.
6. Proceed as for Room Temperature measurement.

Using The System To Measure Hall Effect At Liquid He Temperatures

1. Cool down the Cryostat with LN_2 for at least one day following steps #1-4 on page #2.
2. Make sure valves #7, #13, #5, #4, #8, #14 are closed.
3. Open valves #1, #2, #3, until Gl gauge reads -30 psi.
4. Close valve #1, #2, #3.
5. Shut down mechanical pump #2.
6. Open He gas tank (next to the door) adjust pressure to 5 psi.
7. Open valve #4 then open valves #3, #2, #1 until Gl gauge reads +5 psi (this is an indication that He gas is filled).
8. Close He gas tank.

Transfer of liquid He

9. Contact technician in SSC/B141 regarding LHe dewar and He return.
10. Open valves #8, #2, #3 and flush to transfer tube with He gas.
11. Connect the outlet of valve #14 to liquid He transfer tube (a U shape tube with a valve) i.e. connect the valve to make sure valve #3 is closed.
12. Insert the transfer tube, one end in the LHe fill located on the Cyrostat, and other end in a liquid He tank which is obtained from room B141 S.S.C.
13. Note (ping pong ball will rise and fall down).
14. Wait until the ping pong ball falls down, then open valve #14, pressurize until G2 gauge reads 20 psi .

15. When the ping pong ball rises and falls down for the second time, the Cryostat will be full of liquid He, and the brass tube will be frozen at this point.
16. Take out the transfer tube and insert a rubber stopper on the He fill.
17. Defreeze the brass tube with hot air gun.
18. Close valve #2.
19. G1 gauge pressure should read about 5 psi.
20. Open throttle valve (c.c.w.) direction 70° - 80°. liquid. He flows through the sample chamber, and the sample is cooled down. The flowmeter will read (probably overscale). Wait for 10-15 minutes or more till -emperatures reaches 4.2°K.
21. To read the temperature, set DVM in (internal mode). DC mode trigger rate fast. The temperature at 4.2°K is -0.980mv in order to double check, switch the GE switch on control to upward position to read GE resistance 19.954 mv at 4.2K.
22. Close throttle valve.
23. Turn V_{VH} dial to 380 (3.8 on heater).
24. Open throttle valve to the 18th position relatively. The flow rate should be about 75 on the flowmeter (heavy ball is the reference point).
25. Wait for 10 minutes until temperature stabilizes.
26. Turn DVM to MAN/EXT mode.
27. Turn on the sample heater.

28. Set interval at 4 minutes for initial run, switch to 7 minutes after 30 runs (depends on how stable the temperature is).
29. Turn the teletype to (external) left hand side, push on button teletype will be read. Note: let the tapepunch punch on "here is" for about 5 feet.
30. Switch to "auto" mode.
31. Turn main power on.
32. Push "start" button.
33. Now the control takes over and it will automatically measure the VC_1 VH_1 TC_1 TG I.
34. At the end of the run, switch the teletype to "internal mode" and push "here is" button.
35. Check whether there is bubbling in the oil bubbler indicating the flow of He.
36. Check G1 gauge pressure.
37. Close valve #8. Note: insert last part of tape first and make a mark on the front side at the beginning.
38. At the end of the run, switch teletype to "internal mode". Push "here is" button and punch tape for 5 feet.
39. After the run is over, the magnet will shut itself off.
40. Let the magnet cool down, then turn off water cooling supply.

Note: TC wires are connected in such a way that it should read positive at room temperature.

To Take the Sample Out When Cryostat is Cold

1. Close valve #8 (this valve should be closed when there is no He bubble in the glass tube and no reading on G1 gauge.
2. Open He tank.
3. Open valves #4, #3, #2, and #1.
4. Release pressure by removing rubber stopper from He fill.
5. Take out the sample, put a rubber stopper in place.
6. Take out TC wire.
7. Close valve #4 then pump down again.

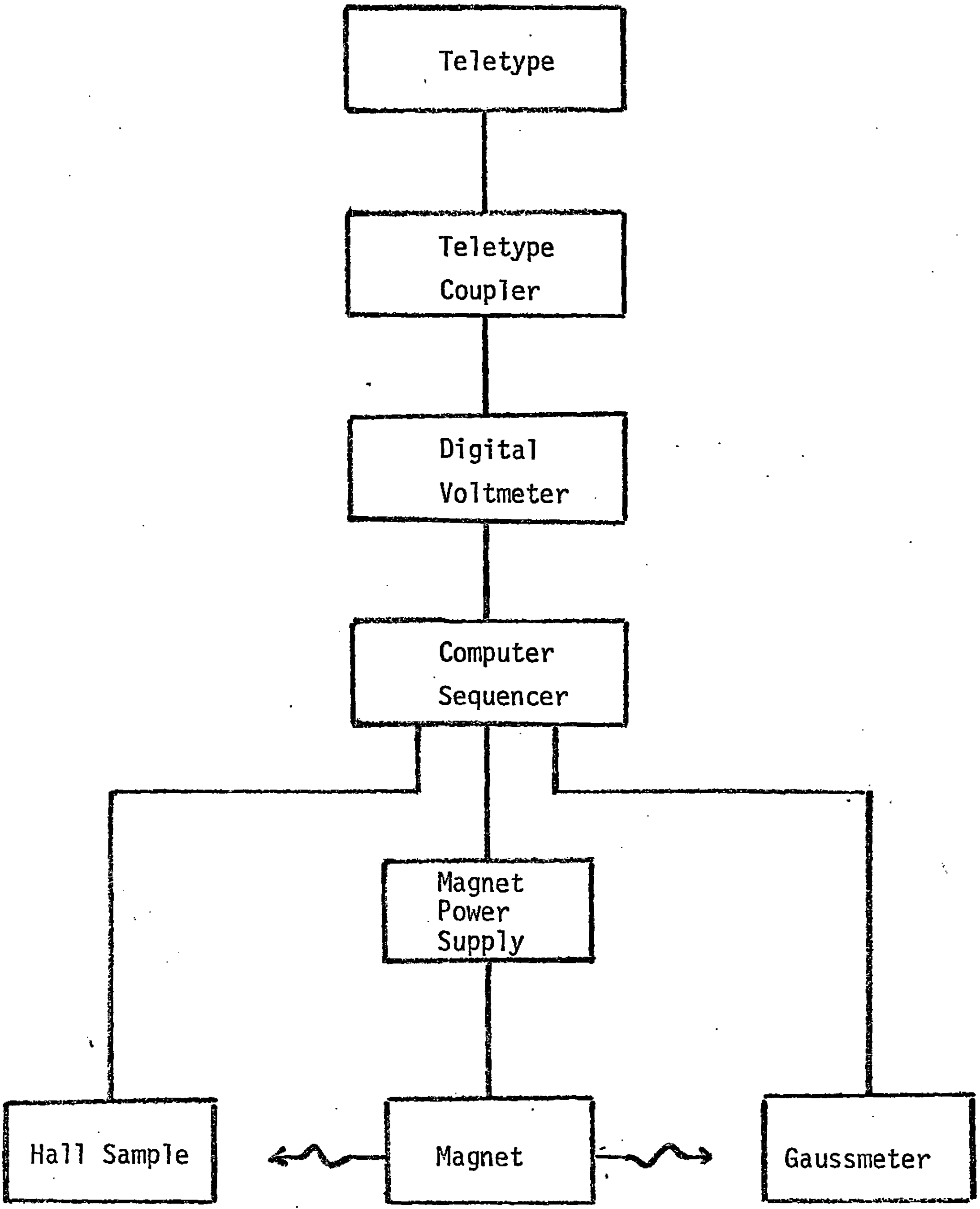

Hall Measurement System

STEP	EVENT
1	Select sample current indicator
2	Record sample current
3	Select sample thermometry
4	Record sample temperature
5	Select conductivity contacts
6	Record V_c (I^+)
7	Reverse sample current
8	Record V_c (I^-)
9	Turn on magnet, select gaussmeter contacts
10	Record magnetic field (B^+)
11	Reverse sample current, select thermometry
12	Record sample temperature
13	Select Hall voltage contacts
14	Record V_h (I^+,B^+)
15	Reverse sample current (I^-)
16	Record V_h (I^-,B^+)
17	Shut down magnet
18	Turn on magnet with reversed field, reverse sample current (I^+)
19	Select Hall voltage contacts
20	Record V_h (I^+,B^-)
21	Reverse sample current (I^-)
22	Record V_h (I^-,B^-)
23	Shut down magnet
24	Select thermometry
25	Record sample temperature
26	Adjust sample current. Wait 0 to 20 minutes.

Hall System Step Sequence

Data Format

The printed output should appear as in Figure II-4, with 12 numbers (1 line of 5, 1 line of 7) in the format ± XXXXXXP. The voltages (V_{GE},V_{TC},V_C,V_H) are interpreted as XXXXXX * 10^{-P} volts, (e.g. +0002216 becomes +221 * 10^{-6} volts). The current range, I, (second datum) is decoded as:

$$\log_{10} I = \left(\frac{XXXXXX * 10^{6-P}}{10^{+4}}\right) - 9$$

where the quotient on the left side of the equation is truncated to the nearest integer. For example, if the second datum is +0377516, the current is I = 10^{-6} amp.

The magnetic field, B, (first datum of the second line) is decoded as:

$$B = \pm\ XXXXXX * 10^{4-P} \text{ Gauss.}$$

For example, if the sixth datum is +0825195, then the field is B = 8.2519 kG.

Sample Calculation

To clarify the principles and methods involved in handling the system output, a sample calculation is given. The data set of Figure II-4-b is used in this example. From the first data set:

$$V_{TC} = \frac{1}{3}\,(3979 + 3975 + 3979) \times 10^{-6} = 3978\mu v$$

This corresponds to a temperature of about 300°K.

$$I = 10^{(3-9)} = 10^{-6} \text{ Amp}$$

$$V_c = \frac{1}{2} (V_c(I^+) - V_c(I^-))$$

$$= \frac{1}{2} (.096119 + .096321) = .09622 \text{ volt}$$

$$B = 78653 \times 10^{4-5} = 7865.3 \text{ Gauss}$$

$$V_H = \frac{1}{4} (V_H(I^+B^+) - V_H(I^-B^+) - V_H(I^+B^-) + V_H(I^-B^-))$$

$$= \frac{1}{4} (123 - 96 - 127 + 110) \times 10^{-6} = 2.5 \mu v$$

It should be noted here that the sign of the Hall voltage is the reverse of what it should be due to an idiosyncrasy of the machine. This is indicated here by a positive Hall voltage for an n-type (CdS) film.

Sample dimensions are:

ℓ = .5 cm

w = .2 cm

t = .0014 cm

Therefore, using the equations of the previous Appendix:

$$R_H = \frac{V_H t}{IB} \times 10^8 \text{ cm}^3/\text{Cb}$$

$$= \frac{(2.5 \times 10^{-6})(.0014)}{(10^{-6})(7.9 \times 10^3)} \times 10^8 = \underline{44 \text{ cm}^3/\text{Cb}}$$

$$n = \frac{1}{q} R_H \ \text{cm}^{-3}$$

$$= 1 \ / \ [1.602 \times 10^{-19} \times 44] = \underline{1.4 \times 10^{17} \ \text{cm}^{-3}}$$

$$\sigma = \frac{I}{V_c} \times \left(\frac{\ell}{wt}\right) \ \text{mho/cm}$$

$$= \frac{10^{-6}}{.096} \times \left(\frac{.5}{.2 \times .0014}\right) = \underline{.019 \ \text{mho/cm}}$$

$$\mu_H = |R_H \sigma| \ \text{cm}^2/\text{v.s}$$

$$= 44 \times .019 = \underline{.82 \ \text{cm}^2/\text{v.s}}$$

Data Evaluation Using CDC 6400

If the system output has been put on tape (with 5 ft. of blank tape before and after data) the calculations of the previous section can be done on the computer using two available fortran decks.

The first, called CONVT, is used to convert the data on tape to cards. It also edits the data to a degree, but this feature is more of an annoyance than a benefit, asit is very sensitive to teletype errors and will simply reject a data set, not correct it. To use this routine, the tape should be wound on a spool (as in Figure II-5) available from the computing centre. The tape spool and program, with control cards as in Figure II-6, are then submitted together and result in an output as in Figure II-7 and a punched data deck.

When the first two labelling cards and the end-of-record cards at the end of the data deck are removed, four data introduction cards should be added to the front and two blank cards at the end as indicated by CONVT. The data is now ready for the Hall evaluation program.

There are two versions of the Hall program available. HALL1, the lengthier version, includes coding to drive the Benson-Lehner Plotting system for publishable output, but HALL2, which produces a printer plot, is faster and more portable, particularly in its binary form. To use the HALL program, simply attach the data deck to the rear of the program between the last end-of-record and the end-of-file cards. Typical output is shown in Figure II-8.

Conclusions

While the system in its present form greatly simplifies the electrical evaluation of semiconductor materials, many improvements can yet be made. As indicated in the previous Appendix the calculations required in the data evaluation are elementary and do not require the large computing facilities of the CDC 6400. A more practical approach would be to use a small programmable calculator on line to evaluate the data real time, thereby entirely bypassing the teletype, tape, and program running time. This concept has already been discussed with the departmental technician (Mr. G. Leinweber) but work has not yet begun on this project.

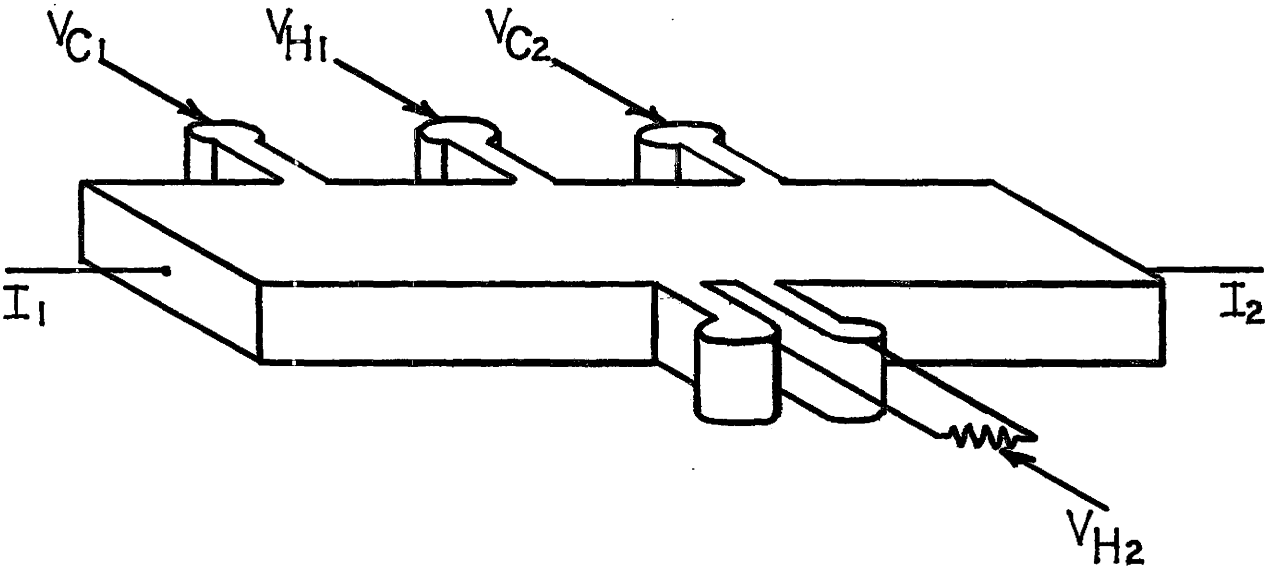

Figure II-1: Modified Hall Sample.

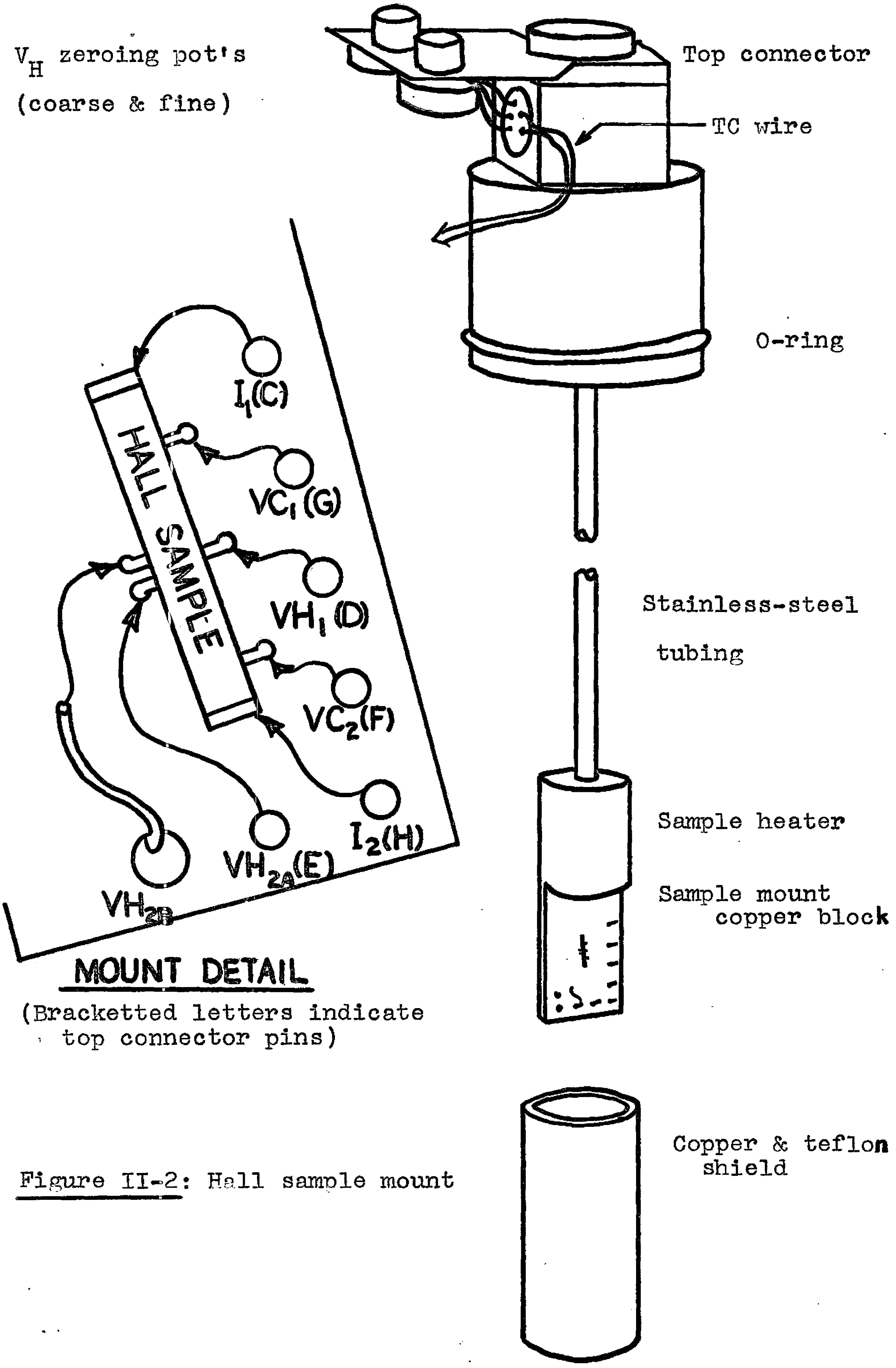

Figure II-2: Hall sample mount

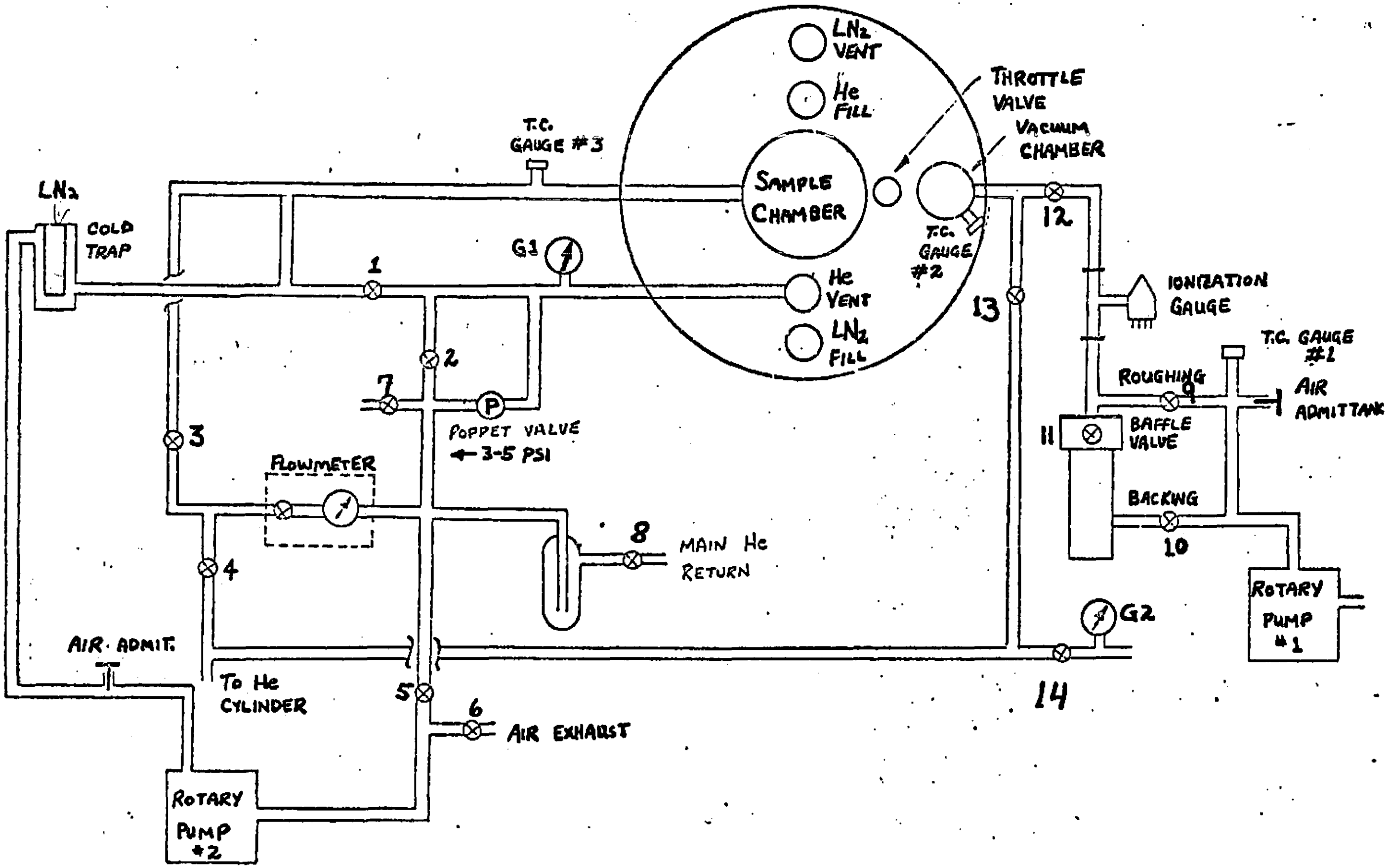

Figure II-3: Hall System Dewar Plumbing.

```
+0001096 +0557646 +0039236 +0715236 -0716436
+0826955 +0039206 +0013106 -0013116 +0019136 -0019066 +0039236
+0001106 +0557686 +0039246 +0714976 -0716236
+0826685 +0039206 +0013106 -0013086 +0019076 -0019116 +0039236
+0001096 +0557606 +0039226 +0714726 -0715996
+0826995 +0039186 +0013106 -0013106 +0019126 -0019076 +0039186
```

Figure II-4-a: System output showing high V_C contribution to V_H.

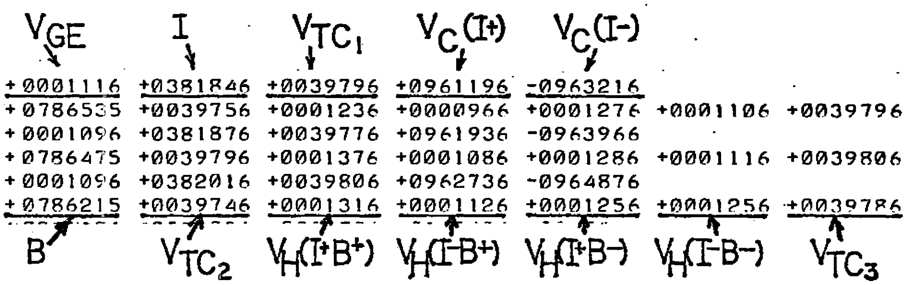

```
+0001116 +0381846 +0039796 +0961196 -0963216
+0786535 +0039756 +0001236 +0000966 +0001276 +0001106 +0039796
+0001096 +0381876 +0039776 +0961936 -0963966
+0786475 +0039796 +0001376 +0001086 +0001286 +0001116 +0039806
+0001096 +0382016 +0039806 +0962736 -0964876
+0786215 +0039746 +0001316 +0001126 +0001256 +0001256 +0039786
```

Figure II-4-b: System output with V_C component of V_H reduced.

(NOTE: Different samples were used

for a. and b.)

Figure II-4: Data format

#1... Have at least 6 ft. of leader on each end of the tape.

#2... Place the tape on the spool as follows:

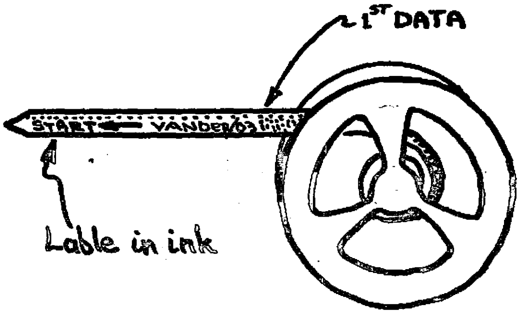

#3... Lable the tape with:

a) START

b) Arrow indicating direction of tape travel

c) Name

d) Reel number

eg:

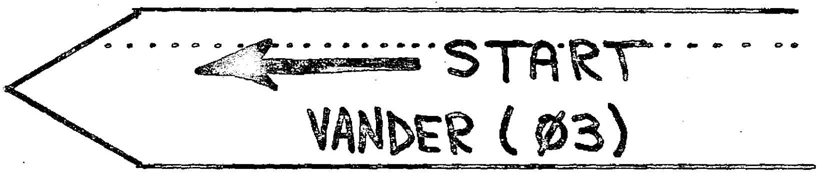

#4... Use Request card (immediately after JOB card)

REQUEST(TAPE1,TR,RTL1)   SPOOL/VANDER(03)

Figure II-5 : Paper tape use

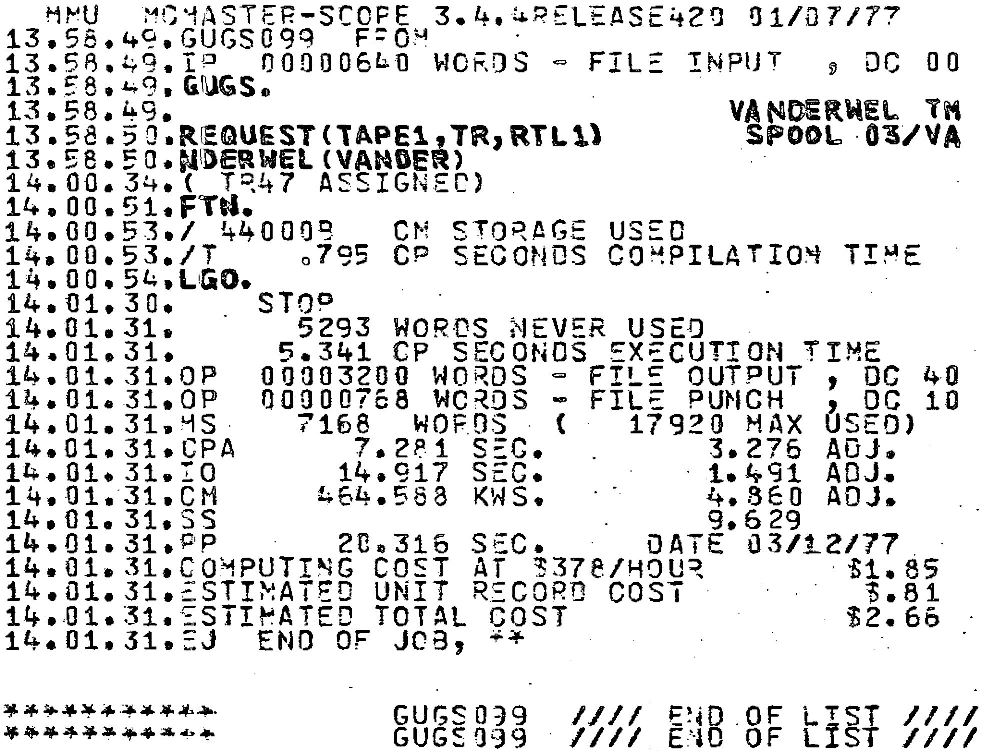

```
  MMU   MCMASTER-SCOPE 3.4.4RELEASE420 01/07/77
13.58.49.GUGS099  FROM
13.58.49.IP  00000640 WORDS - FILE INPUT   , DC 00
13.58.49.GUGS.
13.58.49.                                 VANDERWEL TM
13.58.50.REQUEST(TAPE1,TR,RTL1)            SPOOL 03/VA
13.58.50.NDERWEL(VANDER)
14.00.34.( TR47 ASSIGNED)
14.00.51.FTN.
14.00.53./ 44000B   CM STORAGE USED
14.00.53./T     .795 CP SECONDS COMPILATION TIME
14.00.54.LGO.
14.01.30.     STOP
14.01.31.        5293 WORDS NEVER USED
14.01.31.       5.341 CP SECONDS EXECUTION TIME
14.01.31.OP   00003200 WORDS - FILE OUTPUT , DC 40
14.01.31.OP   00000768 WORDS - FILE PUNCH  , DC 10
14.01.31.MS     7168  WORDS  (   17920 MAX USED)
14.01.31.CPA        7.281 SEC.          3.276 ADJ.
14.01.31.IO        14.917 SEC.          1.491 ADJ.
14.01.31.CM       464.588 KWS.          4.860 ADJ.
14.01.31.SS                             9.629
14.01.31.PP        20.316 SEC.     DATE 03/12/77
14.01.31.COMPUTING COST AT $378/HOUR         $1.85
14.01.31.ESTIMATED UNIT RECORD COST           $.81
14.01.31.ESTIMATED TOTAL COST                $2.66
14.01.31.EJ  END OF JOB, **

***********           GUGS099  //// END OF LIST ////
***********           GUGS099  //// END OF LIST ////
```

Figure II-6: Dayfile for program CONVT showing control cards used.

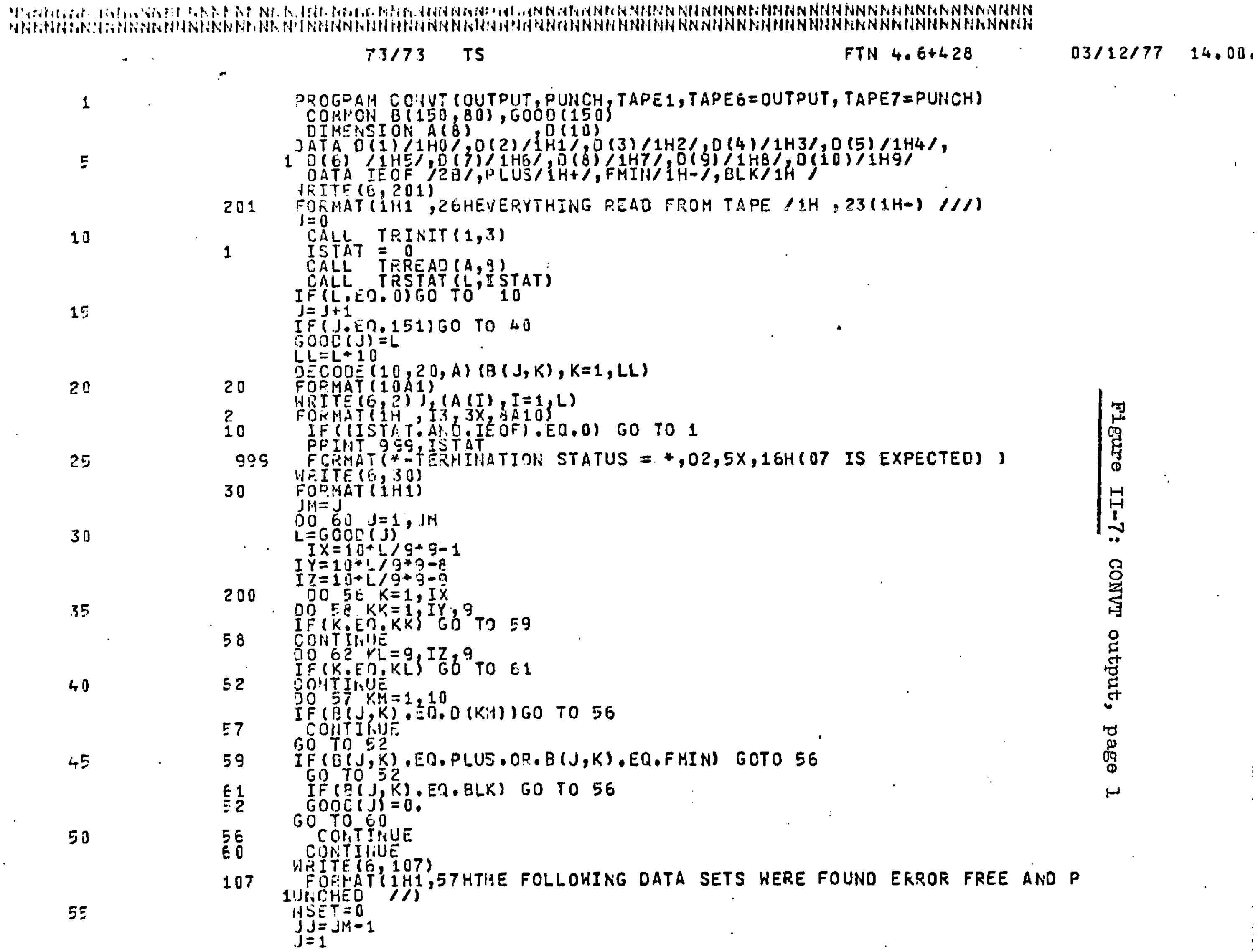

```
                 73/73    TS                              FTN 4.6+428         03/12/77  14.00.

                PROGPAM CONVT(OUTPUT,PUNCH,TAPE1,TAPE6=OUTPUT,TAPE7=PUNCH)
                 COMMON B(150,80),GOOD(150)
                 DIMENSION A(8)      ,D(10)
                DATA D(1)/1H0/,D(2)/1H1/,D(3)/1H2/,D(4)/1H3/,D(5)/1H4/,
               1 D(6) /1H5/,D(7)/1H6/,D(8)/1H7/,D(9)/1H8/,D(10)/1H9/
                 DATA IEOF /2B/,PLUS/1H+/,FMIN/1H-/,BLK/1H /
                WRITE(6,201)
        201     FORMAT(1H1 ,26HEVERYTHING READ FROM TAPE /1H ,23(1H-) ///)
                J=0
                 CALL  TRINIT(1,3)
        1        ISTAT = 0
                 CALL  TRREAD(A,8)
                 CALL  TRSTAT(L,ISTAT)
                IF(L.EQ.0)GO TO  10
                J=J+1
                IF(J.EQ.151)GO TO 40
                GOOD(J)=L
                LL=L+10
                DECODE(10,20,A)(B(J,K),K=1,LL)
        20      FORMAT(10A1)
                WRITE(6,2) J,(A(I),I=1,L)
        2       FORMAT(1H ,I3,3X,8A10)
        10       IF((ISTAT.AND.IEOF).EQ.0) GO TO 1
                 PRINT 999,ISTAT
         999     FORMAT(*-TERMINATION STATUS = *,O2,5X,16H(07 IS EXPECTED) )
                WRITE(6,30)
        30      FORMAT(1H1)
                JM=J
                DO 60 J=1,JM
                L=GOOD(J)
                 IX=10*L/9*9-1
                IY=10*L/9*9-8
                IZ=10*L/9*9-9
        200      DO 56 K=1,IX
                DO 58 KK=1,IY,9
                IF(K.EQ.KK) GO TO 59
        58      CONTINUE
                DO 62 KL=9,IZ,9
                IF(K.EQ.KL) GO TO 61
        62      CONTINUE
                DO 57 KM=1,10
                IF(B(J,K).EQ.D(KM))GO TO 56
        57       CONTINUE
                GO TO 62
        59      IF(B(J,K).EQ.PLUS.OR.B(J,K).EQ.FMIN) GOTO 56
                 GO TO 62
        61       IF(B(J,K).EQ.BLK) GO TO 56
        62       GOOD(J)=0.
                GO TO 60
        56        CONTINUE
        60       CONTINUE
                WRITE(6,107)
        107      FORMAT(1H1,57HTHE FOLLOWING DATA SETS WERE FOUND ERROR FREE AND P
               1UNCHED  //)
                NSET=0
                JJ=JM-1
                J=1
```

Figure II-7: CONVT output, page 1

```
 102     JP=J+1
       IF( J-JJ)100,100,150
 100     IF(GOOD(J).EQ.5.0.AND.GOOD(J+1).EQ.7.0)GO TO 101
       J=J+1
       GO TO 102
 101     NSET=NSET+1
         L1=GOOD(J)*9.-1.
         L2=GOOD(J+1)*9.-1.
       WRITE(6,103)NSET,(B(J,K),K=1,L1)
 103     FORMAT(1H0,I3,3X,80A1)
       WRITE(6,104)(B(JP,K),K=1,L2)
 104       FORMAT(1H ,6X,80A1)
       WRITE(7,105)(B(J,K),K=1,L1)
 105       FORMAT(80A1)
       WRITE(7,106)(B(JP,K),K=1,L2)
 106       FORMAT(80A1)
       J=J+2
       GO TO 102
 150     WRITE(6,120)
 120     FORMAT(1H1,44HTHE FOLLOWING TTY LINES (IF ANY) HAVE ERRORS  //)
       DO 130  J=1,JM
       IF(GOOD(J).NE.0.0) GO TO 130
       WRITE(6,131)J,(B(J,K),K=1,80)
 131     FORMAT(1H0,I3,3X,80A1)
 130     CONTINUE
       WRITE(6,140)
 140     FORMAT(1H1,10(57H DONT FORGET 4 CARDS BEFORE DATA AND 2 BLANK CAR
      1DS AFTER  /)///
      21H ,     53HFIRST CARD ---TITLE CARD (NAME DATE ETC )           /
      31H ,     53HSECOND CARD----WIDTH LENGTH THICKNESS OF SAMPLE     /
      41H ,20X,53HIN CM.  USING 3F10.3 NUMBERS STARTING IN             /
      51H ,20X,53HCOLS. 1, 11 AND 21                                   )
        WRITE(6,141)
 141    FORMAT(
      11H ,11X,53H----STARTING COL 31, ANY COMBINATION OF              /
      21H ,20X,53HPLOTS---FOR PLOTS OF THE DATA                        /
      31H ,20X,53HPUNCH---FOR PUNCHED OUTPUT OF THE CALCULATIONS       /
      41H ,20X,53HGAP ---FOR ENERGY GAP CALCULATIONS                   /
      51H ,20X,53H.    ---(A PERIOD) AFTER LAST WORD                   )
        WRITE(6,142)
 142     FORMAT(
      11H ,     53HTHIRD CARD----5 PARAMETERS FOR E-GAP  CALCULATIONS   /
      21H ,20X,53HUSING FIVE E10.3 FORMAT NUMBERS                      /
      31H ,     53HFOURTH CARD---LABEL FOR PEN PLOT                    /
      41H ,20X,53HNAME AND ACCT TOTALLING 18 CHARS STARTING COL. 1     /
      51H ,20X,53H                                                     /
      61H ,20X,53H                                                     /
      71H ,20X,53H                                                     )
       STOP
 40     WRITE(6,41)
 41    FORMAT(1H1,10(33H TOO MANY LINES FOR CORE RESERVED  /))
       STOP
       END
```

CONVT output, page 2

```
EVERYTHING READ FROM TAPE
-------------------------

  1     +0001016  +0557746  +0039586  +0726776  -0728216  !!!!!
  2     +0820865  +0039606  +0013355  -0013406  +0019366  -0019386  +0039606  !!!!!!!
  3     +0001046  +0557546  +0039596  +0727036  -0728426  !!!!!
  4     +0822005  +0039566  +0013366  -0013356  +0019406  -0019326  +0039576  !!!!!!!
  5     +0001096  +0558196  +0039636  +0726746  -0728096  !!!!!
  6     +0822635  +0039616  +0013416  -0013366  +0019386  -0019346  +0039626  !!!!!!!
  7     +0001096  +0558116  +0039576  +0726166  -0727556  !!!!!
  8     +0823435  +0039576  +0013376  -0013346  +0019366  -0019326  +0039616  !!!!!!!
  9     +0000996  +0557856  +0039556  +0725426  -0726856  !!!!!
 10     +0823705  +0039556  +0013356  -0013326  +0019356  -0019296  +0039566  !!!!!!!
 11     +0001066  +0558176  +0039586  +0724566  -0725916  !!!!!
 12     +0824025  +0039606  +0013286  -0013366  +0019256  -0019346  +0039536  !!!!!!!
 13     +0001036  +0558096  +0039556  +0723746  -0725086  !!!!!
 14     +0824365  +0039456  +0013316  -0013276  +0019316  -0019296  +0039526  !!!!!!!
 15     +0001116  +0558116  +0039485  +0723056  -0724296  !!!!!
 16     +0824665  +0039486  +0013296  -0013276  +0019296  -0019256  +0039496  !!!!!!!
 17     +0001036  +0557896  +0039436  +0722336  -0723746  !!!!!
 18     +0824605  +0039446  +0013246  -0013296  +0019266  -0019266  +0039426  !!!!!!!
 19     +0001066  +0558056  +0039446  +0721636  -0722996  !!!!!
 20     +0824995  +0039396  +0013236  -0013296  +0019246  -0019246  +0039456  !!!!!!!
 21     +0001006  +0557966  +0039366  +0721156  -0722476  !!!!!
 22     +0825195  +0039376  +0013236  -0013256  +0019256  -0019206  +0039406  !!!!!!!
 23     +0001136  +0558006  +0039376  +0720636  -0721956  !!!!!
 24     +0825155  +0039366  +0013306  -0013176  +0019206  -0019256  +0039426  !!!!!!!
 25     +0001026  +0557926  +0039376  +0720256  -0721586  !!!!!
 26     +0825335  +0039346  +0013266  -0013196  +0019226  -0019206  +0039386  !!!!!!!
 27     +0001056  +0558016  +0039376  +0719846  -0721196  !!!!!
 28     +0825505  +0039336  +0013216  -0013226  +0019206  -0019236  +0039366  !!!!!!!
 29     +0001046  +0558036  +0039366  +0719436  -0720816  !!!!!
 30     +0825605  +0039356  +0013206  -0013196  +0019246  -0019166  +0039396  !!!!!!!
 31     +0001096  +0557956  +0039376  +0719116  -0720486  !!!!!
 32     +0825725  +0039326  +0013206  -0013196  +0019246  -0019176  +0039366  !!!!!!!
 33     +0001036  +0557966  +0039356  +0718556  -0720166  !!!!!
 34     +0825655  +0039306  +0013176  -0013196  +0019216  -0019166  +0039376  !!!!!!!
 35     +0001056  +0558036  +0039316  +0718476  -0719936  !!!!!
 36     +0825855  +0039296  +0013156  -0013236  +0019146  -0019246  +0039316  !!!!!!!
 37     +0001026  +0558016  +0039316  +0718266  -0719646  !!!!!
 38     +0825955  +0039296  +0013196  -0013196  +0019196  -0019146  +0039326  !!!!!!!
 39     +0001016  +0557826  +0039316  +0718146  -0719476  !!!!!
 40     +0826065  +0039306  +0013186  -0013175  +0019196  -0019156  +0039336  !!!!!!!
 41     +0001066  +0558026  +0039306  +0717946  -0719366  !!!!!
 42     +0826195  +0039286  +0013156  -0013186  +0019156  -0019186  +0039276  !!!!!!!
 43     +0001056  +0558035  +0039275  +0717876  -0719216  !!!!!
 44     +0826165  +0039276  +0013166  -0013195  +0019166  -0019166  +0039356  !!!!!!!
 45     +0001066  +0558145  +0039296  +0717806  -0719026  !!!!!
 46     +0826345  +0039246  +0013195  -0013136  +0019136  -0019196  +0039316  !!!!!!!
 47     +0001056  +0558106  +0039356  +0717636  -0718856  !!!!!
 48     +0826675  +0039326  +0013166  -0013136  +0019166  -0019146  +0039296  !!!!!!!
 49     +0001066  +0557926  +0039255  +0717446  -0718716  !!!!!
 50     +0826435  +0039246  +0013216  -0013116  +0019196  -0019146  +0039316  !!!!!!!
 51     +0001096  +0558126  +0039256  +0717236  -0718446  !!!!!
 52     +0826495  +0039286  +0013186  -0013136  +0019206  -0019096  +0039306  !!!!!!!
 53     +0001046  +0558086  +0039296  +0717106  -0718356  !!!!!
 54     +0826515  +0039226  +0013146  -0013146  +0019206  -0019096  +0039336  !!!!!!!
 55     +0001106  +0557866  +0039276  +0716946  -0718236  !!!!!
 56     +0826905  +0039296  +0013136  -0013196  +0019146  -0019156  +0039246  !!!!!!!
```

CONVT output, page 3

```
 57   +0001076 +0557986 +0039326 +0716826 -0718016 !!!!!
 58   +0826945 +0039276 +0013145 -0013136 +0019166 -0019126 +0039276 !!!!!!!
 59   +0001076 +0557876 +0039285 +0715626 -0717916 !!!!!
 60   +0826975 +0039276 +0013145 -0013156 +0019126 -0019146 +0039276 !!!!!!!
 61   +0001126 +0557966 +0039286 +0716465 -0717746 !!!!!
 62   +0826805 +0039286 +0013156 -0013096 +0019116 -009136 +0039256 !!!!!!!!
 63   +0001056 +0557796 +0039266 +0716326 -0717586 !!!!!
 64   +0826955 +0039236 +0013156 -0013156 +0019136 -0019116 +0039236 !!!!!!!
 65   +0001056 +0557836 +0039266 +0716156 -0717386 !!!!!
 66   +0826595 +0039236 +0013135 -0013146 +0019076 -0019136 +0039276 !!!!!!!
 67   +0001056 +0557936 +0039286 +0715926 -0717136 !!!!!
 68   +0826835 +0039236 +0013125 -0013126 +0019156 -0019076 +0039256 !!!!!!!
 69   +0001086 +0557836 +0039236 +0715676 -0716896 !!!!!
 70   +0826915 +0039206 +0013116 -0013116 +0019106 -0019146 +0039276 !!!!!!!
 71   +0001086 +0557706 +0039206 +0715486 -0716696 !!!!!
 72   +0826945 +0039216 +0013145 -0013126 +0019116 -0019106 +0039186 !!!!!!!
 73   +0001096 +0557646 +0039236 +0715236 -0716436 !!!!!
 74   +0826955 +0039206 +0013105 -0013116 +0019136 -0019066 +0039236 !!!!!!!
 75   +0001106 +0557686 +0039245 +0714976 -0716236 !!!!!
 76   +0826885 +0039206 +0013105 -0013086 +0019076 -0019116 +0039236 !!!!!!!
 77   +0001096 +0557606 +0039226 +0714726 -0715996 !!!!!
 78   +0826995 +0039186 +0013106 -0013106 +0019126 -0019076 +0039186 !!!!!!!
 79   +0001116 +0557656 +0039216 +0714546 -0715746 !!!!!
 80   +0826835 +0039176 +0013056 -0013096 +0019106 -0019056 +0039236 !!!!!!!
 81   +0001066 +0557706 +0039226 +0714346 -0715566 !!!!!
 82   +0826935 +0039206 +0013056 -0013116 +0019086 -0019096 +0039206 !!!!!!!
 83   +0001086 +0557786 +0039186 +0714176 -0715356 !!!!!
 84   +0827045 +0039156 +0013086 -0013046 +0019076 -0019086 +0039176 !!!!!!!
 85   +0001086 +0557596 +0039196 +0713896 -0715156 !!!!!
 86   +0827055 +0039146 +0013066 -0013086 +0019086 -0019056 +0039146 !!!!!!!
 87   +0001076 +0557686 +0039196 +0713776 -0714936 !!!!!
 88   +0826975 +0039166 +0013065 -0013066 +0019056 -0019116 +0039206 !!!!!!!
 89   +0001036 +0557686 +0039166 +0713546 -0714816 !!!!!
 90   +0827055 +0039166 +0013055 -0013076 +0019106 -0019026 +0039186 !!!!!!!
 91   +0001106 +0557606 +0039196 +0713446 -0714626 !!!!!
 92   +0827065 +0039156 +0013076 -0013076 +0019096 -0019006 +0039176 !!!!!!!
 93   +0001086 +0557536 +0039185 +0713346 -0714506 !!!!!
 94   +0827045 +0039146 +0013056 -0013076 +0019046 -0019096 +0039166 !!!!!!!
 95   +0001056 +0557626 +0039165 +0713156 -0714386 !!!!!
 96   +0827125 +0039146 +0013086 -0013016 +0019076 -0019086 +0039166 !!!!!!!
 97   +0001106 +0557476 +0039176 +0712976 -0714176 !!!!!
 98   +0827035 +0039116 +0013035 -0013046 +0019066 -0019056 +0039156 !!!!!!!
 99   +0001166 +0557516 +0039156 +0712846 -0714086 !!!!!
100   +0826835 +0039126 +0013076 -0013046 +0019126 -0018986 +0039156 !!!!!!!
101   +0001116 +0557626 +0039176 +0712626 -0713806 !!!!!
102   +0826945 +0039096 +0013065 -0013026 +0019046 -0019046 +0039136 !!!!!!!
103   +0001076 +0557506 +0039136 +0712466 -0713726 !!!!!
104   +0826935 +0039106 +0013076 -0013046 +0019075 -0019016 +0039136 !!!!!!!
105   +0001046 +0557446 +0039136 +0712456 -0713686 !!!!!
106   +0827085 +0039116 +0013016 -0013066 +0019016 -0019066 +0039116 !!!!!!!
107   +0001116 +0557426 +0039146 +0712336 -0713556 !!!!!
108   +0826895 +0039156 +0013056 -0013016 +0019016 -0019046 +0039146 !!!!!!!
109   +0001096 +0557466 +0039126 +0712216 -0713376 !!!!!
110   +0827005 +0039115 +0013026 -0013046 +0019065 -0019016 +0039106 !!!!!!!
111   +0001066 +0557526 +0039126 +0712076 -0713256 !!!!!
112   +0826945 +0039056 +0013076 -0013036 +0019076 -0018996 +0039156 !!!!!!!
113   +0001056 +0557536 +0039136 +0711996 -0713236 !!!!!
114   +0826945 +0039096 +0013066 -0013006 +0019076 -0018996 +0039136 !!!!!!!
115   +0001066 +0557486 +0039116 +0711876 -0713096 !!!!!
116   +0826885 +0039086 +0012975 -0013076 +0019046 -0019046 +0039126 !!!!!!!
117   +0001146 +0557516 +0039126 +0711766 -0712946 !!!!!
```

CONVT output, page 4

```
118    +0326965 +0039096 +0013006 -0013026 +0019036 -0019006 +0039136 !!!!!!!
119    +0001116 +0557606 +0039096 +0711556 -0712736 !!!!!
120    +0326965 +0039066 +0013026 -0012996 +0019056 -0019016 +0039066 !!!!!!!
121    +0001086 +0557546 +0039086 +0711426 -0712676 !!!!!
122    +0326915 +0039116 +0012976 -0013046 +0019046 -0018966 +0039096 !!!!!!!
123    +0001106 +0557406 +0039146 +0711276 -0712506 !!!!!
124    +0326895 +0039046 +0013056 -0012976 +0019086 -0018936 +0039056 !!!!!!!

TERMINATION STATUS = 07      (07 IS EXPECTED)
```

```
THE FOLLOWING DATA SETS WERE FOUND ERROR FREE AND PUNCHED


  1    +0001016 +0557746 +0039586 +0726776 -0728216
       +0820485 +0039606 +0013356 -0013406 +0019366 -0019386 +0039606

  2    +0001046 +0557846 +0039596 +0727036 -0728426
       +0822005 +0039566 +0013386 -0013356 +0019406 -0019326 +0039576

  3    +0001096 +0558196 +0039636 +0726746 -0728096
       +0822685 +0039616 +0013416 -0013366 +0019386 -0019346 +0039626

  4    +0001096 +0558116 +0039576 +0726166 -0727556
       +0823435 +0039576 +0013376 -0013346 +0019366 -0019326 +0039616

  5    +0000996 +0557856 +0039556 +0725426 -0726856
       +0823705 +0039556 +0013356 -0013326 +0019356 -0019296 +0039566

  6    +0001056 +0558176 +0039566 +0724566 -0725916
       +0824025 +0039506 +0013286 -0013366 +0019256 -0019346 +0039536

  7    +0001036 +0558096 +0039556 +0723746 -0725086
       +0824365 +0039456 +0013316 -0013276 +0019316 -0019296 +0039526

  8    +0001116 +0558116 +0039486 +0723056 -0724296
       +0824665 +0039486 +0013296 -0013276 +0019296 -0019256 +0039496

  9    +0001036 +0557896 +0039436 +0722336 -0723746
       +0824605 +0039446 +0013245 -0013296 +0019266 -0019266 +0039426

 10    +0001066 +0558056 +0039446 +0721636 -0722996
       +0824995 +0039396 +0013236 -0013286 +0019246 -0019246 +0039456

 11    +0001006 +0557966 +0039366 +0721156 -0722476
       +0825195 +0039376 +0013236 -0013256 +0019256 -0019206 +0039406

 12    +0001136 +0558006 +0039376 +0720636 -0721956
       +0825155 +0039366 +0013306 -0013176 +0019206 -0019256 +0039426

 13    +0001026 +0557926 +0039376 +0720256 -0721586
       +0825335 +0039346 +0013266 -0013186 +0019226 -0019206 +0039386

 14    +0001056 +0558016 +0039376 +0719846 -0721196
       +0825505 +0039336 +0013216 -0013226 +0019206 -0019236 +0039366

 15    +0001046 +0558036 +0039366 +0719436 -0720816
       +0825605 +0039356 +0013206 -0013196 +0019246 -0019166 +0039396

 16    +0001096 +0557956 +0039376 +0719116 -0720486
       +0825725 +0039326 +0013206 -0013196 +0019246 -0019176 +0039366

 17    +0001036 +0557966 +0039356 +0718856 -0720166
       +0825655 +0039306 +0013176 -0013196 +0019216 -0019166 +0039376

 18    +0001056 +0558036 +0039316 +0718476 -0719936
       +0825855 +0039296 +0013156 -0013236 +0019146 -0019246 +0039316

 19    +0001026 +0558016 +0039316 +0718266 -0719646
       +0825955 +0039296 +0013196 -0013196 +0019196 -0019146 +0039326
```

```
20    +0001016 +0557826 +0039316 +0718146 -0719476
      +0326065 +0039306 +0013186 -0013176 +0019196 -0019156 +0039336

21    +0001066 +0558026 +0039306 +0717946 -0719366
      +0326185 +0039286 +0013156 -0013186 +0019156 -0019186 +0039276

22    +0001056 +0558036 +0039276 +0717876 -0719216
      +0326165 +0039276 +0013166 -0013196 +0019166 -0019166 +0039356

23    +0001066 +0558146 +0039296 +0717806 -0719026
      +0326345 +0039246 +0013196 -0013136 +0019136 -0019196 +0039316

24    +0001056 +0558106 +0039356 +0717636 -0718856
      +0326675 +0039326 +0013166 -0013136 +0019166 -0019146 +0039296

25    +0001066 +0557926 +0039256 +0717446 -0718716
      +0326435 +0039246 +0013216 -0013116 +0019196 -0019146 +0039316

26    +0001096 +0558126 +0039256 +0717236 -0718446
      +0326495 +0039286 +0013186 -0013136 +0019206 -0019096 +0039306

27    +0001046 +0558086 +0039296 +0717106 -0718356
      +0326515 +0039226 +0013146 -0013146 +0019206 -0019096 +0039336

28    +0001106 +0557886 +0039276 +0716946 -0718236
      +0326805 +0039296 +0013136 -0013196 +0019146 -0019156 +0039246

29    +0001076 +0557986 +0039326 +0716826 -0718016
      +0326945 +0039276 +0013146 -0013136 +0019166 -0019126 +0039276

30    +0001076 +0557876 +0039286 +0716626 -0717916
      +0326875 +0039276 +0013146 -0013156 +0019126 -0019146 +0039276

31    +0001056 +0557796 +0039266 +0716326 -0717586
      +0326955 +0039236 +0013156 -0013156 +0019136 -0019116 +0039236

32    +0001056 +0557836 +0039266 +0716166 -0717386
      +0326895 +0039236 +0013136 -0013146 +0019076 -0019136 +0039276

33    +0001056 +0557936 +0039266 +0715926 -0717136
      +0326835 +0039236 +0013126 -0013126 +0019156 -0019076 +0039256

34    +0001086 +0557676 +0039236 +0715676 -0716896
      +0326915 +0039206 +0013116 -0013116 +0019106 -0019146 +0039276

35    +0001086 +0557706 +0039206 +0715486 -0716696
      +0326945 +0039216 +0013146 -0013126 +0019116 -0019106 +0039186

36    +0001096 +0557646 +0039236 +0715236 -0716436
      +0326955 +0039206 +0013106 -0013116 +0019136 -0019066 +0039236

37    +0001106 +0557686 +0039246 +0714976 -0716236
      +0326885 +0039206 +0013106 -0013086 +0019076 -0019116 +0039236

38    +0001096 +0557606 +0039226 +0714726 -0715996
      +0326995 +0039186 +0013106 -0013106 +0019126 -0019076 +0039186

39    +0001116 +0557656 +0039216 +0714546 -0715746
      +0326835 +0039176 +0013056 -0013096 +0019106 -0019056 +0039236

40    +0001056 +0557706 +0039226 +0714346 -0715566
```

```
        +0326935 +0039206 +0013056 -0013116 +0019086 -0019096 +0039206

 41     +0001086 +0557786 +0039186 +0714176 -0715356
        +0327045 +0039156 +0013096 -0013046 +0019076 -0019086 +0039176

 42     +0001086 +0557596 +0039196 +0713896 -0715156
        +0327055 +0039146 +0013066 -0013086 +0019086 -0019056 +0039146

 43     +0001076 +0557686 +0039196 +0713776 -0714936
        +0326975 +0039166 +0013066 -0013066 +0019056 -0019116 +0039206

 44     +0001086 +0557686 +0039166 +0713546 -0714816
        +0327055 +0039166 +0013056 -0013076 +0019106 -0019026 +0039186

 45     +0001106 +0557606 +0039196 +0713446 -0714626
        +0327065 +0039156 +0013076 -0013076 +0019096 -0019006 +0039176

 46     +0001086 +0557536 +0039186 +0713346 -0714506
        +0327045 +0039146 +0013056 -0013076 +0019046 -0019096 +0039166

 47     +0001056 +0557626 +0039166 +0713156 -0714386
        +0327125 +0039146 +0013086 -0013016 +0019076 -0019086 +0039166

 48     +0001106 +0557476 +0039176 +0712976 -0714176
        +0327035 +0039116 +0013036 -0013046 +0019066 -0019056 +0039156

 49     +0001166 +0557516 +0039156 +0712846 -0714086
        +0326835 +0039126 +0013076 -0013046 +0019126 -0018986 +0039156

 50     +0001116 +0557626 +0039176 +0712626 -0713906
        +0326945 +0039096 +0013066 -0013026 +0019046 -0019046 +0039136

 51     +0001076 +0557506 +0039136 +0712466 -0713726
        +0326935 +0039106 +0013076 -0013046 +0019076 -0019016 +0039136

 52     +0001046 +0557446 +0039136 +0712456 -0713686
        +0327085 +0039116 +0013016 -0013066 +0019016 -0019066 +0039116

 53     +0001116 +0557426 +0039146 +0712336 -0713556
        +0326695 +0039156 +0013056 -0013016 +0019016 -0019046 +0039146

 54     +0001096 +0557486 +0039126 +0712216 -0713376
        +0327005 +0039116 +0013026 -0013046 +0019066 -0019016 +0039106

 55     +0001066 +0557526 +0039126 +0712076 -0713256
        +0326945 +0039056 +0013076 -0013036 +0019076 -0018996 +0039156

 56     +0001056 +0557536 +0039136 +0711996 -0713236
        +0326945 +0039096 +0013066 -0013006 +0019076 -0018996 +0039136

 57     +0001066 +0557486 +0039116 +0711876 -0713096
        +0326885 +0039066 +0012976 -0013076 +0019046 -0019046 +0039126

 58     +0001146 +0557516 +0039126 +0711766 -0712946
        +0326965 +0039096 +0013006 -0013026 +0019036 -0019006 +0039136

 59     +0001116 +0557606 +0039096 +0711556 -0712736
        +0326965 +0039066 +0013026 -0012995 +0019056 -0019016 +0039066

 60     +0001086 +0557546 +0039066 +0711426 -0712676
        +0327115 +0039116 +0012976 -0013046 +0019046 -0018986 +0039096
```

```
 61    +0001106 +0557406 +0039146 +0711276 -0712506
       +0326595 +0039046 +0013056 -0012976 +0019086 -0018936 +0039056



THE FOLLOWING TTY LINES (IF ANY) HAVE ERRORS

 62    +0326805 +0039286 +0013156 -0013096 +0019116 -009136 +0039256 ::::::::≡≡≡≡≡≡≡≡≡≡
```

```
 DONT FORGET 4 CARDS BEFORE DATA AND 2 BLANK CARDS AFTER
DONT FORGET 4 CARDS BEFORE DATA AND 2 BLANK CARDS AFTER
DONT FORGET 4 CARDS BEFORE DATA AND 2 BLANK CARDS AFTER
DONT FORGET 4 CARDS BEFORE DATA AND 2 BLANK CARDS AFTER
DONT FORGET 4 CARDS BEFORE DATA AND 2 BLANK CARDS AFTER
DONT FORGET 4 CARDS BEFORE DATA AND 2 BLANK CARDS AFTER
DONT FORGET 4 CARDS BEFORE DATA AND 2 BLANK CARDS AFTER
DONT FORGET 4 CARDS BEFORE DATA AND 2 BLANK CARDS AFTER
DONT FORGET 4 CARDS BEFORE DATA AND 2 BLANK CARDS AFTER
DONT FORGET 4 CARDS BEFORE DATA AND 2 BLANK CARDS AFTER


FIRST CARD ---TITLE CARD (NAME DATE ETC )
SECOND CARD----WIDTH LENGTH THICKNESS OF SAMPLE
                    IN CM.  USING 3F10.3 NUMBERS STARTING IN
                    COLS. 1, 11 AND 21
           ----STARTING COL 31, ANY COMBINATION OF
                    PLOTS---FOR PLOTS OF THE DATA
                    PUNCH---FOR PUNCHED OUTPUT OF THE CALCULATIONS
                    GAP ---FOR ENERGY GAP CALCULATIONS
                    .    ---(A PERIOD) AFTER LAST WORD
THIRD CARD----5 PARAMETERS FOR E-GAP  CALCULATIONS
                    USING FIVE E10.3 FORMAT NUMBERS
FOURTH CARD---LABEL FOR PEN PLOT
                    NAME AND ACCT TOTALLING 18 CHARS STARTING COL. 1
```

CONVT output, page 10

```
  100377   P(100) , 10 OHM-CM

          RAW TEMPERATURE DATA

          GERMANIUM VOLTS       .......THERMOCOUPLE VOLTAGES.......        AVERAGE

CAUTION   RESID SET TO -1028. ***********

    1              80.0         907.0          907.0          912.0          908.7
    2              79.0         938.0          938.0          949.0          941.7
    3              81.0         995.0          997.0         1004.0          998.7
    4              82.0        1061.0         1065.0         1073.0         1066.3
    5              82.0        1245.0         1254.0         1261.0         1253.3
    6              84.0        1361.0         1363.0         1376.0         1366.7
    7              88.0        1485.0         1488.0         1502.0         1491.7
    8              93.0        1633.0         1638.0         1659.0         1643.3
    9              95.0        1909.0         1922.0         1954.0         1928.3
   10              99.0        2256.0         2269.0         2296.0         2273.7
   11             103.0        2660.0         2677.0         2709.0         2682.0
   12             105.0        2948.0         2956.0         2974.0         2959.3
   13             108.0        3108.0         3118.0         3131.0         3119.0
   14             109.0        3240.0         3244.0         3252.0         3245.3
   15             107.0        3338.0         3337.0         3356.0         3343.7
   16             109.0        3434.0         3436.0         3441.0         3437.0
   17             113.0        3501.0         3505.0         3515.0         3507.0
   18             112.0        3562.0         3560.0         3575.0         3565.7
   19             108.0        3612.0         3611.0         3621.0         3614.7
   20             114.0        3657.0         3655.0         3668.0         3660.0
   21             116.0        3694.0         3690.0         3702.0         3695.3
   22             108.0        3720.0         3718.0         3725.0         3721.0
   23             107.0        3750.0         3741.0         3752.0         3747.7
   24             106.0        3767.0         3764.0         3771.0         3767.3
   25             117.0        3790.0         3785.0         3794.0         3789.7
   26             113.0        3805.0         3799.0         3806.0         3803.3
   27             115.0        3820.0         3813.0         3822.0         3818.3
   28             118.0        3830.0         3826.0         3830.0         3828.7
   29             113.0        3835.0         3830.0         3844.0         3836.3
   30             113.0        3844.0         3841.0         3847.0         3844.0
   31             114.0        3849.0         3849.0         3859.0         3852.3
   32             113.0        3858.0         3857.0         3862.0         3859.0
   33             117.0        3863.0         3860.0         3871.0         3864.7
   34             112.0        3878.0         3871.0         3886.0         3876.3
   35             114.0        3886.0         3885.0         3885.0         3885.3
   36             111.0        3891.0         3887.0         3894.0         3890.7
   37             119.0        3893.0         3889.0         3902.0         3894.7
   38             120.0        3899.0         3899.0         3902.0         3900.0
   39             123.0        3910.0         3904.0         3907.0         3907.0
   40             121.0        3914.0         3906.0         3912.0         3910.7
   41             116.0        3909.0         3909.0         3915.0         3911.0
   42             116.0        3916.0         3909.0         3918.0         3914.3
```

Figure II-8: HALL2 output, page 1

```
              VGE          TGE    GIVES V          VTC        RESID      TEMP

  1         65.000          -I          -I      905.667          -I     136.186
  2         79.000          -I          -I      941.667          -I     138.157
  3         81.000          -I          -I      998.667          -I     141.525
  4         82.000          -I          -I     1066.333          -I     145.473
  5         87.000          -I          -I     1253.333          -I     156.240
  6         84.000          -I          -I     1356.667          -I     162.645
  7         88.000          -I          -I     1491.667          -I     169.617
  8         63.000          -I          -I     1543.333          -I     177.947
  9         96.000          -I          -I     1928.333          -I     193.317
 10         99.000          -I          -I     2273.667          -I     211.398
 11        103.000          -I          -I     2682.000          -I     232.381
 12        105.000          -I          -I     2959.333          -I     246.374
 13        106.000          -I          -I     3119.000          -I     256.371
 14        109.000          -I          -I     3245.333          -I     265.536
 15        107.000          -I          -I     3343.667          -I     272.670
 16        109.000          -I          -I     3437.000          -I     279.441
 17        113.000          -I          -I     3507.000          -I     284.519
 18        112.000          -I          -I     3565.667          -I     288.775
 19        108.000          -I          -I     3614.667          -I     292.330
 20        114.000          -I          -I     3660.000          -I     295.619
 21        116.000          -I          -I     3695.333          -I     298.182
 22        108.000          -I          -I     3721.000          -I     300.045
 23        107.000          -I          -I     3747.667          -I     301.979
 24        106.000          -I          -I     3767.333          -I     303.405
 25        117.000          -I          -I     3789.667          -I     305.026
 26        113.000          -I          -I     3803.333          -I     306.018
 27        115.000          -I          -I     3818.333          -I     307.106
 28        118.000          -I          -I     3828.667          -I     307.855
 29        113.000          -I          -I     3836.333          -I     308.412
 30        113.000          -I          -I     3844.000          -I     308.968
 31        114.000          -I          -I     3852.333          -I     309.572
 32        113.000          -I          -I     3859.000          -I     310.056
 33        117.000          -I          -I     3864.667          -I     310.467
 34        112.000          -I          -I     3878.333          -I     311.459
 35        114.000          -I          -I     3885.333          -I     311.967
 36        111.000          -I          -I     3890.667          -I     312.353
 37        119.000          -I          -I     3894.667          -I     312.644
 38        120.000          -I          -I     3900.000          -I     313.031
 39        123.000          -I          -I     3907.000          -I     313.538
 40        121.000          -I          -I     3910.667          -I     313.804
 41        116.000          -I          -I     3911.000          -I     313.829
 42        116.000          -I          -I     3914.333          -I     314.070

REFFERANCE TEMP.      77.33K
CORRESPONDING VOLTAGE  -1028.00 ABSOLUTE
```

HALL2 output, page 2

```
  100377    P(100) , 10 OHM-CM

          DATA SCREENING
          --------------

MORE THAN 10 P.C. VARIATION IN CONDUCTIVITY VOLTAGE FOR FOLLOWING SETS OF DATA

SIGN AMBIGUITY IN HALL VOLTAGES

               1         -.000984     .000991     .006457     -.006470
               2         -.000877     .000885     .006514     -.006521
               3         -.000728     .000740     .006599     -.006605
               4         -.000522     .000535     .006727     -.006730
THE FOLLOWING SETS WERE SET EQUAL TO ZERO AS DATA FORMAT NOT ACCEPTABLE
```

HALL2 output, page 3

```
G2377   P(100) , 10 OHM-CM

  TEMP      RECIP       I          VC         B          VH        HALL       RHO       MOBC       MOBH       CONC
            TEMP                                                   COEFF

 136.19   .73E-02   .10E-02   .13E+00   .82E+04   .27E-02   .83E+03   .12E+01   .70E+03   .70E+03   .75E+16
 138.16   .72E-02   .10E-02   .13E+00   .82E+04   .28E-02   .85E+03   .12E+01   .70E+03   .70E+03   .73E+16
 141.52   .71E-02   .10E-02   .13E+00   .82E+04   .29E-02   .89E+03   .13E+01   .70E+03   .70E+03   .70E+16
 145.47   .69E-02   .10E-02   .14E+00   .82E+04   .31E-02   .94E+03   .13E+01   .70E+03   .70E+03   .66E+16
 150.24   .67E-02   .10E-02   .16E+00   .82E+04   .36E-02   .11E+04   .15E+01   .71E+03   .71E+03   .57E+16
 162.64   .61E-02   .10E-02   .18E+00   .82E+04   .39E-02   .12E+04   .17E+01   .71E+03   .71E+03   .53E+16
 169.62   .59E-02   .10E-02   .19E+00   .82E+04   .43E-02   .13E+04   .18E+01   .71E+03   .71E+03   .48E+16
 177.95   .56E-02   .10E-02   .21E+00   .82E+04   .48E-02   .15E+04   .20E+01   .72E+03   .72E+03   .43E+16
 193.32   .52E-02   .10E-02   .26E+00   .82E+04   .58E-02   .18E+04   .24E+01   .73E+03   .73E+03   .35E+16
 211.40   .47E-02   .10E-02   .32E+00   .82E+04   .73E-02   .22E+04   .30E+01   .73E+03   .73E+03   .28E+16
 232.38   .43E-02   .10E-02   .40E+00   .82E+04   .92E-02   .28E+04   .38E+01   .73E+03   .73E+03   .22E+16
 246.37   .41E-02   .10E-02   .47E+00   .82E+04   .11E-01   .32E+04   .44E+01   .73E+03   .73E+03   .19E+16
 256.37   .39E-02   .10E-02   .51E+00   .82E+04   .12E-01   .35E+04   .48E+01   .73E+03   .73E+03   .18E+16
 265.54   .38E-02   .10E-02   .54E+00   .82E+04   .12E-01   .37E+04   .51E+01   .73E+03   .73E+03   .17E+16
 272.67   .37E-02   .10E-02   .56E+00   .82E+04   .13E-01   .39E+04   .53E+01   .73E+03   .73E+03   .16E+16
 279.44   .36E-02   .10E-02   .59E+00   .82E+04   .13E-01   .41E+04   .56E+01   .73E+03   .73E+03   .15E+16
 284.52   .35E-02   .10E-02   .61E+00   .82E+04   .14E-01   .42E+04   .57E+01   .73E+03   .73E+03   .15E+16
 286.78   .35E-02   .10E-02   .62E+00   .82E+04   .14E-01   .43E+04   .59E+01   .73E+03   .73E+03   .15E+16
 292.33   .34E-02   .10E-02   .64E+00   .82E+04   .14E-01   .44E+04   .60E+01   .73E+03   .73E+03   .14E+16
 295.62   .34E-02   .10E-02   .65E+00   .82E+04   .15E-01   .45E+04   .61E+01   .73E+03   .73E+03   .14E+16
 298.18   .34E-02   .10E-02   .66E+00   .82E+04   .15E-01   .45E+04   .62E+01   .73E+03   .73E+03   .14E+16
 300.04   .33E-02   .10E-02   .66E+00   .82E+04   .15E-01   .46E+04   .63E+01   .73E+03   .73E+03   .14E+16
 301.96   .33E-02   .10E-02   .67E+00   .82E+04   .15E-01   .46E+04   .63E+01   .73E+03   .73E+03   .14E+16
 303.41   .33E-02   .10E-02   .68E+00   .82E+04   .15E-01   .46E+04   .64E+01   .73E+03   .73E+03   .13E+16
 305.03   .33E-02   .10E-02   .68E+00   .82E+04   .15E-01   .47E+04   .64E+01   .73E+03   .73E+03   .13E+16
 306.02   .33E-02   .10E-02   .69E+00   .82E+04   .16E-01   .47E+04   .65E+01   .73E+03   .73E+03   .13E+16
 307.11   .33E-02   .10E-02   .69E+00   .82E+04   .16E-01   .47E+04   .65E+01   .73E+03   .73E+03   .13E+16
```

```
307.56   .32E-02   .10E-02   .69E+00   .82E+04   .16E-01   .47E+04   .65E+01   .73E+03   .73E+03   .13E+16
308.41   .32E-02   .10E-02   .69E+00   .82E+04   .16E-01   .48E+04   .66E+01   .73E+03   .73E+03   .13E+16
308.97   .32E-02   .10E-02   .70E+00   .82E+04   .16E-01   .48E+04   .66E+01   .73E+03   .73E+03   .13E+16
309.57   .32E-02   .10E-02   .70E+00   .82E+04   .16E-01   .48E+04   .66E+01   .73E+03   .73E+03   .13E+16
310.06   .32E-02   .10E-02   .70E+00   .82E+04   .16E-01   .48E+04   .66E+01   .73E+03   .73E+03   .13E+16
310.47   .32E-02   .10E-02   .70E+00   .82E+04   .16E-01   .48E+04   .66E+01   .73E+03   .73E+03   .13E+16
311.46   .32E-02   .10E-02   .71E+00   .82E+04   .16E-01   .48E+04   .67E+01   .73E+03   .73E+03   .13E+16
311.07   .32E-02   .10E-02   .71E+00   .82E+04   .16E-01   .48E+04   .67E+01   .73E+03   .73E+03   .13E+16
312.35   .32E-02   .10E-02   .71E+00   .82E+04   .16E-01   .49E+04   .67E+01   .73E+03   .73E+03   .13E+16
312.64   .32E-02   .10E-02   .71E+00   .82E+04   .16E-01   .49E+04   .67E+01   .73E+03   .73E+03   .13E+16
313.03   .32E-02   .10E-02   .71E+00   .82E+04   .16E-01   .49E+04   .67E+01   .73E+03   .73E+03   .13E+16
313.54   .32E-02   .10E-02   .71E+00   .82E+04   .16E-01   .49E+04   .67E+01   .73E+03   .73E+03   .13E+16
313.30   .32E-02   .10E-02   .71E+00   .82E+04   .16E-01   .49E+04   .67E+01   .73E+03   .73E+03   .13E+16
313.83   .32E-02   .10E-02   .71E+00   .82E+04   .16E-01   .49E+04   .68E+01   .73E+03   .73E+03   .13E+16
314.07   .32E-02   .10E-02   .72E+00   .82E+04   .16E-01   .49E+04   .68E+01   .73E+03   .73E+03   .13E+16
```

HALL2 output, page 5

```
SCALED LIMITS,  XMIN=  2.91954  XMAX=  3.69092,  YMIN= -7.34291  YMAX= -3.18400      42 POINTS PLOTTED( ≠ DE
```

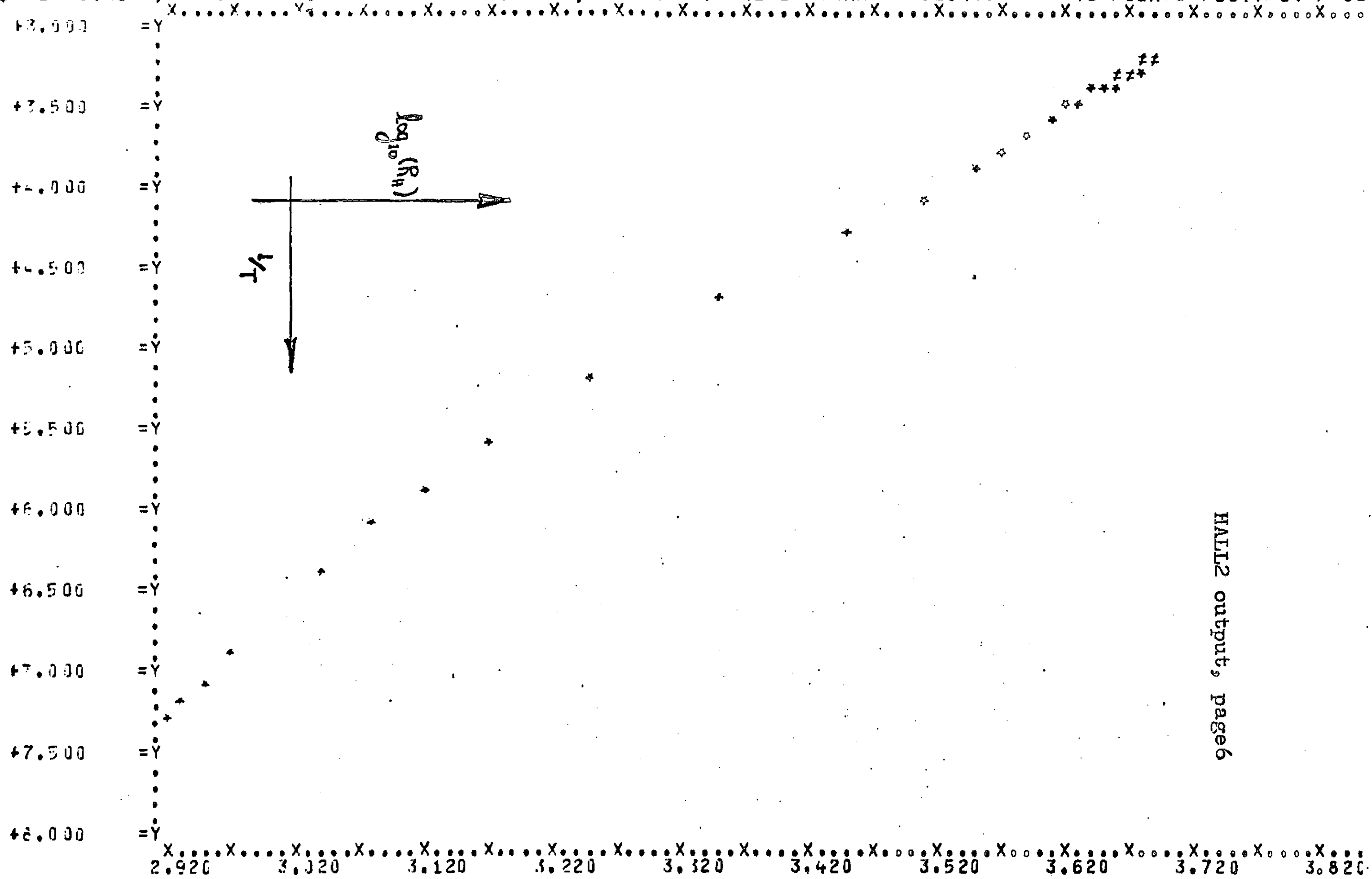

```
          SCALING---- X VALUES TIMES 10 TO POWER   0,  Y VALUES TIMES 10 TO POWER  -3
LOG10(RH)  VS 1/T
  100377    P(100) , 10 OHM-CM
```

HALL2 output, page6

```
SCALED LIMITS, XMIN=  1.51044  XMAX=  1.58752,  YMIN= -7.34291  YMAX= -3.18400      42 POINTS PLOTTED( ≠ E
```

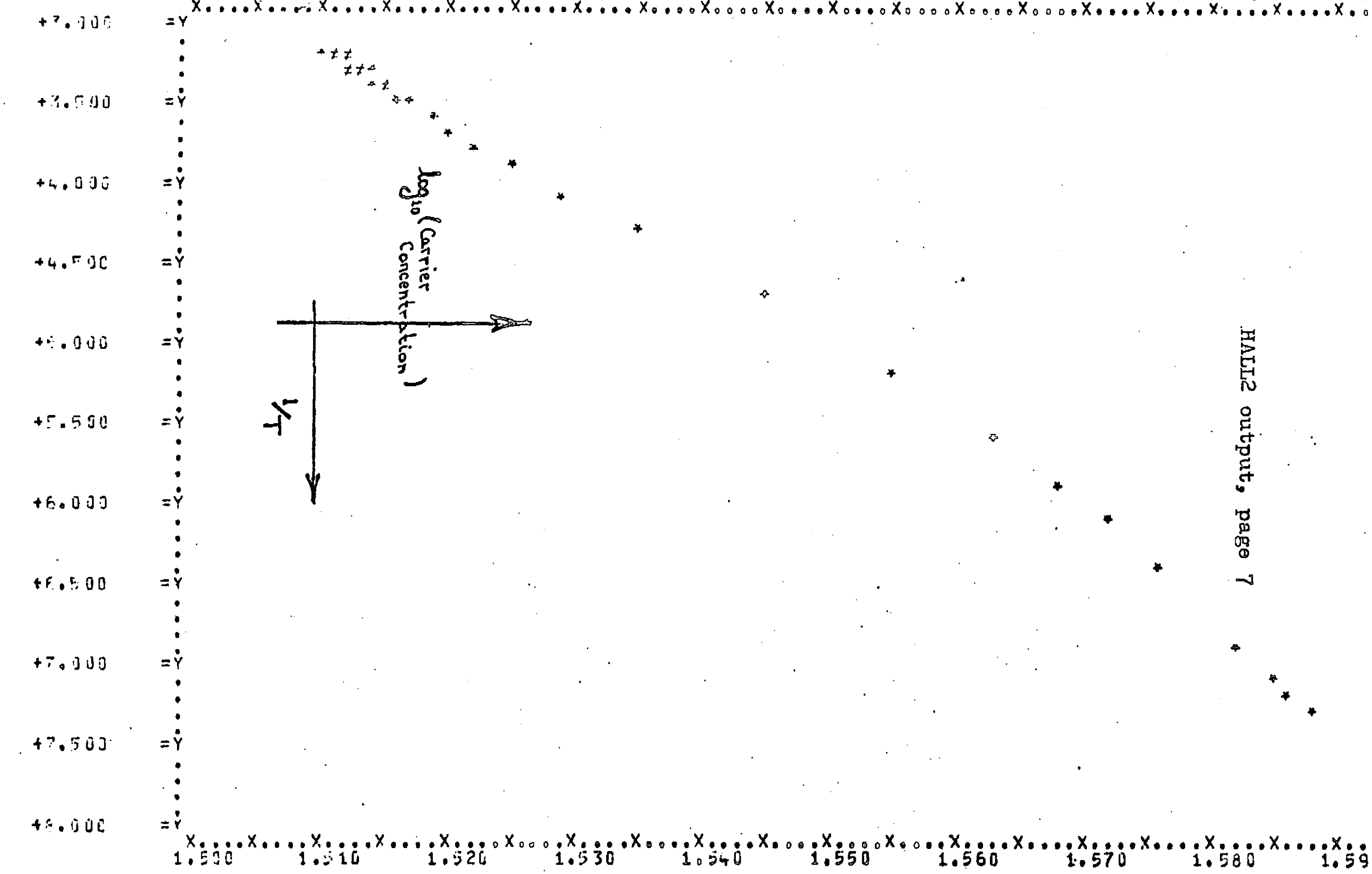

HALL2 output, page 7

```
SCALING---- X VALUES TIMES 10 TO POWER   1,  Y VALUES TIMES 10 TO POWER  -3
LOG10(CN) VS 1/T
  100377   R(100) , 10 OHM-CM
```

```
SCALED LIMITS, XMIN= -8.30313  XMAX= -.76083,  YMIN= -7.34291  YMAX= -3.18400     42 POINTS PLOTTED( ≠ 0
```

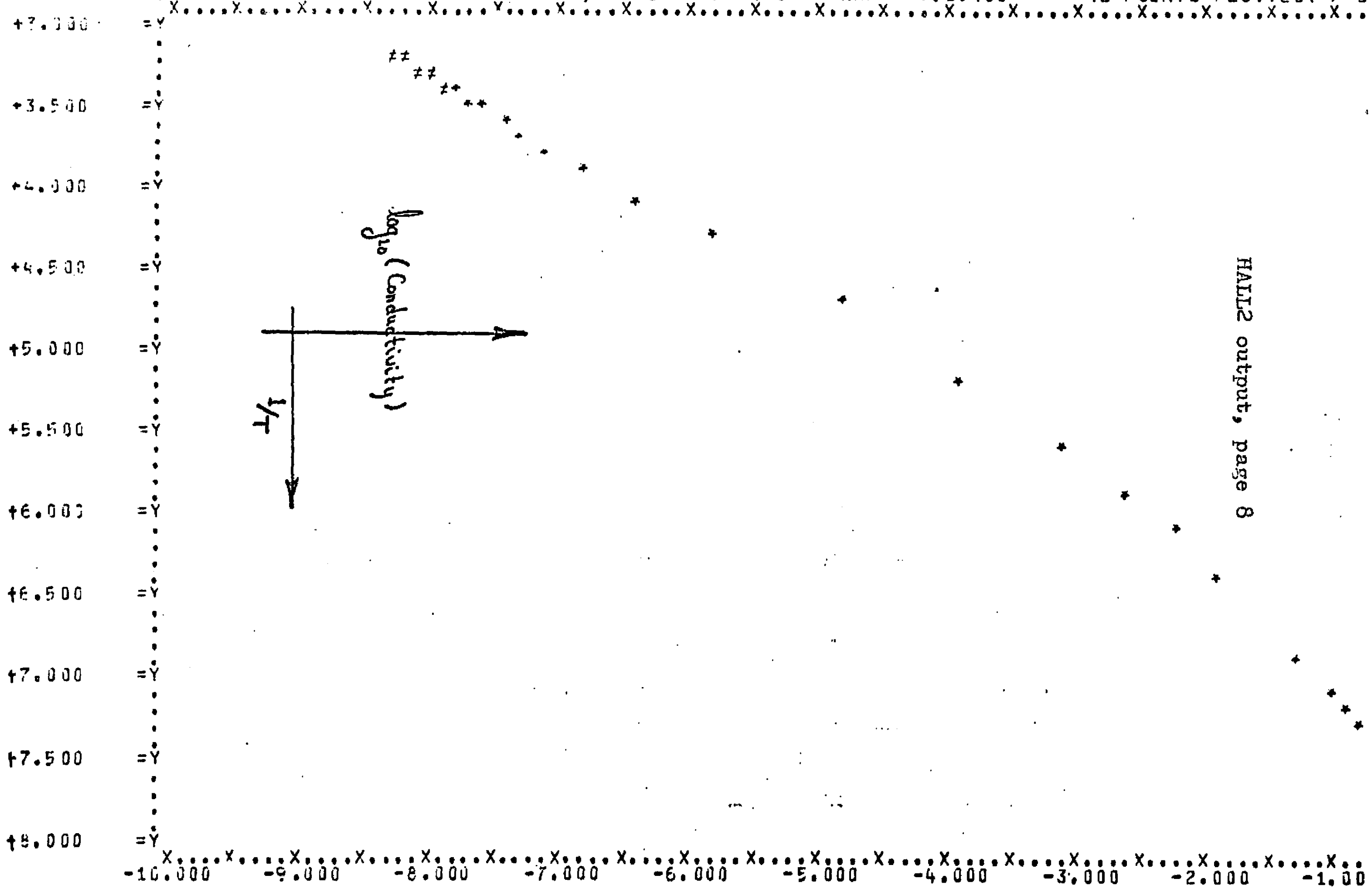

```
SCALING---- X VALUES TIMES 10 TO POWER  -1,  Y VALUES TIMES 10 TO POWER  -3
LOG10(CC) VS 1/T
 100377   P(100) , 10 OHM-CM
```

HALL2 output, page 8

```
SCALED LIMITS,  XMIN=  2.84345  XMAX=  2.86579,  YMIN= -2.49703  YMAX= -2.13413       42 POINTS PLOTTED( ≠ D
```

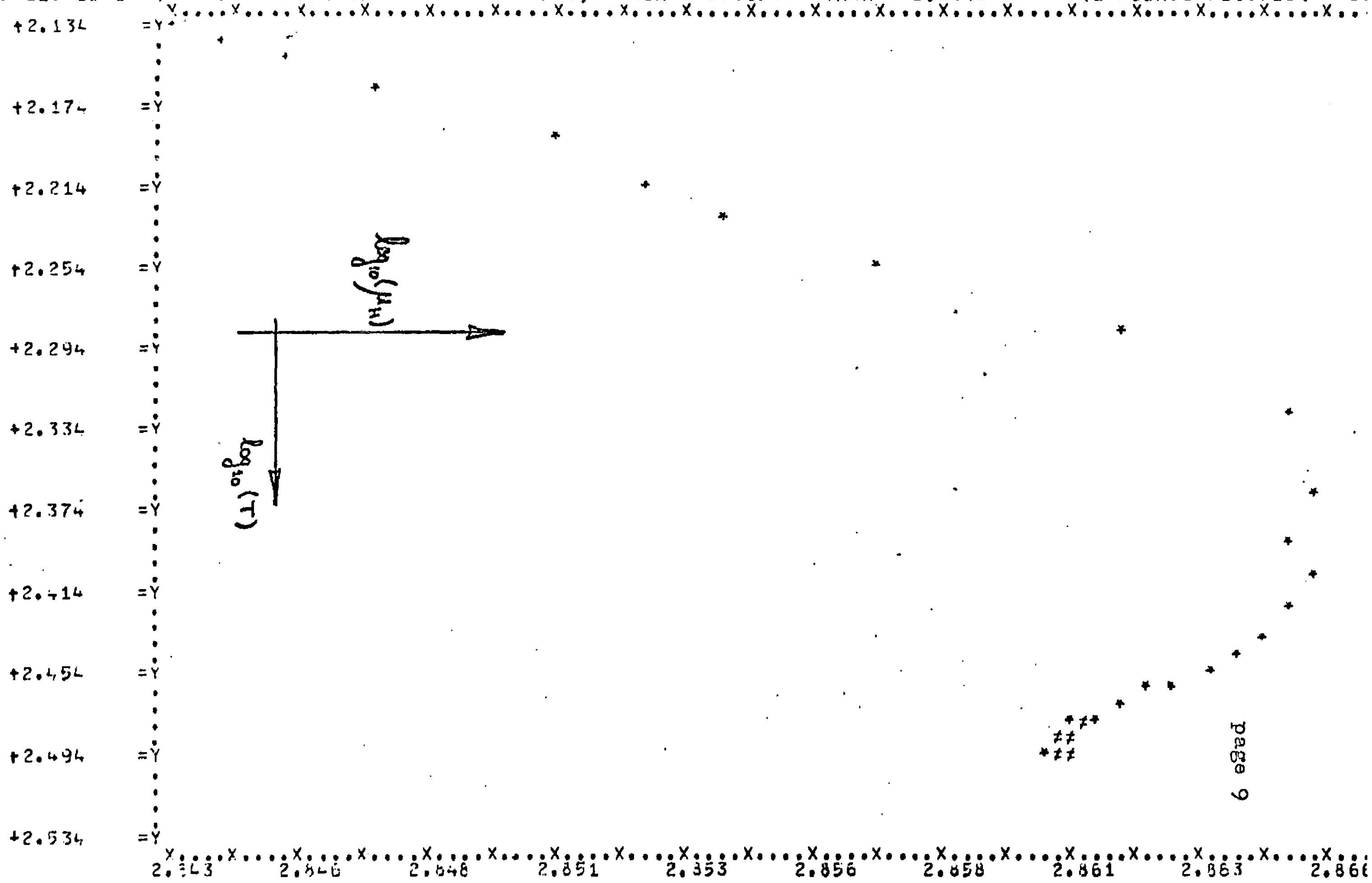

```
                SCALING---- X VALUES TIMES 10 TO POWER    0,  Y VALUES TIMES 10 TO POWER   0
LOG10(MO)  VS LOG10(TMP)
  100377    P(100) , 10 OHM-CM
```

REFERENCES

1. J.T. Burrill, W.J. King, S. Harrison, P. McNally; IEEE Trans. Elect. Dev ED-14, Nol. 1, 10 (1967).
2. J.P. Ponpon and P. Siffert; Proc 11th Photovoltaic Spec. Conf., 342 (1975).
3. J. Lindmayer and J. Allison; Proc. 9th Photovoltaic Spec. Conf., 83 (1973).
4. J.J. Loferski, N. Ramaganathan, E.E. Crisman, and L.Y. Chen; Proc. 9th Photovoltaic Spec. Conf., 19 (1973).
5. J.F. Gibbons, W.S. Johnson, and S.W. Nylroie; Projected Range Statistics, 2nd edition, Halstead Press, 1975.
6. S.M. Sze; Physics of Semiconductor Devices, Wiley-Interscience, 1969.
7. R.S. Walker and D.A. Thompson; Nucl. Instr. and Methods 135, 489 (1976).
8. E. Baldo, F. Cappellani, and G. Restelli; Rad Effects 19, 271 (1973).
9. J.B. Mitchell; "An Investigation into the Electrical and Radiation Damage Properties of Nitrogen Implanted Silicon, Germanium and Silicon-Carbide", Ph.D. Thesis, Elect. Eng., McMaster University (1974).

10. J. Shewchun, K.M. Ghanakar, R. Yager, H.D. Barber, and D.A. Thompson; The Rev. Sci. Instrum. 42, 1797 (1971).

11. J.W. Mayer, L. Erikson, and J.A. Davies; Ion Implantation in Semiconductors, Academic Press, 1970.

12. J.W. Mayer, O.J. Marsh, G.A. Shifrin, and R. Baron; Can. J. of Phys., Vol. 45, 4073 (1967).

13. M. Wolf; Energy Convers., 1112, 63 (1971).

14. D.A. Davies, Solid State Electron 13, 229 (1970).

15. J.F. Gibbons, A. El-Hoshy, K.E. Manchester, and F.L. Vogel; Appl. Phys. Lett. 8.2, 46 (1966).

16. J.J. Loferski; "Principles of Photovoltaic Solar Energy Conversion", 25th Annual Proc. Power Sources Conf. (1972).

17. J.P. McKelvey; Solid State and Semiconductor Physics, Harper & Row, 1966.

18. R.A. Smith; Semiconductors, Cambridge at the Univ. Press, (1959).

19. V.P. Tovizi; "Electrical Properties of Nitrogen and Oxygen Ion Implanted Silicon", M.Eng. Project Report, Engineering Physics, McMaster University (1976).